SURFACE ELECTRON PROPERTIES AND CATALYTIC ACTIVITY OF RARE EARTH OXIDES

THESIS SUBMITTED TO THE
COCHIN UNIVERSITY OF SCIENCE AND TECHNOLOGY
IN PARTIAL FULFILMENT OF THE
REQUIREMENTS FOR THE DEGREE OF
DOCTOR OF PHILOSOPHY
IN
CHEMISTRY
IN THE FACULTY OF SCIENCE

By

JALAJA J. MALAYAN

DEPARTMENT OF APPLIED CHEMISTRY
COCHIN UNIVERSITY OF SCIENCE AND TECHNOLOGY
KOCHI - 682 022, INDIA

DECEMBER 1994

CERTIFICATE

This is to certify that the thesis bound herewith is the authentic record of research work carried out by the author under my supervision in partial fulfilment of the requirements for the Degree of Doctor of Philosophy and no part thereof has been presented before for any other degree.

Dr.S.Sugunan
(Supervising Teacher)
Professor, Department of
Applied Chemistry
Cochin University of
Science and Technology

Kochi 682 022

30 December 1994

DECLARATION

I hereby declare that the work presented in this thesis is based on the original work done by me under the guidance of Dr.S.Sugunan, Professor, Department of Applied Chemistry, Cochin University of Science and Technology, Kochi 682022, and no part of this thesis has been included in any other thesis submitted previously for the award of any degree.

Kochi 682022
30 December 1994

Jalaja. J. Malayan
JALAJA. J. MALAYAN

ACKNOWLEDGEMENT

It gives me great pleasure to record my deep-felt gratitude and obligation to my supervising guide Dr.S.Sugunan, Professor in Physical Chemistry, Department of Applied Chemistry, Cochin University of Science and Technology, for introducing me into the area of research. I am extremely thankful to him for his guidance, support and encouragement throughout the course of my work. My studentship with him was indeed a source of inspiration to me.

I feel grateful to Prof.P.Madhavan Pillai, Head of the Department of Applied Chemistry for providing the necessary facilities for my work. I am indebted to him for the constant encouragement he has given me throughout this period. I am greatly indebted to my teachers in the Department of Applied Chemistry for their help and encouragement which was essential for the fruitful completion of the work.

I thank Dr.N.K.Pillai, Chief Chemist, Process Control, FACT-PD and Shri B.Radhakrishnan, Manager, Process Control, FACT-PD for providing facilities for GC analysis in the PD Lab. I also extend my sincere thanks to Mr.V.Karunakaran, Chemist, FACT-PD for his assistance in the GC analysis.

I wish to thank Prof.C.S.Swamy, Co-ordinator, Catalysis Division, Indian Institute of Technology, Madras

for providing me the BET data for surface area determination and the authorities of Regional Sophisticated Instrumentation Centre, Madras, for providing the infrared and ESR spectral data.

Sincere thanks are due to my friends in the Department of Applied Chemistry for their co-operation and timely help.

I wish to acknowledge my sincere gratitude to the University Grants Commission, New Delhi, India for awarding Junior and Senior Research Fellowships.

Finally I extend my sincere thanks to Mr.Sibi and Mrs.Bharathi for the excellent typing of this thesis.

Jalaja J. Malayan

JALAJA. J. MALAYAN

CONTENTS

CHAPTER I
INTRODUCTION

INTRODUCTION

The rare earths have provided fascinating field for chemists confronted with problems of their separation and purification. The rare earths become available in relatively pure form in recent years due to the development of efficient separation methods, largely as a byproduct of the atomic energy programmes of various countries. The rare earths often called lanthanides from La (Z=57) to Lu (Z=71) display subtle variation of properties through the series, while the differences become appreciable for the elements that are farther apart.

Gradation in properties such as ionic radii, ionization potential and oxidation potential of the elements give rise to a corresponding gradual variation in the properties of the compound. The development of the technology and application of the rare earths has not lagged behind. A symposium [1] on the subject has focussed attention on their availability and application.

Hitherto the main applications were in polishing and colouring of glass, as core material in carbon

electrodes and as 'mishmetal' for flints and alloys. More recent applications are in fuel elements for atomic reactors and materials for laser application.

Rare earth oxides of the type Ln_2O_3, (Ln = a lanthanide element) are formed by calcination of salts such as hydroxides, carbonate, oxalate, nitrate and sulfate among others. Basicity of the tripositive species Ln^{+3} decreases with increasing atomic number, while the order of basicity for different oxidation states of a particular element where they exist would be as follows:

$$Ln^{+2} > Ln^{+3} > Ln^{+4}$$

The rare earth sesquioxides Ln_2O_3 exist in three polymorphic forms: the hexagonal 'A' form, the monoclinic 'B' form and the cubic 'C' form.

Rare earth oxides have been classified as solid base catalysts on the basis of the O_{18} binding energy study of the oxides [2]. A number of studies have been reported in oxidative coupling of methane to C_2-hydrocarbons over rare earth oxides [3-9]. Otsuka et al examined the activity

of lanthanide oxides to catalyse the oxidative coupling of methane to form ethylene and ethane. They reported that Sm_2O_3 which gave a C_2-selectivity of 75% was active in the production of C_2-compounds [3]. All of the lanthanide oxides studied except for Ce, Pr and Tb gave high C_2-selectivity.

Among the rare earth oxides studied the highest C_2-selectivity and C_2-yield are shown by the La_2O_3 catalyst whereas the lowest selectivity and yield are observed for the CeO_2 catalyst. The order of the La_2O_3, Sm_2O_3 and CeO_2 for their activity/selectivity is consistent with that observed by Camphell et al for hydrothermally treated rare earth oxides [7]. The hydrothermal treatment given to La_2O_3 and Sm_2O_3 may be responsible for the change in their order for activity/selectivity. Korf et al have observed a large drop in both activity and C_2 selectivity of Sm_2O_3 at higher activation temperature, due to a change in its crystal structure from cubic to monoclinic [9].

Rare earth oxides exhibit activity as oxidation catalysts and have low work functions. Taking advantage of this property of rare earth oxides negative oxide ions can

be produced by negative surface ionization. J.E.Delmore observed the in situ formation of ReO_4^- and ReO_3^- gas phase ions from rare earth oxide catalysed reaction of water with metallic rhenium using a surface ionization mass spectrometer [10].

In selective formation of ethene from CO hydrogenation reaction over In_2O_3-CeO_2, La_2O_3 and Y_2O_3 mixed oxide catalysts, In_2O_3-CeO_2 is highly active due to reduction behaviour of CeO_2. Thus the active centers for hydrocarbon formation exist on cerium ions in In_2O_3-CeO_2 [11].

When heated to high temperatures or treated in reducing atmosphere cerium oxide is known to show large deviation from its stoichiometry. However, subsequent treatment with oxygen leads to rapid reestablishment of its normal stoichiometry [12]. Ahmidov Leechir and V.Perrichon have shown that these redox properties of CeO_2 are utilised in catalytic devices developed for the automotive post combustion process, since the cerium oxide is a regulator of the oxygen partial pressure over the catalyst [13].

A high oxygen storage capacity (OSC) of cerium oxide is one of the reasons why they have been effectively employed as a base component of automotive three way catalysts [14,15].

Takita et al studied the effect of rare earth oxides (Dy_2O_3, Nd_2O_3, Yb_2O_3 and La_2O_3) on the catalytic properties of $Rh-Al_2O_3$ catalyst in the hydrogenation of carbon monoxide. They found that a linear relationship exists between the carbon skeleton propagation of the hydrocarbons formed and basicity of the rare earth oxide [16].

The $CO-H_2$ reaction in the presence of H_2O, formed ketones and secondary alcohols over cerium oxide catalyst around 653 K [17].

To investigate the relationship between structure and catalytic behaviour of ceria and alumina supported cerium oxides, the oxides were subjected to 'OSC' measurements as well as kinetic studies for methane oxidation. The highest 'OSC' was achieved in the finely divided nonstoichiometric cerium oxides. Kinetic studies

for methane oxidation reaction is first order with respect to oxygen in the cerium dioxide and cerium aluminate but in finely divided nonstoichiometric cerium oxides half order with respect to oxygen was obtained [18].

Bernal et al studied the dehydration of 2-butanol on several 4f oxides. Among the sesqioxides studied the highest percentage of 1-butene corresponds to holmia and ytterbia and lowest to lanthana [19]. Galway has reported the existence of linear relationship between the activation energy and the logarithm of the pre-exponential factor corresponding to the dehydration of several butanols and pentanols studied by Knozinger et al [20,21].

In the case of 4f oxides studied the temperature has a little effect on the butene distribution, 1-alkene preference exists over a wide range of temperatures. This would be related to higher pre-exponential factor for 1-butene formation [19]. Siddhan suggests the existence of a correlation between catalyst basicity and terminal alkene formation. The comparison of the acid-base properties of catalysts has also been carried out on the basis of the selectivity data [22-24].

E.R.S. Winter examined the catalytic activity of rare earth oxides for the decomposition of nitric oxide and found that the reaction showed similarity to N_2O decomposition and was first order with respect to pressure [25]. Several studies have been made of the N_2O decomposition on lanthanide oxides [26,27]. Winter analysed the results for decomposition of N_2O over lanthanide oxides pre-treated with oxygen [28]. Read extended the work of Winter to provide a detailed analysis of the effect of pressure on kinetics of decomposition of N_2O on neodymium oxide, dysprosium oxide and erbium oxide [29]. Read suggested that the surface of lanthanide oxides contain a large number of anion vacancies and these centers form the active site for the decomposition of nitrous oxide.

Adsorbed species over heterogenous catalysts are often regarded as reaction intermediates. The reactivity and the stability of the adsorbed species under the reaction conditions are the important factors in elucidating the function of heterogenous catalysts. For the synthesis of methanol from CO and H_2 and hydrocarbons from CO and H_2 and from methanol, methoxide is one of the

important surface intermediate species on the catalyst [30-34]. The reactivity of surface methoxides have been studied over a series of lanthanide oxide catalysts by in situ IR spectroscopy and have observed C-D/C-H exchange in surface methoxide species over Sm_2O_3 in hydrogen [35]. The results reflect the characteristic properties of the Sm_2O_3 surface.

Samarium oxide is an active and selective catalyst in the oxidative coupling of methane [3]. LiCl-Sm_2O_3 was a selective catalyst in the synthesis of C_2H_6 from CH_4. The addition of LiCl to Sm_2O_3 depresses the oxidation of CH_4 and C_2H_6 to CO and CO_2 [36].

A considerable interest in the use of lanthanide compounds as reagent in organic transformations has been developed in the last decades [37]. Among them low valent lanthanide derivatives mainly Sm(II) compounds have been used as promoters for various coupling reactions between carbonyl compounds and organic halides. Sm(II) derivatives have strong reducing properties and react as one electron transfer reagents in the C-C bond forming reactions. In these coupling reactions Sm(II) is transformed into Sm(III) [38].

The use of rare earths as promoters or supports in catalytic reactions have been grown extensively due to its interesting properties encountered in pollution control by catalysis or syngas conversion [39]. In syngas conversion both reducibility and basicity of rare earth oxides have been invoked [40]. On rare earth oxide supports the high selectivity of Pd or Al towards methanol synthesis is explained by the easy decomposition of carbon monoxide on basic sites of the support [41]. Normand et al tested the influence of the support on the reactivity of Pd/rare earth oxide catalysts [42]. According to the results they classified oxides into three classes, (a) oxides of the type Re_2O_3 which are unreducible, (b) CeO_2, where anion vacancies can be created extrinsically by reduction process, (c) Pr_6O_{11} and Tb_4O_7 where anion vacancies exist due to nonstoichiometric nature of these oxides. In syngas conversion production of higher alcohols is found to be favoured by the presence of intrinsic anion vacancies on Pr_6O_{11} and Tb_4O_7 supports.

The oxidative coupling of methane is commonly accepted to proceed by dimerization of methyl radicals produced at the surface as a catalyst, usually an oxide

[43]. By supporting and/or mixing oxide systems, the formation of new phases that either have improved performances with respect to the pure oxides or are clearly inactive is obtained. The oxidative dimerization of methane has been studied over samarium oxide supported on alumina as a function of the samarium loading and the calcination temperature [44]. The structure of the supported phase has been determined by Extended X-ray Absorption Fine Structure (EXAFS). This result states that all the samarium ions are present at the catalyst surface for Sm_2O_3 contents lower than 20% w/w. At the higher loadings crystalline phases containing Sm appear, their structure depending upon the calcination temperature. The activity/selectivity toward C_2-compounds per exposed samarium ion is higher for samples containing less than a monolayer of samarium. Here the coordination polyhedron around samarium ions points to a nonordered structure that blocks highly reactive sites on the alumina surface. On increasing the samarium loading two phases develop depending upon the calcination temperature. At low temperature an oxide like structure grows over the alumina support, while at higher temperatures a perovskite like phase evolves. For the same samarium loading the oxide

like structure shows better selectivity towards C_2-compounds than the $SmAlO_3$ phase.

The nitrogen oxides NO_x are the major air pollutants that cause photochemical smog and acid rain, Iwamoto et al reported the catalytic reduction of nitrogen oxides by using hydrocarbons as reductants in excess of oxygen over copper ion exchanged zeolite [45]. Misono et al reported that Ce-Zeolite was active for the reduction of nitrogen monoxide by propene in presence of oxygen [46]. The activity was further increased by the addition of alkaline earths or on increase of Ce doping [47]. They have also obtained a good correlation between the production of nitrogen and the cumbustion of hydrocarbons [48].

In the oxidation of butene on a series of lanthanide oxides a good correlation has been obtained between the catalytic activity of lanthanide oxides and the fourth ionization potential of the lanthanide elements, which can be interpreted well by assuming that the rate determining step is the oxidation of the trivalent ion to the tetravalent ion [49]. The highest activity of cerium

oxide is due to the least coulomb attraction energy and also due to the change of the exchange energy being zero. The second highest activity of terbium is due to the fact that the latter is zero but the former is larger than cerium ion. The decrease in the activity as the atomic number increases from cerium to qadolinium and from terbium to lutetium is due to the increase in both factors.

The conversion of methane and selectivity to various products on the four catalysts studied ie., Sm_2O_3, CeO_2, La_2O_3 and Pr_6O_{11} showed significant differences for each of these solids in the absence and presence of carbon tetrachloride [50]. Under the reaction conditions employed CeO_2 is the least selective catalyst to C_2 hydrocarbons with essentially all of the methane being converted to CO and CO_2, while La_2O_3 is the most selective to the desired products.

Camphell *et al* [7] have indicated that the abstraction of hydrogen atom from methane molecule to form methyl radicals can best be related to basicity of the oxides, the more basic oxides being more active. It seems that the acid-base pair $[M^{n+}_{Lc} \quad O^{2-}_{Lc}]$ on the surface is

involved in the abstraction of H atom from adsorbed methane molecule by its polarization followed by heterolytic C-H bond rupture. The resulting CH_3^- and H^+ ions interact with the acid and base site respectively.

Although investigations on the catalytic properties of rare earth sesquioxides have multipled in recent years, the primary mode of surface interactions on these materials remain largely undefined. So we have carried out an investigation on the strength and distribution of electron donor sites on the rare earth oxide surfaces (Sm_2O_3 and CeO_2) by adsorption of some electron acceptors.

REFERENCES

1. The Rare Earths, Ed. P.B.Spedding and A.H.Daane (John Wiley & Sons Inc., New York, 1961).

2. H.Vinek, H.Noller, M.Ebel and K.Schwarz, J. Chem. Soc. Faraday Trans 1, 73, 734 (1977).

3. K.Otsuka, K.Jinno and A.Morikawa, Chem. Lett., p.499 (1985).

4. C.H.Lin, K.D.Camphell, J.K.Wang and J.H.Lunsford, J. Phys. Chem., 90, 534 (1986).

5. K.Otsuka, K.Jinno and A.Morikawa, J. Catal., 108, 853 (1986).

6. K.Otsuka and T.Komatsu, Chem. Lett., p.483 (1987).

7. K.D.Camphell, H.Zhang and J.H.Lunsford, J. Phys. Chem., 92, 750 (1988).

8. Y.Tong, M.P.Rosynek and J.H.Lunsford, J. Phys. Chem., 93, 289 (1989).

9. S.J.Korf, J.A.Roos, J.M.Diphoorn, R.H.J.Veehof, J.G.Van Ommen and J.R.H.Russ., Catal. Today, 4, 279 (1989).

10. J.E.Delmore, J. Phys. Chem., 91, 2883 (1987).

11. T.Arai, K.Maruya, K.Domen and T.Onishi, Bull. Chem. Soc. Jap., 62, 349 (1989).

12. K.Otsuka, K.Hattori and A.Morikawa, J. Catal., 79, 493 (1983).

13. A.Leechir and V.Perrichon, J. Chem. Soc. Faraday Trans., 87, 1601 (1991).

14. H.S.Gandhi and M.Shelef, Stud. Surf. Sci. Catal., 30, 199 (1987).

15. R.K.Herz and J.A.Sell, J. Catal., 94, 166 (1985).

16. Y.Takita, T.Yoko, N.Egashira and F.Hori, Bull. Chem. Soc. Jap., 55, 2653 (1982).

17. K.Kushihashi, K.Maruya, K.Domen and T.Onishi, J. Chem. Soc. Chem. Commun., No.3, 259 (1992).

18. H.Honeda, T.Mizushima, N.Kakuta, A.Uene and Y.Sato, Bull. Chem. Soc. Jap., 66, 1279 (1993).

19. S.Bernal and J.M.Trillo, J. Catal., 66, 184 (1980).

20. A.N.Galway, Adv. Catal., 27, 247 (1977).

21. H.Knozinger, H.Bubl and K.Kochloeff, J. Catal., 21, 57 (1972).

22. S.Siddhan, J. Catal., 57, 191 (1979).

23. T.Yamaguchi, H.Saseki and K.Tanabe, Chem. Lett., p.1017 (1973).

24. S.S.Jewur and J.B.Moffat, J. Catal., 57, 167 (1979).

25. E.R.S.Winter, J. Catal., 22, 158 (1971).

26. E.Cremer and E.Marschell, Monatsh. Chem., 82, 840 (1951).

27. Y.Saito, Y.Yoneda and S.Makishima, Actes. Congr. Catal., 2nd, 1960, 1937 (1961).

28. E.R.S.Winter, J. Catal., 15, 144 (1969).

29. J.F.Read, J. Catal., 28, 428 (1973).

30. S.Tsuchiya and T.Shiba, Bull. Chem. Soc. Jap., 38, 1728 (1965).

31. Y.Ono and T.Mori, J. Chem. Soc. Faraday Trans 1, 71, 2209 (1981).

32. M.Y.He and J.G.Ekerdt, J. Catal., 90, 17 (1984).

33. T.Onishi, K.Maruya, K.Domen, H.Abe and K.Kundo, Proc. 9th Int. Congr. Catal., Canada, Vol.2, 507 (1988).

34. K.Maruya, T.Fujisawa, A.Takesawa, K.Domen and T.Onishi, Bull. Chem. Soc. Jap., 62, 11 (1989).

35. Y.Sakata, M.Yoshina, H.Imamura and S.Tsuchiya, J. Chem. Soc. Faraday Trans., 86, 3489 (1990).

36. K.Otsuka, Q.Liu and A.Morikawa, J. Chem. Soc. Chem. Commun., 586 (1986).

37. H.B.Kagan and L.J.Namy, Tetrahedron Report, 213 (1986).

38. E.Leonard, E.Dunech and J.Perichon, J. Chem. Soc. Chem. Commun., 276 (1989).

39. K.C.Tayor, Catalysis Science and Technology, Vol.5, p.119 (Springer Verley, Berlin, 1984).

40. C.Diagne, M.Idriss, I.Pepin, J.P.Hindermann and A.Kiennemann, Appl. Catal., 50, 42 (1989).

41. M.A.Vannice, G.Sudhakar and M.Freemen, J. Catal., 108, 970 (1987).

42. F.Le. Normand, J.Harrault, R.Breauolt, L.Hilaire and A.Kiennemann, J. Phys. Chem., 95, 257 (1991).

43. Y.Aminomiya, V.I.Birss, M.Goled Zinowski, J.Galuszka and A.R.Sanger, Catal. Rev. Sci. Eng., 32, 165 (1990).

44. M.J.Capitan, P.Malet, M.A.Centeno, A.Muhoz-Paez and J.A.Odriozola, J. Phys. Chem., 97, 9233 (1993).

45. M.Iwamoto, Proc. of Meeting of Catalytic Technology for Removal of Nitrogen Oxides, Catalytic Society of Japan, p.17 (1990).

46. M.Misono and K.Kondo, Chem. Lett., p.1001 (1991).

47. C.Yokoyama and M.Misono, Chem. Lett., p.1669 (1992).

48. C.Yokoyama and M.Misono, Bull. Chem. Soc. Jap., 67, 557 (1994).

49. Y.Hattori, J.J.Inoko and Y.Murakami, J. Catal., 42, 60 (1976).

50. S.Sugiyama, Y.Matsumura and J.B.Moffat, J. Catal., 139, 338 (1993).

CHAPTER II
SURFACE ELECTRON PROPERTIES

SURFACE ELECTRON PROPERTIES

2.1 ELECTRON DONOR-ACCEPTOR PROPERTIES

Acid-base interactions during the adsorption of acidic and basic molecules on inorganic powders such as iron oxide, silica and titania have been studied by Fowkes et al [1-3]. they have also extended the acid-base interaction theory to polymer powder interfaces [4]. When strong electron acceptors or donors are adsorbed on metal oxides the corresponding radicals are formed as a result of electron transfer between the adsorbate and the metal oxide surface [5-8]. Flockhart et al associated the electron donor sites with unsolvated hydroxyl ions and defect centers involving oxide ions [9]. Such electron donor-acceptor interactions at surfaces are quite important in elucidating the adhesion forces at these interfaces.

During the past decades there has been much discussion about the nature of the acid and base present on the metal oxide surfaces, and their relevance in catalysis has been extensively investigated. Spectroscopic studies have established the existence of strong electrophilic centers on the silica-alumina surface and formation of

cation radical from hydrocarbons at the same centers [10-12]. The nature of site responsible for electron transfer process is of wide interest [13].

The electron donor strength of metal oxide can be defined as the conversion power of an electron acceptor adsorbed on the metal oxide into its anion radical. If a strong electron acceptor is adsorbed on the metal oxide, the anion radical is formed at every donor site present on the metal oxide surface. On the other hand, if a weak electron acceptor is adsorbed the formation of anion radical will be expected only at the strong donor site. Finally in the case of a very weak electron acceptor adsorption its anion radical will not be formed even at the strongest donor site. Therefore the electron donor strength of a metal oxide can be defined as the limiting electron affinity value of the electron acceptor at which free anion radical formation of the corresponding electron acceptor is not expected on the metal oxide surface [14].

It has been shown that dehydroxylation of a silica surface reduces the extent and heat of adsorption of aromatic and unsaturated hydrocarbons from the gas phase

[15]. Dehydration of surfaces (silica gel, aerosil, aerosilogel) is normally carried out at 900-1000°C. Sintering of the wide porous silica gel and aerosilogel does not occur at this temperature in vacuuo. The effect of dehydroxylation of the silica surface on the state of the adsorbate is clearly seen in its heat of adsorption [15] and in the infrared spectra of silica surface on which various molecules have been adsorbed [16,17].

Terephthalic acid adsorbed on to alumina from alcohol solution was studied by using inelastic electron tunnelling spectroscopy [18]. A comparison with tunnelling spectrum of p-acetylbenzoic acid showed that terephthalic acid is adsorbed predominantly as a monocarboxylate ion on the alumina surface.

Flockhart et al [9] found that when catalytic aluminas are heated to a high temperature, sites are produced on the surface which are capable of oxidising polynuclear aromatic hydrocarbons to corresponding ion radical at room temperature provided O_2 is present.

Studies by Peri [19,20] have presented a clear picture of the surface of partially dehydrated catalytic

aluminas. During dehydration of alumina surface hydroxyl ions combine to form water molecules which are then desorbed leaving a surface lattice containing both hydroxyl and oxide ions. For each molecule of water formed one oxide ion is left in the top layer and one aluminium ion is left in an octahedral site in the next lower layer. The surface lattice develops in such a way as dehydration proceeds, that there are separate domains in each of which the oxide ions are regularly arranged. Remaining hydroxyl ions tend to concentrate in boundaries between these domains and isolated hydroxyl ions may occur within them.

Further dehydration of the surface results in the formation of two kinds of defects at domain boundaries. At one of these two or more immediately adjoining vacancies in the surface layer results in an abnormally exposed aluminium ion (site (a) in the Fig.1). The resultant

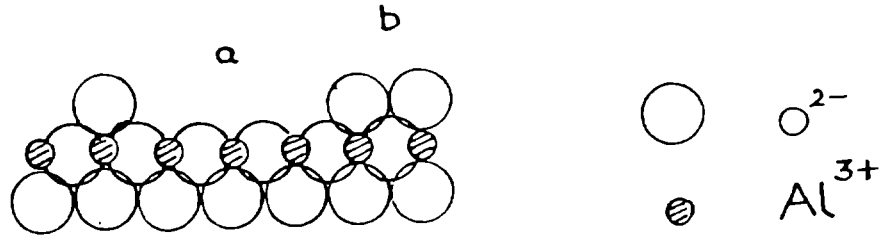

Fig.1 Electron acceptor defect site (a) and electron donor defect site (b) on the surface of alumina dehydrated above 500°C.

localised positive charge makes this site an electron acceptor and gives its oxidising character. At the second type of active site two or more oxide ions occupy immediately adjoining surface sites and a potential electron donor site is created.

The type of defect which may be regarded as an abnormally exposed Al^{3+} ion with resultant localised positive charge possesses the character of Lewis acid. The experiment in which an electron rich hydrocarbon is adsorbed on alumina surface, the potentially active adsorption site is clearly the defect which is electron deficient [6,12]. Interest in the nature of catalytic aluminas has centered mainly on the electron deficient sites on the alumina surface.

Flockhart et al described a detailed investigation of the reduction of tetracyanoethylene (TCNE) on the surface of alumina and silica-alumina catalysts [9]. They found that in the dehydration of catalytic aluminas, sites are formed on the surface which are capable of reducing TCNE to corresponding anion radical. Two different surface sites are responsible for reducing properties. One formed during dehydration at low temperatures ($<350°C$) may be associated with the presence on the surface of unsolvated

hydroxyl ions. At higher temperature (>500°C) a different site is produced which is believed to be a defect centre involving oxide ions

Fomin et al have shown that electron transfer from the hydroxyl ions can and does occur in certain solvent systems provided a suitable acceptor molecule is present [21]. The steep fall in radical forming activity between 250 and 350°C corresponds to a reduction in the number of hydroxyl ions on the surface as dehydration proceeds. Above 500°C dehydration of the surface results in formation of two types of defects. As a result of oxide ion defect described by Peri [19] a potential electron donor site is created and this is mainly responsible for TCNE anion radical in the temperature range 500-1000°C.

A.J.Tench and R.L.Nelson studied the adsorption of nitro compounds on the surface of magnesium oxide powder by ESR and reflectance spectroscopy [7].

On studying the adsorption of TCNE on alumina, silica and silica-alumina it was observed that the electron donating sites decreased initially when silica was added to

alumina and passed through a minimum at about 50% silica [22]. It is interesting to note that the amount of electron donating sites present in silica-alumina is less than silica or alumina and are in the following sequence:

alumina > silica > silica - alumina.

H.Hosaka, T.Fujiwara and K.Meguro investigated the electron donor properties of metal oxides such as magnesia, alumina, silica, titania, zinc oxide and nickel oxide by 7,7,8,8-tetracyanoquinodimethane (TCNQ) adsorption [8]. They found that when TCNQ was adsorbed, the surface of metal oxides acquired the colouration characteristic of each electron acceptor. The colouration was caused by formation of TCNQ anion radicals on metal oxide surfaces. The order of radical forming activity determined by ESR spectroscopy was magnesia > zinc oxide > alumina > titania > silica > nickel oxide. Hosaka et al suggested that electron donor property of metal oxide surfaces depend on the nature of semiconductors and surface hydroxyl ions.

M.Che, C.Naccache and B.Imelik [23] investigated the electron donor properties of titanium dioxide and

magnesium oxide. They found that electron donor centers are associated with hydroxyl groups present on the surfaces of solids activated at low temperature ($< 300°C$), at higher temperatures weakly coordinated oxide ions are formed on their surfaces and these are responsible for the reducing property of these solids.

K.Meguro and K.Esumi have reported the adsorption of some electron acceptors having different electron affinity on alumina [24]. For this they employed electron acceptors such as 7,7,8,8-tetracyanoquinodimethane (TCNQ), 2,5-dichlorobenzoquinone (DCQ), p-dinitrobenzene (PDNB) and m-dinitrobenzene (MDNB). They found that when electron acceptors are adsorbed from solutions in acetonitrile, alumina surface showed remarkable colouration characteristic with the kind of acceptor. They suggested the possibility of its participation of an oxidation-reduction process which is of the type:

$$OH^- + A \longrightarrow A^- + OH$$

where A is an electron acceptor.

M.A.Enriquez and J.P.Fraissard carried out a comparative study of variation of surface properties and catalytic activity of TiO_2 samples with pretreatment temperature in vacuuo [25]. The results showed that active sites are electron donor centres, number of which has been determined by adsorption of tetracyanoethylene and trinitrobenzene. These centers are Ti^{3+} ions and O-Ti-OH groups for high and low pretreatment temperatures respectively.

It has been shown that silica has stronger electron acceptor properties for phenothiazine than alumina [26]. Electron donor properties of these substances measured by the formation of anion radicals of tetracyano-ethylene and 7,7,8,8-tetracyanoquinodimethane decreases in the opposite sequence.

K.Esumi and K.Meguro described an investigation of strength and distribution of electron donor sites on alumina, titania and zirconia-titania by adsorption of electron acceptors such as 7,7,8,8-tetracyanoquino-dimethane (TCNQ), 2,5-dichloro p-benzoquinone (DCQ), p-dinitrobenzene (PDNB) and m-dinitrobenzene (MDNB) by means

of an ESR spectrophotometer [27]. They suggested that the electron donor sites of alumina, titania and zirconia-titania are mainly associated with surface hydroxyl ions.

The electronic state of adsorbed species was studied by UV-Visible spectroscopy in addition to ESR spectroscopy [8,14,24]. The observed bands near 600 nm were related to the dimeric TCNQ anion radical which absorbs light at 643 nm [28]. This tentative attribution was supported by the characteristic features that neutral TCNQ absorbs only at 395 nm. TCNQ has a high electron affinity and TCNQ anion radicals are stable even at room temperature [29-32]. ESR and electronic spectra provided evidence that TCNQ anion radicals are formed as a result of electron transfer from metal oxide surface to adsorbed TCNQ.

On studying the adsorption of electron acceptors with electron affinities varying from 2.84 eV to 1.26 eV on the surface of titania Esumi and Meguro have shown that the limiting radical concentration decreases with decreasing electron affinity of the electron acceptor and steeply between PDNB and MDNB [33]. This suggests that adsorption sites of titania act as electron donor to the adsorbed

molecule with electron affinity larger than 1.77 eV but not to those smaller than 1.26 eV. Accordingly the limit of electron transfer from electron donor sites of titania to electron acceptor molecule is located between 1.77 and 1.26 eV in the electron affinity of the electron acceptor.

On comparing the model of Lewis acidity or basicity of a surface with surface state model Morrison suggested that basic centers can in many cases be coincident with sites providing surface state [34]. D.Cordishi and V.Indovina investigated the electron donor properties of CaO, MgO, ZnO, Al_2O_3 and SiO_2-Al_2O_3 activated in vacuuo at temperatures upto 1200 K using ESR of adsorbed nitro radicals as a probe [35]. The results indicated the existence of a correlation between electron donor activity of oxides and their Lewis base strength.

Ishikawa et al have shown that there are two kinds of irreversible adsorption site for CO_2 on non-stoichiometric strontium-calcium hydroxy apatites (SrCa HAP) [36]. Irreversible adsorption of CO_2 on these samples depends on the nonstoichiometry.

The study of the adsorption of anion radical salts on metal oxides can provide useful information concerning the interaction between anion radical salts and metal oxide surfaces [37]. Esumi and Meguro reported the adsorption of TCNQ anion radical salts such as Li^+ TCNQ, Na^+ $TCNQ^{--}$ and K^+ $TCNQ^-$ on alumina from a solution in acetonitrile by measuring the adsorption isotherms and the ESR and electronic spectra of these adsorbed TCNQ anion radical salts. They found that TCNQ anion radicals were adsorbed at electron deficient sites on the alumina surface.

Recently plasma treatment has become attractive as a method for surface treatment, probably because it is a dry process at low temperatures with a relatively low pressure gas [38]. Esumi et al have studied the surface modification of meso carbon microbeads [39-41] by various plasma treatments and found that oxygen plasma treatment renders the surface more acidic owing to the formation of carbonyl groups, whereas nitrogen or ammonia plasma treatment renders the surface more basic owing to the formation of amino groups. The interaction of plasma treated metal oxide with TCNQ in acetonitrile solution was

studied by measuring their adsorption intensity of TCNQ in acetonitrile solution [42]. The electron donicity is increased by the ammonia and nitrogen plasma treatments.

Fowkes et al [2,4] have studied the interaction between inorganic solids and basic adsorbates by using the Drago correlations of the heats of acid-base interactions, and have determined the Drago parameters for several solids such as silica, rutile and magnetite. Esumi et al when studied the adsorption of tetrachloro-p-benzoquinone from various solvents on metal oxides, interpreted their adsorption results in terms of acid-base theory [43]. For this they employed the Drago equation [44],

$$-\Delta H^{ab} = C_A C_B + E_A E_B$$

where E and C are the Drago constants for the acidic compound (A) and the basic compound (B). They suggested that a useful approach for relating interfacial interactions quantitatively has been the Drago equation of enthalpy in acid-base complexation.

K.Esumi, K.Miyata and K.Meguro examined the electron donor-acceptor interactions on metal oxides by

means of 7,7,8,8-tetracyanoquinodimethane (TCNQ) adsorption from various solvents [45]. They found that amount of TCNQ adsorbed on metal oxides decreased with an increase in acid-base interaction between TCNQ and basic solvents.

Skourtis et al have shown that electron transfer (ET) reactions play a significant role in biology [46]. They constitute important steps in processes such as photosynthesis and oxidative phosphorylation. Biological ET reactions are also important from a physico-chemical point of view, because they involve the tunnelling of an electron over a long distance.

2.2 SOLID ACIDS AND BASES

The acidic and basic properties of oxide catalysts are very important for the development of scientific criteria in catalyst application. The methods for determination of surface acidity were critically reviewed [47] by H.A.Benesi and B.H.C.Winquist. Surface acidic and basic sites of oxides are involved in the catalytic activity for various reactions such as cracking, isomerization and polymerization [48].

The microcalorimetric measurements of the heats of adsorption of ammonia and carbon dioxide have been used to elucidate the acidic and basic properties of a number of oxides [49]. The results showed that greater the degree of covalency of the oxide expressed by higher value of charge/radius ratio, the more likely is the acidity to be observed. An oxide with a low value of charge/radius ratio is more ionic in nature and present more basic sites.

The aqueous methods for the determination of acidity consists of direct titration of an aqueous suspension of the sample of powdered solid with a dilute base to a neutral end point. Webb et al gave a method of measuring the amount of acid sites by the extent to which they neutralise a solution of KOH as revealed by subsequent titration with HCl using phenolphthalien as indicator [50]. This method is least suitable because the state of the surface of the solid catalyst in a water suspension is radically different from its state during use as an acidic catalyst.

Non-aqueous methods for the determination of surface acidity represent a considerable improvement over aqueous methods, because the solvents used (eg., benzene,

iso-octane) do not react with catalyst surface. Of the available non-aqueous methods [48,51,52] simplest is that employing adsorbed indicators.

Following Walling [53] the acid-strength of a solid surface can be defined as its proton donating ability, quantitatively expressed by Hammett and Deyrup's H_o function [54,55].

$$H_o = -\log a_{H^+} f_B / f_{BH^+}$$

$$H_o = pKa + \log[B]/[BH^+]$$

where a_{H^+} is the proton activity, [B] and $[BH^+]$ are the concentration of the neutral base and its conjugate acid, f_B and f_{BH^+} are the corresponding activity coefficients. If the reaction takes place by electron pair transfer from adsorbate to the surface, H_o is expressed by

$$H_o = -\log a_A f_B / f_{AB}$$

$$H_o = pKa + \log[B]/[AB].$$

where a_A is the activity of the Lewis acid or electron pair acceptor.

The basic strength of a solid surface is defined as the ability of the surface to convert an adsorbed electrically neutral acid indicator to its conjugate base, the ability of the surface to donate an electron pair to an adsorbed acid.

When an electrically neutral acid indicator is adsorbed on a solid base from a nonpolar solvent, the base strength is determined from the colour changes of the indicator over a range of pKa values. For the reaction of an indicator AH with a solid base B

$$AH + B = A^- + BH^+$$

$$H_o = pK_a + \log[A^-]/[AH]$$

where [AH] is the concentration of the acidic form of the indicator and $[A^-]$, that of the basic form.

The initial colour change and the subsequent change in the intensity are observed at values of $pK_a \pm 1$. If we assume that the intermediate colour appears when the basic form reaches 50% ie., when $[A^-]/[AH] = 1$, we have $H_o = pK_a$.

Solid acids and bases are characterized by amount, strength and nature of acid and base centers. The characterization not only depend upon the purity of the materials and the method of preparation but also upon the heat treatment, compression and irradiation.

The amount of base (basic sites) or acid (acidic sites) on a solid is usually expressed as the number (or mmol) of basic sites per unit weight or unit surface area of the solid.

Wail Malherbe and Weiss was the first to note that weakly basic indicators adsorbed on clays gave some colours as those formed when such indicators were added to concentrated sulfuric acid [56]. Walling [53] suggested that such colour tests could be used to measure acid strength of solid surfaces in terms of Hammett acidity function. This approach was extended by Benesi [57].

The indicator method is by far the easiest and quickest way of screening surface acidities of solid catalysts, but it has two drawbacks. First of all, the number of suitable indicator is limited, because of the

visual requirement that the colour of the acid form mask that of the basic form. Secondly the acid colour of many of the Hammett indicators can be produced by processes other than simple proton addition.

After the acid strength of a catalyst surface has been bracketed by means of colours of adsorbed indicator, the next step in the determination of surface acidity is the measurement of number of acid groups. This is generally done by titrating a suspension of the catalyst with a solution of a suitable indicator in an inert solvent.

Amine titration method, one of the several methods used to determine acidity was reported first by Benesi [57] and is based on O.Johnson's experiment [58], and has been subsequently modified [59,60]. The acid amount measured is the sum of Bronsted and Lewis acid sites.

The amine titration method is obviously limited to white or light coloured surfaces. Titration of dark coloured solids can be carried out by adding a small amount of white solid acid [61]. The end point of the titration

is taken when the colour change is observed on white solid and a correction is made for the amount of n-butyl amine used for the added white material. Using this method both acid amount and acid strength have been measured for titanium trichloride by employing silica-alumina as the white material.

There are many methods for the measurements of acid strength like visual colour change method [62], spectrophotometric method using fluorescent indicators [63], and gaseous adsorption method [50]. For basic strength, method using indicators [64], phenol vapour adsorption method [65] and temperature programmed desorption technique [66] are generally employed.

The very significant work of Hirschler has shed some light on acid strength distribution of cracking catalysts [62]. The use of a series of substituted aryl cerbinols gave an acid strength distribution curve which is in keeping with the heterogenous distribution of energy sites determined by other physical studies. The formation of coloured carbonium ion led to the conclusion that acid sites on the surface of the catalyst is protonic (Bronsted) [67].

Parry showed that adsorption of pyridine on silica involved association through surface hydrogen bonds [68]. Basila et al have gone one step further and have proposed that primary sites on silica-alumina are of the Lewis type (centered on aluminium atoms) and that appreciably Bronsted sites are produced by a second order interaction between the molecule chemisorbed on a Lewis site and nearby surface hydroxyl group [69].

To evaluate the catalytic activity of zeolite it is necessary to determine the nature, strength and distribution of acid sites. Zeolite acidity can be determined by n-butyl amine titration [70]. UV spectrophotometry has been applied for measurement of acid strength of silica-alumina catalysts using 4-benzene azodiphenylamine, 4-nitroaniline and 2,4-dinitroquinoline [71].

Quantitative information on the base strength distribution of solid base surfaces are essential for studies of solid base catalysts. The relative base strength of solid bases such as MgO and CaO was determined from the adsorption power for phenol vapour [72].

T.Yamanaka and K.Tanabe determined the basicity of a series of oxides and found that basicity at basic strength ($H_o \geqslant 1.5$) has the order, $ZnO > TiO_2 > \gamma Al_2O_3 > BaO >$ activated $Al_2O_3 > B_2O_3 > ZrO_2 > MgSO_4 > MoO_3$ [73].

The amount of basic sites can be determined by titrating a suspension of a solid in benzene on which an indicator has been adsorbed on its conjugate base form with benzoic acid dissolved in benzene [48]. The benzoic acid titres are a measure of the amount of basic sites having basic strength corresponding to the pK_a value of the indicator. Malinowski and Sczepanska have devised titration methods for use with aqueous solution and with anhydrous acetic acid [64].

J.Take, N.Kikuchi and Y.Yoneda developed a method for the determination of basic strength of solid surfaces which consists of titration of solids suspended in cyclohexane with benzoic acid using a series of Hammett indicators [74]. They found that base strength of alkaline earth oxides increased remarkably upon heat treatment in vacuuo and basicity decreased in the order SrO = CaO > MgO.

T.Itzuka, K.Ogasawara and K.Tanabe examined the acid strength of $Nb_2O_5.nH_2O$ by indicator adsorption method [75]. The surface of $Nb_2O_5.nH_2O$ showed strong acidic character which disappears on heat treatment at higher temperature. P.A.Burke and E.I.Ko also observed that acidity of niobia diminishes with increase in calcination temperature [76].

A method of determining the basicity at various base strength by titrating a solid suspended in benzene with trichloroacetic acid using a series of Hammett indicators was proposed by K.Tanabe and Y.Yamanaka [73]. The method makes it possible to determine the basic strength expressed by a Hammett acidity function and hence the acid base strength distribution of solid surface on a common scale. This method permits the determination of basicity at relatively weak basic strength which was not previously proposed.

It is necessary to distinguish between Bronsted and Lewis acid sites for the catalytic action of solid acids. The number of Bronsted sites on a solid surface may be derived from the number of free protons in aqueous solution arising from the exchange of proton or hydrogen atom. Malinowski and Sczepanska measured the amount of

Bronsted acid by potentiometric titration of solid acid in anhydrous picoline with 0.1N solution of sodium methoxide [64]. Leftin and Hall reported that the amount of Lewis acid can be determined from the amount of triphenyl carbonium ion formed, when the solid acid abstract a hydride ion from triphenyl methane as shown below [77].

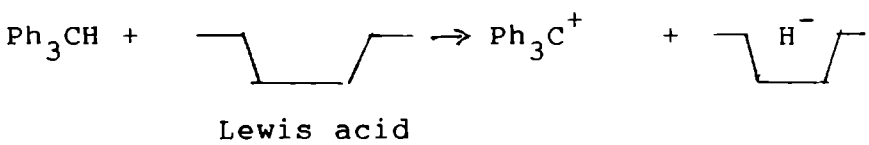

Lewis acid

In an infra red study of pyridine chemisorbed on silica-alumina catalysts of varying silica content, Schwarz described a new method for the measurement of Lewis and Bronsted acid sites [78]. Gay and Liang have investigated the surface acidities of silica, alumina and silica-alumina by ^{13}C NMR spectra of a variety of aliphatic and aromatic amines adsorbed on these solids [79]. In the case of silica, only weak interactions of amines with surface hydroxyl groups are observed. Much stronger interactions are observed in the case of alumina. In silica-alumina chemical shift due to protonation is observed. Yoshizumi et al determined acid strength distribution on silica-alumina catalyst calorimetrically by measuring the heat of adsorption of n-butylamine from benzene solution [80].

Silica-magnesia is an important binary oxide because of the potential utility as a matrix in zeolite containing cracking catalysts [81]. An infra red study by Kermarec et al shows that the surface acidity of silica-magnesia appears to be more complex than that of silica-alumina [82]. From infra red spectra of pyridine and 2,6-dimethyl pyridine chemisorbed on silica-magnesia, they deduce that Bronsted and Lewis acid sites are present.

Shibata and Kiyoura measured surface acidities by the n-butylamine titration method of the TiO_2-ZrO_2 system as a function of composition and method of preparation. Highest titer of strong acid sites [$H_o \leq 5.6$] was obtained at a composition of 50% m (mole %) ZrO_2 [83].

Surface acidities of Al_2O_3-TiO_2, SiO_2-TiO_2 and TiO_2-ZrO_2 preparations heated at various temperatures have been reported by Walvekar and Halgeri [84]. Butylamine titers of each binary oxide increase as calcination temperature is increased, go through maximum value and finally decrease.

Tanabe et al found that silica-titania is highly acidic and has high catalytic activity for phenol amination

with ammonia and for double bond isomerization in butenes [85,86]. The highest acidity per unit weight of catalyst was obtained when TiO_2-SiO_2 (1:1 molar ratio) was heated at 500°C.

Silica is an ideal host oxide with high electronegativity and the oxygen coordination is two which leads to the existence of coordinatively unsaturated dopant cations on the surface [87]. For two-cations in similar coordination and bonding sites the cation with higher electronegativity to be a stronger Lewis acid site [87]. Microcalorimetric measurement of the differential heat of pyridine adsorption were used to probe the distribution of acid strength on a series of silica supported oxide catalysts [88]. Depositing oxides of the following cations ie., Ga^{2+}, Zn^{2+}, Al^{3+}, Fe^{3+} Fe^{2+} Mg^{2+} and Sc^{2+} on to silica increased the acid strength of the catalyst. Gallium oxide is the most electronegative oxide and when it is added to silica strong acid sites are generated and that both Lewis and Bronsted acid sites are present on the surface [89,90].

According to Tanabe the acid-base properties of mixed metal oxides can be varied by choosing different metal oxide composition at different concentrations and by changing the treatment of the sample [91].

Infra red spectroscopic studies of benzene adsorbed on several KH β zeolites where the extent of potassium exchange K/Al (%) varied from 0 to 88.32% have been undertaken under different conditions. The bands of adsorbed benzene on KH β zeolites is in the range 2050-1700 cm^{-1} [92]. KH β zeolite exhibits basicity when K/Al $\leq$ 88.32% where its basicity is stronger and acidity is weaker. The order of stability of various adsorbed benzene species on the samples is as follows:

O^- (benzene) > H^+ (benzene) > K^+ benzene > benzene.

V.R.Choudhary and V.H.Rane have showed that rare earth oxide catalysts differ widely in their acidity and basicity and in the site energy distribution of both the acid and basic sites [65]. The acid and basic sites on the catalysts are the accessible M^{n+}_{Lc} cations and O^{2-}_{Lc} anions on the oxide surface and the site energy distributions of acid and base sites is mostly attributed to the M^{n+}_{Lc} and O^{2-}_{Lc} ions

in different coordination, the lower coordinated ion site being responsible for the stronger acid-base sites.

2.3 CATALYTIC ACTIVITY

Although the fundamental catalytic and surface properties of alkali, alkaline earth and other basic oxides have been extensively studied [48], equivalent information about the series of basic rare earth oxides is much less. Empirical studies have demonstrated that following appropriate pretreatment, rare earth oxides are active catalysts for a number of reactions.

Taylor and Diamond have shown that paramagnetic oxides Gd_2O_3 and Nd_2O_3 are more active in catalysing ortho-para hydrogen conversion [93]. Minachev compared the catalytic activity in oxidation of hydrogen and propylene with that in the isotopic exchange of oxygen and suggested that the catalytic activity depends on the binding energy of oxygen with the surface and on the valence of lanthanide ions [94].

Hopkins and Taebel have measured the catalytic activity of rare earths for oxidation, hydrogenation,

decomposition and synthesis of organic compounds [95]. Oxidation-reduction reactions are important in organic chemistry. Rare earth oxides like La_2O_3 and Dy_2O_3 are effective in Meerwein-Ponndorf-Verley type reduction of ketones [96,97].

The reduction of multiple bonds using an organic molecule as a hydrogen donor in place of hydrogen gas or metal hydride is known as hydrogen transfer reaction [98]. Reduction of carbonyl groups is one of the most fundamental operations in organic chemistry. This is called Meerwein Ponndorf-Verley reduction. It was discovered in 1925 and has been used successfully in a number of instances [99].

Aluminium isopropoxide has been found to be the best reagent for this reaction. This method calls for both addition of at least 100-200% excess aluminium isopropoxide and neutralisation of alkoxide salt with strong acid. Heterogenous catalysts for the reduction reaction are known [100]. The mechanism of the reduction reaction involves a hydride transfer from aluminium isopropoxide to the carbonyl carbon of the ketone. Kibby and Keithhall have reported on hydrogen transfer reaction over hydroxy apatite catalyst and proposed a mechanism similar to that of the Meerwein-Ponndorf-Verley reduction [101].

M.Shibagaki *et al* studied the liquid phase reduction of aldehydes and ketones with 2-propanol over hydrous zirconium oxide [102]. Kinetic experiments have indicated that the reaction rate is of first order dependence on each of the concentration of the carbonyl compound, 2-propanol and the catalyst. An observation of the primary isotope effect has suggested that a step of hydride transfer from adsorbed 2-propanol to adsorbed carbonyl compound constitute the rate determining step for the reduction. Tin(IV) oxide is an effective catalyst in the vapour phase reduction of carboxylic acid with 2-propanol [103]. Tin(IV) oxide is analogous to hydrous zirconium(IV) oxide regarding its characteristic reactivity. The reverse reaction which is known as Oppenauer oxidation has been used for the oxidation of alcohols.

In 1937 Oppenauer showed that unsolvated steroid alcohols could be oxidised to the corresponding ketone in excellent yields through the use of aluminium t-butoxide in the presence of a large amount of acetone, that compound functioning as the hydrogen acceptor and the large excess serving to shift the equilibrium in the desired direction

[104]. In view of the reversible nature of the reaction, many statements as to the mechanism of the Meerwein-Ponndorf-Verley reduction [99] are equally applicable to the Oppenauer oxidation. Activation of the alcoholic hydrogen atom by the aluminium resulting in hydrogen bonding has also been proposed [105] by Woodward et al.

The Oppenauer oxidation has not been used as a preparative method for the oxidation of primary alcohols to aldehydes because the aldehydes condensed with the hydrogen acceptor. Schinz and Lauehensuer have developed a general preparative method for the Oppenauer oxidation of low molecular weight primary alcohols to aldehydes. The procedure is essentially a reversal of the MPV reduction but does not require an excess of alcohol [106].

The three most common catalysts in the Oppenauer oxidation are aluminium t-butoxide, isopropoxide and phenoxide. Aluminium isopropoxide and in particular phenoxide is easier to prepare. Aluminium isopropoxide is the most powerful oxidising agent [107]. In the modified Oppenauer oxidation benzophenone was found to be satisfactory oxidising agent [108] since it cannot undergo condensation in the presence of a strongly basic catalyst.

According to Oppenauer a solvent is necessary for the oxidation of alcohols [105]. Toluene is employed occasionally [109]. Time and temperature can be varied over a wide range, depending upon the alcohol to be oxidised, although the choice of solvent and hydrogen acceptor naturally controls the maximum temperature that can be reached. This method has several disadvantages such as need for tedious purification and unreusability of the catalyst.

Heterogenous catalysts for the oxidation are known. Silica, MgO and Al_2O_3 have been reported to be successful catalysts [110,111]. This process has several advantages in the isolation of products and require a high reaction temperature.

Kuno et al have shown that liquid phase oxidation of primary and secondary alcohols proceeds efficiently using benzophenone as the hydrogen acceptor [112,113].

Correlation between acid-base properties and catalytic activity

Rare earth oxides have been recognized as solid base catalysts. The solid acids and bases have been

usefully employed as catalysts in various acid-base catalysed reactions. A parallel has been found between the base strength of various solids as measured by the phenol vapour adsorption method and that the catalytic activity for the dehydrogenation of isopropyl alcohol [114].

The dehydration of isopropyl alcohol to propylene is a measure of the acidity of the catalyst [115,116], and the (dehydrogenation rate/dehydration rate) ratio is a measure of the basicity [117]. The dehydration is catalysed at acidic sites and the dehydrogenation is catalysed at both acidic and basic sites.

It has been reported by several workers [118-120] that a large part of the basic sites determined by the adsorption of acidic substances consist of surface lattice oxygen, O^{2-} ions. Keulks and Wragg *et al* have reported that the active oxygen species available for oxidation is lattice oxygen O^{2-} ions. The acidic sites contribute to the activation of electron donor type reactants such as olefins and are connected with the oxidising sites [121-122].

Fukuda et al studied the decomposition of 4-hydroxy-4-methyl 2-pentanone over La_2O_3, Y_2O_3 and CeO_2 [123]. It was found that maximum activity was obtained by pretreatment at 500°C for La_2O_3 and at 700°C for Y_2O_3. In the case of La_2O_3 variation on the activity with the pretreatment temperature was similar to that of the basicity. The activities of three oxides for the decomposition reaction are in the following order, $La_2O_3 > Y_2O_3 > CeO_2$.

Good correlation have been found in many cases between the total amount of acid (Bronsted plus Lewis type usually measured by the amine titration method) and the catalytic activities of solid acids. The rates of both the catalytic decomposition of cumene and the polymerization of propylene over SiO_2-Al_2O_3 catalysts were found to increase with increasing acid amount at strength $H_o \leq +3.3$ [125,126].

Catalytic activity of alumina in a range of reactions such as isomerization of hydrocarbons, polymerization of olefins have all been attributed to the acidic properties of the surface [127].

Minachev et al studied the hydrogenation of ethylene at low temperature as part of a study of catalytic

activity of rare earth oxides [128]. They found that La_2O_3 is highly active for hydrogenation when pretreated at high temperatures. They also correlated basicity with catalytic activity.

The catalytic activity of lanthanide sesquioxides for the double bond isomerization of n-butenes has been studied in the temperature range 0-50°C [129]. Activity increases with increasing pretreatment temperature due to removal of surface hydroxyls and then decreases with increase in pretreatment temperature due to decrease of surface anion disorder. Rosynek et al reported that basic sites in La_2O_3 were essential for the isomerization of butenes [130].

As a measure of the base strength of metal oxide catalysts Davis suggested the alcohol conversion selectivity [131]. The amount of alkene produced by the water elimination depends on the base strength. It was found that ZnO is a stronger base than CaO and MgO, and the oxides of Zr, In, Th and Y are stronger base than ZnO [132]. Vapour phase conversion of cyclohexanol to cyclohexanone in the presence of different basic catalysts showed that some of them are able to activate dehydration

and dehydrogenation simultaneously. The dehydrogenation activity is related to the existence of basic sites originating from the oxygen in the oxide lattice.

The catalytic isomerization of butenes over samarium oxide has been investigated in view of acid-base catalysis [133]. The ratio cis/trans 2-butenes formed from 1-butene isomerization was 22.2. The reaction profile of the butene isomerization obtained from the relative rate constant was of the cis-convex type. The basic sites on the oxide surface have been revealed by the benzoic acid titration method.

The adsorption and mechanism of surface reactions of 2-propanol on ceria calcined at different temperatures is known to change the surface species on the oxide and remove surface bound OH groups with Bronsted type acidity at high temperatures with the formation of new sites of Lewis acidity from exposed metal cations [134]. Upon calcination dehydration activity of ceria increases. According to the mechanism proposed for this reaction it is suggested that exposed couples of Ce^{4+} and O^{2-} ions are active sites.

Zhang et al have investigated the aldol addition of butyraldehyde on alkaline earth oxides, zirconium oxide and lanthanum oxide, to compare the active site and mechanism with those for aldol addition of acetone [135]. It is found that active site is the surface O^{2-} and the rate determining step is the α-H abstraction.

Catalytic properties of chromium oxide are very sensitive to its method of preparation. Dyne et al have found an increase in activation energy and specific activity for hydrogenolysis and polymerization of cyclopropane after recrystallization of an amorphous sample [136]. L.Nondek and M.Kraus have found that catalytic properties of chromium oxide depends mainly on its temperature of calcination which governs the surface concentration of hydroxyl groups and the state of coordination of surface Cr^{3+} ions [137].

The surface of $Nb_2O_5.nH_2O$ showed considerably strong acidic character and rather weak basic property. The acidic sites on these catalyst surface are thought to be the isolated OH groups as Bronsted acid sites and exposed metal ions as heavier acid sites; both of which appear after vigorous heat treatment [75].

Selectivity of butenes produced from 2-butanol is very sensitive to the surface acidic and basic property [138]. The oxide catalysts which have both acidic and basic sites such as ThO_2 and ZrO_2 produces 1-butene dominantly [139]. Polymerization of propylene proceeds on Bronsted acid sites on $Nb_2O_5.nH_2O$ pretreated at low temperatures; but Lewis acid sites become main active sites after treatment at lower temperatures [75].

Usually the reactions which are catalysed by solid bases are polymerization, isomerization, alkylation, condensation, addition and dehydrohalogenation. The oxides, carbonates and hydroxides of alkali metals and alkaline earth metals (MgO, CaO, SrO, Na_2CO_3, $CaCO_3$, $SrCO_3$, NaOH, $Ca(OH)_2$) have been found active in the high polymerization of formaldehyde, ethylene oxide, propylene oxide and propiolactone [140-143].

A first order rate constant for the formation of benzyl benzoate from benzaldehyde over calcium oxide calcined at various temperatures is found to change in parallel with the change in catalyst basicity. There is a good correlation between catalytic activity and amount of base per unit surface area [144].

Hydrous zirconium oxide is an amorphous solid and has several catalytic activity [145]. The oxide was changed to crystalline zirconium by calcination at high temperature and the catalytic activities were lowered. The correlation between surface property and catalytic activity was investigated on hydrous zirconium oxide calcined at several temperatures, the best activity was obtained on the oxide calcined at 300°C. The quantity of surface acid or basic sites was measured by the butylamine or trichloro acetic acid titration method respectively using various Hammett indicators.

Investigations are carried out to have a systematic comparison of the acidic properties and catalytic activities of single oxides SiO_2, TiO_2, Al_2O_3 etc., their binary oxides and the ternary oxide TiO_2-SiO_2-Al_2O_3 [146]. The acidity distribution is measured by using butylamine titration technique and the reaction selected for the catalytic activity measurements are alkylation of toluene with 2-propanol and dehydration of 2-propanol. On comparing acid properties with catalytic activity it appears that the isopropylation of toluene requires acid sites of strength $H_o \leq + 1.5$.

Mizuno et al carried out olefin polymerization over silica-alumina and found that strong Lewis acid sites are active in this reaction [147]. Binary metal oxides such as SiO_2-Al_2O_3, SiO_2-MgO, SiO_2-ZrO_2 and Al_2O_3-B_2O_3 have been used as solid acid catalysts, since their surface acidic properties are well known [148]. Many other combinations such as TiO_2-Al_2O_3 [149], TiO_2-ZnO [150], SiO_2-ZnO [151], SiO_2-TiO_2 [85] and Al_2O_3-MgO [152] have been found to show remarkable acid properties and catalytic activities in various acid catalysed reactions.

The acidity and basicity of the ternary system MoO_3-Bi_2O_3-P_2O_5 catalysts have been studied by adsorption of acidic and basic compounds in the gas phase. Catalytic activity for oxidation and olefin isomerization have also been studied and established the concept that the catalytic activity and selectivity in mild oxidation can be well interpreted in terms of the acid and base properties between the catalyst and the reactant [153].

M.Ai used static and pulse methods to study acidity and basicity of a series of TiO_2-V_2O_5-P_2O_5 system by the adsorption of acidic and basic molecules in the gas phase [154]. The vapour phase oxidation of electron donor

type reactants such as butadiene, 1-butene and that of acetic acid as an acidic reactant was carried out and the relationship between the catalytic behaviour and the acid-base properties was investigated. The acid-base properties of the catalyst and oxygen mobilities are responsible for the catalytic action. The acidic sites (probably consisting of metal ions with a high electron affinity) play a role in electron transfer from the reactant sites resulting in the formation of a cationic intermediates and a reduced metal ion [155] ie., the acidic sites contribute to the activation of the reactant.

The basic sites owing to their ability to donate electrons to oxygen contribute to adsorb and activate the gaseous oxygen and also reoxidise the reduced metal ions, ie., basic sites are connected with the oxidising site, probably consisting of lattice oxygen O^{2-} [156]. The combination of the metal oxides contribute to the modification of both the acidic and basic properties of the catalyst.

REFERENCES

1. S.T.Joslin and F.A.Fowkes, Ind. Eng. Chem. Prod. Dev., **24**, 369 (1985).

2. F.M.Fowkes, D.C.Me Carthy and J.A.Wolfe, J. Polym. Sci. Polym. Chem. Ed., **22**, 547 (1984).

3. F.M.Fowkes, Y.C.Huang, B.A.Shah, M.J.Kulp and T.B.Lloyd, Colloids. Surf., 29, 243 (1988).

4. F.M.Fowkes, in "Physico Chemical Aspects of Polymer Surfaces", K.L.Mittal (Ed.), Vol.2, p.583, (Plenum Press, New York, 1983).

5. J.J.Booney and R.C.Pink, Trans. Faraday Soc., 58, 1632 (1962).

6. B.D.Flockhart, J.A.N.Scott and R.C.Pink, Trans. Faraday Soc., 62, 730 (1966).

7. A.J.Tench and R.L.Nelson, Trans. Faraday Soc., 63, 2254 (1967).

8. H.Hosaka, T.Fujiwara and K.Meguro, Bull. Chem. Soc. Jap., 44, 2616 (1971).

9. B.D.Flockhart, I.R.Leith and R.C.Pink, Trans. Faraday Soc., 65, 542 (1969).

10. H.P.Leftio and M.C.Hobson, J. Adv. Catal., 14, 372 (1963).

11. R.P.Porter and W.K.Hall, J. Catal., 5, 336 (1966).

12. A.Terenin, Adv. Catal., 15, 256 (1964).

13. B.D.Flockhart, C.Naccache, J.A.N.Scott and R.C.Pink, Chem. Commun., p.238 (1965).

14. K.Esumi and K.Meguro, J. Colloid. Interface Sci., 66, 192 (1978).

15. A.V.Kiselev and Y.I.Yashin, "Gas Adsorption Chromatography", (Plenum Press, New York, 1969).

16. L.H.Little, "Infrared Spectra of Adsorbed Species" (Academic Press, London, 1966).

17. G.Curthoys and B.A.Elkington, J. Phys. Chem., 72, 347 (1968).

18. S.Kamata and M.Higo, Chem. Lett., p.2017 (1984).

19. J.B.Peri, J. Phys. Chem., 69, 220 (1965).

20. J.B.Peri and R.B.Hannan, J. Phys. Chem., 64, 1524 (1960).

21. G.V.Fomin, L.A.Blyumenfeld and V.I.Sukhorukov, Proc. Acad. Sci. (USSR), 157, 819 (1964).

22. K.C.Khulbe, A.Kumar and R.S.Mann, React. Kinet. Catal. Lett., 17(3-4), 317 (1982).

23. M.Che, C.Naccacha and B.Imelik, J. Catal., 24, 328 (1972).

24. K.Meguro and K.Esumi, J. Colloid. Interface Sci., 59, 93 (1977).

25. M.A.Enriquiz and J.P.Fraissard, J. Catal., 74, 77 (1982).

26. A.Grigoryan and A.M.Aikazyan, React. Kinet. Catal. Lett., 20(1-2), 127 (1982).

27. K.Meguro and K.Esumi, J. Adhesion Sci. Technol., 4(5), 393 (1990).

28. R.H.Boyd and W.D.Philips, J. Chem. Phys., 43, 2927 (1965).

29. D.S.Acker, R.J.Harder, W.R.Hertler, L.Mahler, L.R.Melby, R.E.Benson and W.E.Mochel, J. Am. Chem. Soc., 82, 6408 (1960).

30. R.C.Kepler, P.E.Bierstedt and R.E.Merrifild, Phys. Rev. Lett., 5, 503 (1960).

31. D.B.Cheanut, H.Fosker and W.D.Philips, J. Chem. Phys., 34, 684 (1961).

32. L.R.Melby, R.J.Harder, W.R.Hertler, W.Mahler, R.E.Benson and W.E.Mochel, J. Am. Chem. Soc., 84, 3374 (1962).

33. K.Esumi and K.Meguro, Bull. Chem. Soc. Jap., 55, 1647 (1982).

34. S.R.Morrison, Surface Sci., 50, 329 (1975).

35. D.Cordishi and V.Indovina, J. Chem. Soc. Faraday Trans., 72(10), 2341 (1976).

36. T.Ishikawa, H.Saito, A.Yosukawa and K.Kandori, J. Chem. Soc. Faraday Trans., 89(20), 3621 (1993).

37. K.Esumi and K.Meguro, J. Colloid. Interface Sci., 61, 191 (1977).

38. J.A.Hollahen and A.T.Bell, "Techniques and Application of Plasma Chemistry" (Wiley, New York, 1974).

39. M.Sugura, K.Esumi, K.Meguro and H.Honda, Bull. Chem. Soc. Jap., 58, 2638 (1985).

40. K.Esumi, M.Suguro, T.Mori, K.Meguro and H.Honda, Colloids Surf., 19, 331 (1986).

41. K.Esumi, K.Nishina, S.Sakureda, K.Meguro and H.Honda, Carbon, 25, 821 (1987).

42. K.Esumi, N.Nishiuchi and K.Meguro, J. Surf. Sci. Tech., 4, 207 (1988).

43. R.S.Drago, I.B.Parr and C.S.Chamberlain, J. Am. Chem. Soc., 99, 3203 (1977).

44. K.Esumi, K.Miyata, F.Waki and K.Meguro, Bull. Chem. Soc. Jap., 59, 3363 (1986).

45. K.Esumi, K.Miyata and K.Meguro, Bull. Chem. Soc. Jap., 58, 3524 (1985).

46. S.S.Skoortis, J.J.Regan and J.N.Onuchic, J. Phys. Chem., 98, 3379 (1994).

47. H.A.Benesi and B.H.C.Winquist, Adv. Catal., 27, 97 (1978).

48. K.Tanabe, Solid Acids and Bases (Academic Press, New York, 1970).

49. A.Aurous and A.Gervassin, J. Phys. Chem., 94, 6371 (1990).

50. A.N.Webb, Ind. Eng. Chem., 267 (1957).

51. M.S.Goldstein in "Experimental Methods in Catalytic Research", (R.B.Anderson, Ed.), p.361 (Academic Press, New York, 1969).

52. F.Forni, Catal. Rev., 8, 69 (1973).

53. C.Walling, J. Am. Chem. Soc., 72, 1154 (1950).

54. I.P.Hammett and A.J.Deyrup, J. Am. Chem. Soc., 54, 2721 (1932).

55. I.P.Hammett, "Physical Organic Chemistry", p.251 (Mc Graw Hill, New York, 1940).

56. H.Wail Malherbe and J.Weiss, J. Chem. Soc., p.2164 (1948).

57. H.A.Benesi, J. Am. Chem. Soc., 5490 (1956).

58. O.Johnson, J. Phys. Chem., 59, 827 (1955).

59. H.A.Benesi, J. Phys. Chem., 61, 979 (1957).

60. A.E.Hirschler and A.Schneider, J. Chem. Eng. Data., 6, 313 (1961).

61. K.Tanabe and Y.Watanabe, J. Res. Inst. Catal., 11, 65 (1963).

62. A.E.Hirschler, J. Catal., 2, 428 (1963).

63. H.P.Leftin and M.C.Hobson, Adv. Catal., 14, 115 (1968).

64. S.Malinowski and S.Sczepanska, J. Catal., 2, 310 (1963).

65. C.Naccache, Y.Kodratoff, R.C.Pink and B.Imelik, J. Chem. Phys., 63, 341 (1966).

66. V.R.Choudhary and V.H.Rane, J. Catal., 130, 411 (1991).

67. H.V.Drushel and A.L.Sommers, Anal. Chem., 38(12), 1723 (1966).

68. E.P.Parry, J. Catal., 2, 371 (1963).

69. M.R.Basila and T.R.Kantner, J. Phys. Chem., 68, 3197 (1955).

70. K.Ashim and E.Ghosh, J. Chem. Soc. Faraday Trans. I, 79, 147 (1983).

71. J.Take, T.Tsuruya, T.Sato and Y.Yoneda, Bull. Chem. Soc. Jap., 45, 3409 (1972).

72. O.V.Krylov and E.A.Fokina, Probl. Kinet. Katal. Akad. Nank. USSR, 8, 218 (1955).

73. T.Yamanaka and K.Tanabe, J. Phys. Chem., 79, 2409 (1975).

74. J.Take, N.Kukuchi and Y.Yoneda, J. Catal., 21, 101 (1977).

75. T.Itzuka, K.Ogasawara and K.Tanabe, Bull. Chem. Soc. Jap., 56, 2927 (1983).

76. P.A.Burke and E.I.Ko, J. Catal., 129, 38 (1991).

77. H.P.Laftin and W.K.Hall, Actes. Congress, Intern. Cat., (1), 58 (1962).

78. J.A.Schwarz, J. Vac. Sci. Technol., 12, 32 (1975).

79. I.D.Gay and S.Liang, J. Catal., 44, 306 (1976).

80. H.Yoshisumi, Y.Shimada and T.Shirosaki, Chem. Lett., p.107 (1973).

81. J.S.Magee and J.J.Blazek, ACS Monogr., No.171, p.615 (1976).

82. M.Kermerec, M.Briend Faure and D.Deleforse, J. Chem. Soc. Faraday Trans. 1, 79, 2180 (1974).

83. K.Shibata and T.Kiyoura, J. Res. Inst. Catal., Hokkaida University, 19, 35 (1971).

84. S.B. Walvekar and A.B.Halgeri, Indian J. Chem., 11, 662 (1973).

85. K.Tanabe, M.Itoh and M.Sato, J. Chem. Soc. Chem. Commun., 676 (1973).

86. M.Itoh, H.Hattori and K.Tanabe, J. Catal., 35, 225 (1974).

87. G.Connell and J.A.Domesic, J. Catal., 101, 103 (1986).

88. N.C.Martinez and J.A.Domesic, J. Catal., 127, 106 (1991).

89. G.Connell, Ph.D. Thesis, University of Wisconsin, Madison (1985).

90. G.Connell and J.A.Domesic, J. Catal., 105, 285 (1987).

91. K.Tanabe, in "Catalytic Science and Technology", Vol.2, p.231 (Springer Verlag, New York, 1981).

92. J.P.Shen, J.Ma, T.Sun and D.Jiang, J. Chem. Soc. Faraday Trans., 90, 1351 (1994).

93. H.S.Taylor and H.Diamond, J. Am. Chem. Soc., 57, 1251 (1935).

94. K.M.Minachev, Proc. Int. Congr. Catal., 5th, 219 (1973).

95. B.S.Hopkins and W.A.Taebel, Trans. Electrochem. Soc., 71, 397 (1934).

96. S.Sugunan and K.B.Sherly, Indian J. Chem., 33A, 937 (1994).

97. S.Sugunan and K.B.Sherly, React. Kinet. Catal. Lett., 51, 533 (1993).

98. G.Brieger and T.J.Nectric, Chem. Rev., 74, 567 (1974).

99. A.L.Wilds, Org. React., 2, 178 (1944).

100. I.H.Klemm and D.R.Taylor, J. Org. Chem., 35, 3216 (1970).

101. C.L.Kibby and L.Keithhall, J. Catal., 31, 65 (1973).

102. M.Shibagaki, K.Takahashi and H.Matsushita, Bull. Chem. Soc. Jap., 61, 3283 (1988).

103. K.Takahashi, M.Shibagaki, H.Kuno and H.Matsushita, Bull. Chem. Soc. Jap., 67, 1107 (1994).

104. Oppenauer, React. Trav. Chim., 56, 137 (1937).

105. Woodward, Wendler and Brutechy, J. Am. Chem. Soc., 67, 1423 (1945).

106. Lauehensuer and Schinz, Helv. Chim. Acta., 32, 1265 (1949).

107. Yamashita and Honjo, J. Chem. Soc. Jap., 63, 133 (1942).

108. C.Djerassi, Org. React., 6, 207 (1951).

109. Marker, Wittla, Jones and Crooke, J. Am. Chem. Soc., 64, 1283 (1942).

110. H.Niiyama and E.Echigoya, Bull. Chem. Soc. Jap., 45, 938 (1972).

111. R.Schwartz and A.Juhasz, Rev. Roum. Chim., 31, 131 (1986).

112. H.Kuno, K.Takahashi, M.Shibagaki and H.Matsushita, Bull. Chem. Soc. Jap., 64, 312 (1991).

113. H.Kuno, K.Takahashi, M.Shibagaki and H.Matsushita, Bull. Chem. Soc. Jap., 63, 1943 (1990).

114. M.P.Rosynek and D.T.Magnuson, J. Catal., 46, 402 (1977).

115. M.Ai and S.Suzuki, Shakabai, 15, 159 (1973).

116. M.Ai and S.Suzuki, Bull. Chem. Soc. Jap., 47, 3074 (1974).

117. M.Ai and S.Suzuki, Bull. Jap. Petrol. Inst., 16, 118 (1974).

118. K.Tanabe and K.Saito, J. Catal., 35, 247 (1974).

119. M.Mohri, K.Tanabe and H.Hattori, J. Catal., 32, 144 (1974).

120. O.V.Krylov, Z.A.Markova and E.A.Fokina, Kinet. Katal., 6, 124 (1965).

121. G.W.Keulks, J. Catal., 19, 232 (1971).

122. R.D.Wragg, P.G.Ashmore and J.A.Hockey, J. Catal., 22, 49 (1971).

123. Y.Fukuda, H.Hattori and K.Tanabe, Bull. Chem. Soc. Jap., 51, 3150 (1973).

124. M.W.Tamele, Discussions Faraday Soc., 8, 270 (1950).

125. H.Pines and J.Ravoire, J. Phys. Chem., 65, 1857 (1961).

126. J.E.Tung and E.Moinich, J. Catal., 3, 229 (1964).

127. J.B.Peri, J.Phys. Chem., 69, 231 (1965).

128. K.M.Minachev, Y.S.Khodakov and V.S.Nakhshunov, J. Catal., 49, 209 (1977).

129. M.P.Rosynek, J.S.Fox and J.L.Jensen, J. Catal., 71, 64 (1981).

130. M.P.Rosynek and J.S.Fox, J. Catal., 49, 285 (1977).

131. D.H.Devis in "Adhesion and Catalysis on Oxide Surfaces", (M.Che and G.Bond, Eds.), Stud. Surf. Sci. Catal., Vol.21, p.309 (Elsevier, Amsterdam, 1985).

132. C.P.Bezouhanova and M.A.Alzihen, Catal. Lett., 11, 245 (1991).

133. Y.Nakashima, Y.Sakato, S.H.Imamura and S.Tsuchiya, Bull. Chem. Soc. Jap., 63 , 3373 (1990).

134. M.I.Zaki and N.Sheppard, J. Catal., 80, 114 (1983).

135. G.Zhang, H.Hattori and K.Tanabe, Bull. Chem. Soc. Jap., 62, 2070 (1989).

136. S.R.Dyne, J.B.Butt and G.L.Haller, J. Catal., 25, 378 (1972).

137. L.Nondek and M.Kraus, J. Catal., 40, 40 (1975).

138. M.E.Winfield, Catalysis, 1, 93 (1960).

139. A.J.Lundeen and R.V.Hoozer, J. Org. Chem., 32, 3386 (1967).

140. P.N.Hill, F.E.Bailey and J.T.Fitzpatric, Ind. Eng. Chem., 50, 5 (1958).

141. O.V.Krylov, M.J.Kushnerev, Z.A.Kurkova and E.A.Fokina, Proc. Intern. Catal. Amsterdam (1964).

142. Japan Pat. Showa, 18-1048 (1943).

143. R.N.Goyce, J. Polymer Sci., 3, 169 (1948).

144. K.Saito and K.Tanabe, J. Polymer Sci., 11, 206 (1969).

145. M.Shibagaki, K.Takahashi, H.Kuno and H.Matsushita, Bull. Chem. Soc. Jap., 63, 258 (1990).

146. K.R.Sabu, K.V.C.Rao and C.G.R.Nair, Bull. Chem. Soc. Jap., 64, 1926 (1991).

147. K.Mizuno, M.Ikeda, T.Imokawa, J.Take and Y.Yoneda, Bull. Chem. Soc. Jap., 49, 1788 (1976).

148. K.Tanabe, Solid Acids and Bases, (Kodansha, Tokyo, Academic Press, New York and London, 1971).

149. R.Rodenas, T.Yamaguchi, H.Hattori and K.Tanabe, J. Catal., 69, 434 (1981).

150. K.Tanabe, C.Ishiya, I.Matsuzaki, I.Ichikawa and H.Hattori, Bull. Chem. Soc. Jap., 45, 47 (1972).

151. K.Tanabe, T.Suniyoshi and H.Hattori, Chem. Lett., 723 (1972).

152. K.Shibata, T.Koyoura, J.Kitagawa and K.Tanabe, Bull. Chem. Soc. Jap., 46, 2985 (1973).

153. M.Ai and T.Ikawa, J. Catal., 40, 203 (1974).

154. M.Ai, Bull. Chem. Soc. Jap., 50, 355 (1977).

155. J.H.Peacock, M.J.Sharp and J.A.Hockey, J. Catal., 15, 379 (1969).

156. M.Ai and T.Ikawa, J. Catal., 40, 201 (1974).

CHAPTER III
EXPERIMENTAL

EXPERIMENTAL

3.1 MATERIALS

3.1.1 Single Oxides

The rare earth oxides (Sm_2O_3 and CeO_2) were prepared by hydroxide method [1] from nitrate salt (purity 99.9%) obtained from Indian Rare Earths Ltd., Udyogamandal, Kerala.

Hydroxide method

Nitrate solution of the sample (250 ml) containing 0.5 g of rare earth oxide was heated to boiling and 1:1 ammonium hydroxide solution was added dropwise with stirring until the precipitation was complete. Concentrated ammonium hydroxide solution (an amount equal to one tenth of volume of solution) was then added with stirring. It was then allowed to digest on a steam bath until precipitate was flocculated and settled. The precipitate was filtered on a Whatmann No.41 filter paper and washed with small portions of an aqueous solution containing 1 g of ammonium nitrate and 10 ml of concentrated ammonium hydroxide in 100 ml, until the precipitate was free from NO_3^{2-} The

precipitate was kept in an air oven at 100°C for overnight and was ignited in a china dish at 300-400°C for 2 hrs.

3.1.2 Mixed Oxides

Mixed oxides of rare earths and aluminium were prepared by co-precipitation method [2] from their nitrate solution.

10% Mixed oxide

Aqueous ammonia (5%) solution was added to an aqueous solution (250 ml) containing rare earth nitrate (2.50 g) and aluminium nitrate (66.15 g, SQ grade obtained from Qualigens Fine Chemicals), until the precipitation was complete. The precipitate was washed with distilled water, dried by keeping overnight at 110°C and then calcined at 500°C for 3 hrs.

Using the same method mixed oxides of samarium (5, 10, 15, 20, 40 and 75% by wt. of rare earth oxide) with aluminium and mixed oxides of cerium (10, 20, 40, 60 and 80% by wt. of rare earth oxide) with aluminium were prepared from the required amount of aluminium nitrate and rare earth nitrate.

3.1.3 Electron acceptors

Electron acceptors employed for the study are 7,7,8,8-tetracyanoquinodimethane (TCNQ), 2,3,5,6-tetrachloro-p-benzoquinone (Chloranil), p-dinitrobenzene (PDNB) and m-dinitrobenzene (MDNB).

TCNQ was obtained from Merck Schuchandt and was purified by repeated recrystallisation from acetonitrile [3].

Chloranil was obtained from Sisco Research Laboratories Pvt. Ltd., and was purified by recrystallisation from benzene [4].

p-Dinitrobenzene was supplied by Koch-Light Laboratories Ltd. and was purified by recrystallisation from chloroform [5].

m-Dinitrobenzene was obtained from Loba-Chemie Industrial Company and was purified by recrystallisation from CCl_4 [6].

3.1.4 Solvents

Acetonitrile

SQ grade acetonitrile obtained from Qualigens Fine Chemicals was first dried by passing through a column filled with silica gel (60-120 mesh) activated at 110°C for 2 hrs. It was then distilled with anhydrous phosphorus pentoxide and the fraction between 79-82°C was collected [7].

1,4-Dioxane

SQ grade 1,4-dioxane was obtained from Qualigens Fine Chemicals. It was dried by keeping over potassium hydroxide pellets for 2-3 days, filtered and refluxed with sodium metal for 6-7 hours till the surface of sodium metal got shining appearance. The refluxed solvent was then distilled and the fraction at 101°C was collected [8].

Ethyl acetate

SQ grade ethyl acetate was obtained from Qualigens Fine Chemicals. A mixture of 1 litre of ethyl acetate, 100 ml of acetic anhydride and 10 drops of concentrated sulphuric acid was heated under reflux for 4

hours and was then fractionated using an efficient column. The distillate was then shaken with 20-30 g of anhydrous potassium carbonate, filtered and redistilled. The fraction boiling at 77°C was collected [9].

3.1.5 Reagents for acidity/basicity measurements

Benzene

Benzene used for the acidity and basicity measurements was purified by the following procedure [10].

SQ grade benzene obtained from Qualigens Fine Chemicals was shaken repeatedly with about 15% of the volume of concentrated sulphuric acid in a stoppered separating funnel until the acid layer is colourless on standing. After shaking, the mixture is allowed to settle and lower layer was drawn off. It was then washed twice with water to remove most of the acid, then with 10% sodium carbonate solution, and finally with water. It was dried with anhydrous $CaCl_2$. It was filtered and distilled and the distillate was kept over sodium wire for 1 day. It was then distilled and fraction boiling at 80°C was collected.

Hammett Indicators

Hammett indicators used for the study are the following:

Methyl red (E.Merck India Pvt. Ltd.)

Dimethyl Yellow (Loba Chemie Industrial Company)

Crystal violet (Romali)

Neutral red (Romali)

Bromothymol blue (Qualigens Fine Chemicals)

Thymol blue (Qualigens Fine Chemicals)

4-Nitroaniline (Indian Drug and Pharmaceuticals Ltd.)

Trichloro acetic acid (SQ grade) obtained from Qualigens Fine Chemicals and n-butylamine (S.d-Fine Chemicals Pvt. Ltd.) were used without further purification.

3.1.6 Reagents used for activity measurements

Cyclohexanone

Commercial cyclohexanone obtained from BDH was purified through the bisulphite method [11]. A saturated solution of sodium bisulphite was prepared from 40 g of finely powdered sodium bisulphite. The volume of the resulting solution was measured and it was treated with 70% of its volume of rectified spirit. Sufficient water was added to dissolve the precipitate which is separated. 20 g of cyclohexanone was introduced into the aqueous alcoholic bisulphite solution with stirring and the mixture was

allowed to stand for 30 minutes. The crystalline bisulphite compound was filtered off at the pump and washed it with a little rectified spirit.

The bisulphite compound was transferred to a separating funnel and decomposed with 80 ml of 10% NaOH solution. The liberated cyclohexanone was removed. The aqueous solution layer was saturated with salt and extracted it with 30 ml of ether. The ether extract was combined with the ketone layer and dried with 5 g of anhydrous magnesium sulphate. The dried etherial solution was filtered into a 50 ml distilling flask, attached with a condenser and distilled off the ether using a water bath. The resultant cyclohexanone was distilled and the fraction at 153°C was collected.

Acetophenone

Extra pure quality acetophenone obtained from Sisco Research Laboratories Pvt. Ltd. was used as such.

Benzophenone

Benzophenone was supplied by Sisco Research Laboratories Pvt. Ltd. and was purified by recrystallisation from ethanol [12].

2-Propanol

LR grade reagent obtained from Merck was further purified by adding about 200 g of quick lime to 1 litre of 2-propanol. It was kept for 3-4 days, refluxed for 4 hours and distilled. The fraction distilling at 82°C was collected [13].

Xylene

Extra pure quality xylene obtained from Merck was used as such.

Cyclohexanol

Cyclohexanol obtained from Merck was refluxed with freshly ignited CaO and then fractionally distilled. The fraction distilling at 161.1°C was collected [14].

Toluene

SQ grade toluene obtained from Qualigens Fine Chemicals was shaken twice with cold concentrated H_2SO_4 (100 ml of acid for 1 litre of toluene), then with water, aq. 5% $NaHCO_3$ and again with water. Then it was dried

successively with $CaSO_4$ and P_2O_5, distilled and fraction distilling at 110°C was collected [15].

n-Decane

LR grade reagent obtained from S.d-Fine Chemicals Pvt. Ltd. was further purified by shaking with conc. H_2SO_4. It was washed with water and aq. $NaHCO_3$. Finally it was washed with more water. Then it was dried with $MgSO_4$, refluxed with sodium and distilled. The fraction distilling at 174°C was collected [16].

3.2 METHODS

3.2.1 Adsorption studies [17]

The oxides were activated at a particular temperature for 2 hrs prior to each experiment. The oxide (0.5 g) was placed in a 25 ml test tube and outgassed at 10^{-5} Torr for 1 hour. Into the test tube which was fitted with a mercury sealed stirrer, 20 ml of a solution of an electron acceptor in organic solvent was then poured in. After the solution had subsequently been stirred for 3 hrs at 25°C in a thermostated bath, the oxide was collected by centrifuging the solution and dried at room temperature in vacuuo. The reflectance spectra of the dried samples were recorded on a Hitachi 200-20 UV-Visible spectrophotometer with a 200-0531 reflectance attachment.

The ESR spectra were measured at room temperature using Varian E-112 X/Q band ESR spectrophotometer. Radical concentrations were calculated by comparison of area obtained by double integration of the first derivative curve for the sample and standard solution of 1,1-diphenyl-2-picryl-hydrazyl in benzene. The amount of electron acceptor adsorbed was determined from the difference in concentration before and after adsorption. The absorbance of electron acceptors was measured by means of a UV-Vis spectrophotometer (Hitachi 200-20) at the λ_{max} of the electron acceptor in the solvent. The λ_{max} of chloranil was 288 nm in acetonitrile, 287 nm in ethyl acetate and 286 nm in 1,4-dioxane, while the λ_{max} for TCNQ was 393.5 nm in acetonitrile, 393 nm in ethyl acetate and 403 nm in 1,4-dioxane. The λ_{max} of PDNB and MDNB in acetonitrile were 262 nm and 237 nm and in 1,4-dioxane 261 nm and 218 nm respectively.

Infra red spectra of oxides were taken on a Perkin Elmer PE-983 infra red spectrophotometer.

The specific surface area of the oxides were determined using Carlo-Erba Strumentazione Sorptomatic series 1800. The values in m^2g^{-1} are given in Tables 1 and 2. Data print out from the instrument are also attached (pages 94-109).

Table 1 Surface area of Sm_2O_3 and CeO_2 activated at different temperatures

Activation temperature (°C)	Surface area (m^2g^{-1})	
	Sm_2O_3	CeO_2
300	65.84	66.42
500	47.97	200.35
800	30.20	210.17

Table 2: Surface area of Sm_2O_3/Al_2O_3 and CeO_2/Al_2O_3 for various compositions (activation temperature 500°C).

Composition % by weight of Sm_2O_3	Surface area M^2g^{-1} Sm_2O_3/Al_2O_3	Composition % by weight of CeO_2	Surface area m^2g^{-1} CeO_2/Al_2O_3
0	193.91	0	193.91
5	195.64	10	217.05
10	219.68	20	216.95
15	193.70	40	160.14
20	186.30	60	143.70
40	130.00	80	125.24
75	77.74	100	66.42
100	47.97		

Carlo Erba Strumentazione — Microstructure Lab.
MI. Le. S. TO. NE. 1 0 0

Calculation parameters of Sorptomatic

Comment	OUTGASSED AT 120 C	Sm_2O_3 activated at 300°C.	
Date (mm/dd/yy)	05-22-1992		
Monolayer thickness (a):	4.3	Total introduction :	9
Satur/Limit pressure (torr):	760	Reduced introduction :	9
Mol.mass. gas ads. (g/mol):	28	Reduction factor :	.5
Gas ads. density (g/cm3):	.808	Constant bur.(cm3/torr):	.1139
Burette temperature (c):	-195.82	Sample weight (g):	1.01755
Operating pressure (torr):	800	Sample Density (g/mm3):	.9255

Initial point (P/P0) for linear regression of B.E.T. region 0

Final point (P/P0) for linear regression of B.E.T. region .3

Correlation factor = .9998779

Monolayer Volume (CM3/G) = 15.06948

Specific surface area (M2/G) = 65.84814

Corrected Burette Constant = .1087965

Adsorption values

P.ADS (Torr)	P/P0 ADS	VI (CM3)	V.ADS(CM3/G)	T(A)	P/(P0-P)Va/g
0.0	0.0000	7.86	7.73	3.3	0.000000000
10.0	0.0132	15.73	14.38	4.5	0.000926899
60.7	0.0799	23.59	16.69	5.4	0.005200445
119.4	0.1571	31.45	18.14	6.0	0.010273865
178.3	0.2346	39.31	19.57	6.5	0.015661405
236.1	0.3107	47.18	21.12	7.0	0.021339558
293.2	0.3858	55.04	22.74	7.5	0.027620768
352.6	0.4639	62.90	24.12	8.0	
406.0	0.5342	70.76	26.13	8.6	

****

CATALYSIS DIVISION
DEPARTMENT OF CHEMISTRY
I.I.T.,MADRAS 600 036

BET SURFACE AREA ANALYSIS

SAMPLE WEIGHT : 0.42315 g
BULK DENSITY : 0.7026 g/cc
OUT GAS TEMPERATURE: 120 C,20microns

Sm_2O_3 activated at 500°C.

DATA POINTS

P/Po	P/(Po-P)*N*28
0.13803	24.1388
0.16136	27.0046
0.19408	30.7046
0.22585	33.9635
0.24469	35.9225
0.26463	37.8062
0.28490	39.7966

SPECIFIC SURFACE AREA = 47 97 sq.m/g

****

****

CATALYSIS DIVISION
DEPARTMENT OF CHEMISTRY
I I T MADRAS 600 036

BET SURFACE AREA ANALYSIS

SAMPLE WEIGHT 1.1736 g
BULK DENSITY 0.9772 g/cc
OUT GAS TEMPERATURE: 120 C 20micron

5% Sm_2O_3/Al_2O_3 activated at 500°C.

DATA POINTS

P/Po	P/(Po-P)*N*28
0.00143	0.04583
0.02646	0.44133
0.13163	1.83086
0.19762	2.65725
0.22809	3.04295
0.24428	3.25736
0.25667	3.40631
0.27517	3.66170

SPECIFIC SURFACE AREA = 195.64 sq.m/g

****

****

CATALYSIS DIVISION
DEPARTMENT OF CHEMISTRY
I I T ,MADRAS 600 036

BET SURFACE AREA ANALYSIS

SAMPLE WEIGHT 0.20285 g
BULK DENSITY 0.9219 g/cc
OUT GAS TEMPERATURE: 120 C 20micron

10% Sm_2O_3/Al_2O_3 activated at 500°C.

DATA POINTS

P/Po	P/(Po-P)*N*28
0.09068	7.22111
0.15925	11.9301
0.19782	14.3188
0.22462	15.9029
0.24259	16.9384
0.26054	17.9709
0.27319	18.5517

SPECIFIC SURFACE AREA = 219.68 sq.m/g

****

CATALYSIS DIVISION
DEPARTMENT OF CHEMISTRY
I I T ,MADRAS 600 036

BET SURFACE AREA ANALYSIS

SAMPLE WEIGHT 0.2759 g
BULK DENSITY 0.9465 g/cc
OUT GAS TEMPERATURE: 120 C 20micron

15% Sm_2O_3/Al_2O_3 activated at 500°C.

DATA POINTS

P/Po	P/(Po-P)*N*28
0.06551	4.32086
0.14979	8.98161
0.19782	11.5091
0.22973	13.1471
0.24830	13.9925
0.25544	14.3247
0.26320	14.7248
0.27020	15.0094

SPECIFIC SURFACE AREA = 193.7 sq m/g

****

****

CATALYSIS DIVISION
DEPARTMENT OF CHEMISTRY
I I T ,MADRAS 600 036

BET SURFACE AREA ANALYSIS

SAMPLE WEIGHT 0.30315 g
BULK DENSITY 0.89175 g/cc
OUT GAS TEMPERATURE: 120 C, 20micron

20% Sm_2O_3/Al_2O_3 activated at 500°C.

DATA POINTS

P/Po	P/(Po-P)*N*28
0.06605	4.50156
0.13911	8.52717
0.18312	10.7324
0.20701	12.4971
0.22490	13.2494
0.23823	13.8719
0.25367	14.6417
0.27100	15.3734

SPECIFIC SURFACE AREA = 186.3 sq.m/g

Carlo Erba Strumentazione Microstructure Lab.
MI. Le. S. TO. NE. 1 0 0

Calculation parameters of Sorptomatic

Comment OUTGASSED AT 120 C 40% Sm_2O_3/Al_2O_3 activated at 500°C

Date (mm/dd/yy) 01-21-1993

Monolayer thickness (a):	4.3	Total introduction :	20
Satur/Limit pressure (torr):	760	Reduced introduction :	20
Mol.mass. gas ads. (g/mol):	28	Reduction factor :	.25
Gas ads. density (g/cm3):	.808	Constant bur.(cm3/torr):	.112
Burette temperature (c):	-195.82	Sample weight (g):	1.486
Operating pressure (torr):	800	Sample Density (g/mm3):	1.169

Initial point (P/P0) for linear regression of B.E.T. region .05

Final point (P/P0) for linear regression of B.E.T. region .33

Correlation factor = .9997464

Monolayer Volume (CM3/G) = 29.88684

Specific surface area (M2/G) = 130.5946

Corrected Burette Constant = .1060994

Adsorption values

P.ADS (Torr)	P/P0 ADS	VI (CM3)	V.ADS(CM3/G)	T(A)	P/(P0-P)Va/g
0.0	0.0000	3.97	2.67	3.3	0.000000000
0.0	0.0000	7.94	5.34	3.3	0.000000000
0.3	0.0004	11.91	7.99	3.7	0.000049422
0.8	0.0011	15.87	10.63	3.9	0.000099175
1.3	0.0017	19.84	13.26	4.0	0.000129221
2.1	0.0028	23.81	15.87	4.1	0.000174558
4.7	0.0062	27.78	18.36	4.3	0.000338960
6.8	0.0089	31.75	20.88	4.4	0.000432408
14.7	0.0193	35.72	22.99	4.7	0.000858098
25.7	0.0338	39.68	24.87	4.9	0.001407269
38.2	0.0503	43.65	26.65	5.1	0.001985980
54.2	0.0713	47.62	28.18	5.3	0.002725394
68.9	0.0907	51.59	29.80	5.5	0.003345784
88.5	0.1164	55.56	31.07	5.7	0.004242041
105.6	0.1389	59.53	32.52	5.9	0.004962418
124.4	0.1637	63.49	33.85	6.0	0.005782597
141.2	0.1858	67.46	35.32	6.2	0.006460919
160.1	0.2107	71.43	36.64	6.3	0.007284062
176.8	0.2326	75.40	38.12	6.5	0.007953324
201.0	0.2645	79.37	39.06	6.7	0.009205732

Carlo Erba Strumentazione Microstructure Lab.
MI. Le. S. TO. NE. 1 0 0

Calculation parameters of Sorptomatic

Comment OUTGASSED AT 120 C 75% Sm_2O_3/Al_2O_3 activated at 500°C.

Date (mm/dd/yy) 04-16-1993

Monolayer thickness (a):	4.3	Total introduction	16
Satur/Limit pressure (torr):	760	Reduced introduction	16
Mol.mass. gas ads, (g/mol):	28	Reduction factor	.25
Gas ads. density (g/cm3):	.808	Constant bur.(cm3/torr):	.1644
Burette temperature (c):	-195.82	Sample weight (g):	1.415
Operating pressure (torr):	800	Sample Density (g/mm3):	1.3455

Initial point (P/P0) for linear regression of B.E.T. region .05

Final point (P/P0) for linear regression of B.E.T. region .33

Correlation factor = .9999961

Monolayer Volume (CM3/G) = 17.83759

Specific surface area (M2/G) = 77.94376

Corrected Burette Constant = .1595184

Adsorption values

P.ADS (Torr)	P/P0 ADS	VI (CM3)	V.ADS(CM3/G)	T(A)	P/(P0-P)Va/g
0.2	0.0003	3.97	2.78	3.6	0.000094618
0.6	0.0008	7.94	5.54	3.8	0.000142580
1.2	0.0016	11.91	8.28	3.9	0.000191034
2.7	0.0036	15.87	10.91	4.1	0.000326679
7.6	0.0100	19.84	13.17	4.4	0.000767210
17.5	0.0230	23.81	14.85	4.7	0.001586673
31.4	0.0413	27.78	16.09	5.0	0.002678140
47.4	0.0624	31.75	17.09	5.2	0.003891545
64.6	0.0850	35.72	17.96	5.4	0.005172911
82.3	0.1083	39.68	18.77	5.6	0.006470823
100.5	0.1322	43.65	19.52	5.8	0.007806722
118.6	0.1561	47.62	20.28	6.0	0.009115877
136.8	0.1800	51.59	21.04	6.1	0.010434602
155.3	0.2043	55.56	21.76	6.3	0.011804682
173.4	0.2282	59.53	22.52	6.5	0.013126212
191.4	0.2518	63.49	23.30	6.6	0.014449977

Carlo Erba Strumentazione — Microstructure Lab.

MI. Lc. S. TO. NE. 1 0 0

Calculation parameters of Sorptomatic

Comment OUTGASSED AT 120 C — CeO_2 activated at 300°C.

Date (mm/dd/yy) 07-27-1993

Monolayer thickness (a):	4.3	Total introduction	10
Satur/Limit pressure (torr):	760	Reduced introduction	10
Mol.mass. gas ads. (g/mol):	28	Reduction factor	.25
Gas ads. density (g/cm3):	.808	Constant bur.(cm3/torr):	.112825
Burette temperature (c):	-195.82	Sample weight (g):	1.012
Operating pressure (torr):	800	Sample Density (g/mm3):	1.69

Initial point (P/P0) for linear regression of B.E.T. region .05

Final point (P/P0) for linear regression of B.E.T. region .33

Correlation factor 9998435

Monolayer Volume (CM3/G) = 15.20129

Specific surface area (M2/G) = 66.42411

C value of B. E. T equation 146.1541

Pore specific volume (CM3/G)

Total volume introduced (CM3) 39.68416
Corrected Burette Constant = 1100454

Adsorption values

P.ADS (Torr)	P/P0 ADS	VT (CM3)	V ADS(CM3/G)	T(A)	P/(P0-P)Va/g
0.5	0.0007	3.97	3.87	3.8	0.000170243
0.5	0.0007	7 94	7 79	3.8	0.000084527
4.5	0.0059	11 91	11.27	4 3	0.000528289
23.4	0 0308	15 87	13 14	4.9	0.002417456
44.7	0 0588	19.84	14 75	5 2	0.004237816
72.2	0 0950	23 81	15 68	5 5	0.006695907
99 0	0 1303	27 78	16 68	5 8	0.008976937
126 1	0 1659	31 75	17 66	6 0	0.011265113
155.0	0 2019	35 72	18 44	6 3	0.013895533
180.2	0 2371	39.68	19.62	6.5	0.01584'

Carlo Erba Strumentazione Microstructure Lab.
MI. Le. S. TO. NE. 1 0 0

Calculation parameters of Sorptomatic

Comment 120 C OUTGASING CeO_2 activated at 500°C.

Date (mm/dd/yy) 05-27-1993

Monolayer thickness (a):	4.3	Total introduction	8
Satur/Limit pressure (torr):	760	Reduced introduction	0
Mol.mass. gas ads. (g/mol):	28	Reduction factor :	1
Gas ads. density (g/cm3):	.808	Constant bur.(cm3/torr):	.116049
Burette temperature (c):	-195.82	Sample weight (g):	1.099
Operating pressure (torr)	800	Sample Density (g/mm3):	1.57

Initial point (P/P0) for linear regression of B.E.T. region .05

Final point (P/P0) for linear regression of B.E.T. region .33

Correlation factor = .9997123

Monolayer Volume (CM3/G) = 45.85192

Specific surface area (M2/G) = 200.3562

C value of B. E. T equation = 47.34838

Pore specific volume (CM3/G) =

Total volume introduced (CM3) = 126.7

Corrected Burette Constant = .1127997

Adsorption values

P.ADS (Torr)	P/P0 ADS	VI (CM3)	V.ADS(CM3/G)	T(A)	P/(P0-P)Va/g
0.1	0.0001	15.84	14.40	3.5	0.000009138
3.4	0.0045	31.68	28.47	4.2	0.000157828
48.0	0.0632	47.51	38.31	5.2	0.001759933
108.5	0.1428	63.35	46.51	5.9	0.003580936
168.2	0.2213	79.19	54.79	6.4	0.005187366
229.7	0.3022	95.03	62.89	6.9	0.006887556
289.6	0.3811	110.86	71.15	7.4	0.008652586
348.7	0.4588	126.70	79.50	8.0	

Carlo Erba Strumentazione Microstructure Lab.

MI. Le. S. TO. NE. 1 0 0

Calculation parameters of Sorptomatic

CeO_2 activated at 800°C.

Date (mm/dd/yy) 05-27-1993

Monolayer thickness	(a)	4.3	Total introduction	: 9
Satur/Limit pressure	(torr):	760	Reduced introduction	: 0
Mol.mass. gas ads.	(g/mol)	28	Reduction factor	: 1
Gas ads. density	(g/cm3):	.808	Constant bur.(cm3/torr):	.159031
Burette temperature	(c)	-195.82	Sample weight (g):	1.009
Operating pressure	(torr):	800	Sample Density (g/mm3):	1.44

Initial point (P/P0) for linear regression of B.E.T. region .05

Final point (P/P0) for linear regression of B.E.T. region .33

Correlation factor = .9983606

Monolayer Volume (CM3/G) = 48.09901

Specific surface area (M2/G) = 210.1752

C value of B. E. T equation = 15.53291

Pore specific volume (CM3/G) =

Total volume introduced (CM3) = 142.5375

Corrected Burette Constant = .1557785

Adsorption values

P.ADS (Torr)	P/P0 ADS	VI (CM3)	V.ADS(CM3/G)	T(A)	P/(P0-P)Va/g
0.3	0.0004	15.84	15.65	3.7	0.000025233
30.1	0.0396	31.68	26.75	5.0	0.001541894
77.6	0.1021	47.51	35.11	5.6	0.003239031
128.6	0.1692	63.35	42.93	6.1	0.004744279
176.1	0.2317	79.19	51.29	6.5	0.005879771
223.9	0.2946	95.03	59.61	6.9	0.007006339
270.1	0.3554	110.86	68.17	7.3	0.008087300
317.8	0.4182	126.70	76.51	7.7	
365.9	0.4814	142.54	84.78	8.2	

Carlo Erba Strumentazione Microstructure Lab.
MI. Le. S. TO. NE. 1 0 0

Calculation parameters of Sorptomatic

Comment : OUTGASSED AT 120 C 10% CeO_2/Al_2O_3 activated at 500°C.
Operator : A.NARAYANAN
Date (mm/dd/yy) 07-27-1993

Monolayer thickness (a):	4.3	Total introduction	17
Satur/Limit pressure (torr):	760	Reduced introduction	17
Mol.mass. gas ads. (g/mol):	28	Reduction factor :	.25
Gas ads. density (g/cm3):	.808	Constant bur.(cm3/torr):	.112155
Burette temperature (c):	-195.82	Sample weight (g):	.991
Operating pressure (torr):	800	Sample Density (g/mm3):	1.101

Initial point (P/P0) for linear regression of B.E.T. region .05

Final point (P/P0) for linear regression of B.E.T. region .33

Correlation factor = .9997838

Monolayer Volume (CM3/G) = 49.66534

Specific surface area (M2/G) = 217.0194

C value of B. E. T equation = 99.7342

Pore specific volume (CM3/G) =

Total volume introduced (CM3) 67.46306

Adsorption values

P.ADS (Torr)	P/P0 ADS	VI (CM3)	V.ADS(CM3/G)	T(A)	P/(P0-P)Va/g
0.3	0.0004	3.97	3.97	3.7	0.000099425
0.3	0.0004	7.94	7.98	3.7	0.000049509
0.5	0.0007	11.91	11.96	3.8	0.000055049
0.5	0.0007	15.87	15.96	3.8	0.000041240
0.5	0.0007	19.84	19.97	3.8	0.000032969
0.5	0.0007	23.81	23.97	3.8	0.000027462
2.1	0.0028	27.78	27.80	4.1	0.000099661
3.9	0.0051	31.75	31.61	4.2	0.000163174
6.8	0.0089	35.72	35.30	4.4	0.000255761
14.7	0.0193	39.68	38.44	4.7	0.000513063
25.0	0.0329	43.65	41.33	4.9	0.000823074
35.7	0.0470	47.62	44.16	5.1	0.001116052
48.9	0.0643	51.59	46.73	5.3	0.001471578
65.2	0.0858	55.56	48.96	5.4	0.001916730
82.0	0.1079	59.53	51.13	5.6	0.002365314
99.0	0.1303	63.49	53.28	5.8	0.002810820
114.3	0.1504	67.46	55.62	5.9	0.003182509

Carlo Erba Strumentazione Microstructure Lab.
MI. Le. S. TO. NE. 1 0 0

Calculation parameters of Sorptomatic

Comment OUTGASSED AT 120 C 20% CeO_2/Al_2O_3 activated at 500°C.

Date (mm/dd/yy) 09-20-1993

Monolayer thickness (a):	4.3	Total introduction :	16
Satur/Limit pressure (torr):	760	Reduced introduction :	16
Mol.mass. gas ads. (g/mol):	28	Reduction factor :	.25
Gas ads. density (g/cm3):	.808	Constant bur.(cm3/torr):	.1141479
Burette temperature (c):	-195.82	Sample weight (g):	.813
Operating pressure (torr):	800	Sample Density (g/mm3):	1.05

Initial point (P/PO) for linear regression of B.E.T. region .05

Final point (P/PO) for linear regression of B.E.T. region .33

Correlation factor = .9997095

Monolayer Volume (CM3/G) = 49.62867

Specific surface area (M2/G) = 216.859

C value of B. E. T equation = 69.97832

Pore specific volume (CM3/G) =

Total volume introduced (CM3) = 63.49464

Corrected Burette Constant = .1105538

Adsorption value

P.ADS (Torr)	P/PO ADS	VI (CM3)	V.ADS(CM3/G)	T(A)	P/(PO-P)Va/g
0.3	0.0004	3.97	4.84	3.7	0.000081583
0.3	0.0004	7.94	9.72	3.7	0.000040620
0.3	0.0004	11.91	14.60	3.7	0.000027042
0.5	0.0007	15.87	19.46	3.8	0.000033835
1.6	0.0021	19.84	24.19	4.0	0.000087220
4.2	0.0055	23.81	28.72	4.2	0.000193516
7.7	0.0101	27.78	33.12	4.4	0.000309024
16.4	0.0216	31.75	36.82	4.7	0.000599000
28.1	0.0370	35.72	40.11	4.9	0.000957206
42.2	0.0555	39.68	43.07	5.2	0.001364892
58.3	0.0767	43.65	45.77	5.4	0.001815430
73.7	0.0970	47.62	48.55	5.5	0.002211780
93.6	0.1232	51.59	50.73	5.7	0.002768830
110.6	0.1455	55.56	53.30	5.9	0.003195502
128.6	0.1692	59.53	55.73	6.1	0.003654622
145.3	0.1912	63.49	58.34	6.2	0.004051623

Carlo Erba Strumentazione Microstructure Lab.

MI. Le. S. TO. NE. 1 0 0

Calculation parameters of Sorptomatic

Comment	OUTGASSED AT 120 C		40% CeO_2/Al_2O_3 activated at 500°C.
Date (mm/dd/yy)	09-16-1993		
Monolayer thickness (a):	4.3	Total introduction	: 12
Satur/Limit pressure (torr):	760	Reduced introduction	: 12
Mol.mass. gas ads. (g/mol):	28	Reduction factor	: .25
Gas ads. density (g/cm3):	.808	Constant bur.(cm3/torr):	.114148
Burette temperature (c):	-195.82	Sample weight (g):	.435
Operating pressure (torr):	800	Sample Density (g/mm3):	1.4

Initial point (P/P0) for linear regression of B.E.T. region .05

Final point (P/P0) for linear regression of B.E.T. region .33

Correlation factor = .9996635

Monolayer Volume (CM3/G) = 36.69608

Specific surface area (M2/G) = 160.3485

C value of B. E. T equation = 104.0673

Pore specific volume (CM3/G) =

Total volume introduced (CM3) = 47.62099

Corrected Burette Constant = .1127057

Adsorption values

P.ADS (Torr)	P/P0 ADS	VI (CM3)	V.ADS(CM3/G)	T(A)	P/(P0-P)Va/g
0.5	0.0007	3.97	8.99	3.8	0.000073202
1.1	0.0014	7.94	17.96	3.9	0.000080703
7.2	0.0095	11.91	25.50	4.4	0.000375027
25.5	0.0336	15.87	29.88	4.9	0.001161730
44.8	0.0589	19.84	34.01	5.2	0.001841991
69.7	0.0917	23.81	36.68	5.5	0.002752896
95.5	0.1257	27.78	39.12	5.8	0.003674113
122.8	0.1616	31.75	41.17	6.0	0.004681526
145.3	0.1912	35.72	44.46	6.2	0.005316724
174.5	0.2296	39.68	46.02	6.5	0.006476772
198.9	0.2617	43.65	48.82	6.7	0.007261447
226.7	0.2983	47.62	50.74	6.9	0.008378282

Carlo Erba Strumentazione Microstructure Lab.

MI. Le. S. TO. NE. 1 0 0

Calculation parameters of Sorptomatic

Comment OUTGASSED AT 120 C 60% CeO_2/Al_2O_3 activated at 500°C.
Operator : A.NARAYANAN
Date (mm/dd/yy) 10-21-1993

Monolayer thickness (a):	4.3	Total introduction	9
Satur/Limit pressure (torr):	760	Reduced introduction	9
Mol.mass. gas ads. (g/mol):	28	Reduction factor	.25
Gas ads. density (g/cm3):	.808	Constant bur.(cm3/torr):	.11112
Burette temperature (c):	-195.82	Sample weight (g):	.468
Operating pressure (torr)	800	Sample Density (g/cm3):	1.8

Initial point (P/P0) for linear regression of B.E.T. region .05

Final point (P/P0) for linear regression of B.E.T. region .33

Correlation factor = .9997021

Monolayer Volume (CM3/G) = 32.88797

Specific surface area (M2/G) 143.7085

C value of B. E. T equation = 64.385

Pore specific volume (CM3/G) =

Total volume introduced (CM3) = 35.71574

Corrected Burette Constant = .1099131

Adsorption values

P.ADS (Torr)	P/P0 ADS	VT (CM3)	V.ADS(CM3/G)	T(A)	P/(P0-P)Va/g
0.5	0.0007	3.97	8.36	3.8	0.000078728
1.0	0.0013	7.94	16.72	3.9	0.000078780
9.4	0.0124	11.91	23.23	4.5	0.000539080
32.1	0.0422	15.87	26.38	5.0	0.001671753
55.9	0.0736	19.84	29.27	5.3	0.002712490
77.1	0.1014	23.81	32.77	5.6	0.003445288
105.3	0.1386	27.78	34.63	5.9	0.004644952
131.2	0.1726	31.75	37.02	6.1	0.005635735
158.1	0.2080	35.72	39.18	6.3	0.006703321

Carlo Erba Strumentazione Microstructure Lab.
MI. Le. S. TO. NE. 1 0 0

Calculation parameters of Sorptomatic

Comment OUTGASSED AT 120 C 80% CeO_2/Al_2O_3 activated at 500°C.
Operator A.NARAYANAN
Dat mm/dd/yy) 10-21-1993

Monolayer thickness (a)	4.3	Total introduction	11
Satur/Limit pressure (torr)	760	Reduced introduction	11
Mol.mass. gas ads. g/mol	28	Reduction factor	.25
Gas ads. density (g/cm3)	.808	Constant bur.(cm3/torr):	.11263
Burette temperature	-195.82	Sample weight (g):	.582
Operating pressure (torr)	800	Sample Density (g/cm3):	1.8

Initial point (P/P0) for linear regression of B.E.T region .05

Final point (P/P0) for linear regression of B.E.T. region .33

Correlation factor = .9994514

Monolayer Volume (CM3/G) = 28.66182

Specific surface area (M2/G) 125.2417

C value of B. E. T equation 58.10911

For specific volume (CM3/G)

For volume introduced (CM3) 43.65257

Corrected Burette Constant = .1111291

Adsorption values

P.ADS (Torr)	P/P0 ADS	VI (CM3)	V.ADS(CM3/G)	T(A)	P/(P0-P)Va/g
0.1	0.0001	3.97	6.80	3.5	0.000019354
0.3	0.0004	7.94	13.58	3.7	0.000029079
6.8	0.0089	11.91	19.16	4.4	0.000471263
25.6	0.0337	15.87	22.39	4.9	0.001557139
47.3	0.0622	19.84	25.06	5.2	0.002648201
71.1	0.0936	23.81	27.14	5.5	0.003775614
97.7	0.1286	27.78	29.07	5.8	0.005071661
123.9	0.1630	31.75	30.89	6.0	0.006305466
148.2	0.1950	35.72	33.07	6.2	0.007325075
173.5	0.2283	39.68	35.06	6.5	0.008438302
197.3	0.2596	43.65	37.33	6.7	0.009392421

3.2.2 Acidity/basicity measurements

The oxides were sieved to prepare powders of 100-200 mesh size and then activated at a particular temperature for 2 hours prior to each experiment.

The acidity at various acid strengths of a solid was measured by titrating 0.1 g of solid suspended in 5 ml of benzene with a 0.1N solution of n-butylamine in benzene. At the end point basic colour of indicators appeared [18].

The basicity was measured by titrating 0.1 g of solid suspended in 5 ml of benzene with a 0.1N solution of trichloroacetic acid in benzene using the same indicators as those for acidity measurement. The colours of indicators on the surface at the end point of the titration were the same as the colours which appeared by adsorption of respective indicators on the acid sites. The colour of the benzene solution was the basic colour of the indicator at the end point but it turned to be the acidic colour by adding an excess of the acid. As the results for a titration lasting 1 hour were the same as those for a titration lasting 20 hrs, 1 hr was taken for titration.

3.2.3 Magnetic susceptibility measurements

Magnetic moments of the oxides before and after the adsorption of electron acceptors, were determined by magnetic susceptibility measurements.

The magnetic susceptibility measurements were done at room temperature on a simple Guoy type balance. The Guoy tube was standardised using ($Hg[Co(CNS)_4]$) as recommended by Figgis and Nyholm [19]. The effective magnetic moment was calculated using the equation

$$\mu_{eff} = 2.8 \, (\chi_M^{corr} \, T)^{\frac{1}{2}}$$

where T is the absolute temperature and χ_M is the molar susceptibility [20].

3.2.4 Catalytic activity measurements

a) Oxidation of the alcohol [21]

In a round bottomed flask (20 cm^3) equipped with a reflux condenser were placed catalyst (100-200 mesh, 0.5 g), 10 cm^3 of a toluene solution of cyclohexanol (0.25 mmol), benzophenone (14.6 mmol) and n-decane (0.20 mmol) as an internal standard. The contents were heated under gentle reflux for 2 hours at 110°C.

b) Reduction of the ketones [22]

To 1 gm of the catalyst placed in a round bottomed flask (20 cm^3) equipped with a reflux condenser, 5 mmol of ketone, 10 cm^3 of 2-propanol and 0.5 mmol of xylene were added. The contents were heated under gentle reflux.

The reaction was followed by product analysis by means of a CHEMITO-8510 Gas Chromatograph, by comparison of its retention time with authentic samples. From the peak area of the product the concentration of the product formed was calculated with reference to that of the internal standard.

REFERENCES

1. Encyclopaedia of Industrial Chemical Analysis, Ed.F.D.Snell and L.S.Ettre, Vol.17, p.475 (Interscience, New York, 1973).

2. T.Arai, K.Maruya, K.Domen and T.Onishi, Bull. Chem. Soc. Jap., 62, 349 (1989).

3. D.S.Acker and W.R.Hertler, J. Am. Chem. Soc., 84, 3370 (1962).

4. L.F.Flesser and Mary Flesser, "Reagents for Organic Synthesis", p.125 (John Wiley, New York, 1967).

5. B.S.Furness, A.J.Hannaford, V.Rogers, P.W.G.Smith and A.R.Tatchell, "Vogel's Text Book of Practical Organic Chemistry", 4th ed., p.708 (ELBS, London, 1978).

6. ibid, p.626.

7. A.I.Vogel, "A Text Book of Practical Organic Chemistry", 3rd ed., p.407 (ELBS, London, 1973).

8. ibid, p.177.

9. B.S.Furness, A.J.Hannaford, V.Rogers, P.W.G.Smith and A.R.Tatchell, "Vogel's Text Book of Practical Organic Chemistry", 4th ed., p.276 (ELBS, London, 1978).

10. A.I.Vogel, "A Text Book of Practical Organic Chemistry", 3rd ed., p.172 (ELBS, London, 1973).

11. ibid, p.342.

12. D.D.Perrin, W.L.F.Armarego and D.R.Perrin, "Purification of Laboratory Chemicals", 2nd ed., p.123 (1983).

13. A.I.Vogel, A Text Book of Practical Organic Chemistry, 3rd ed., p.886 (ELBS, London, 1973).

14. ibid, p.185.

15. ibid, p.487.

16. ibid, p.190.

17. K.Esumi, K.Miyata and K.Meguro, Bull. Chem. Soc. Jap., 59, 3363 (1986).

18. Y.Yamanaka and K.Tanabe, J. Phys. Chem., 79, 2409 (1978).

19. B.N.Figgis and R.S.Nyholm, J. Chem. Soc., 4190 (1958).

20. B.N.Figgis and J.Lewis, "Modern Co-ordination Chemistry" (Interscience, New York, 1960).

21. H.Kuno, K.Takahashi, M.Shibagaki and H.Matsushita, Bull. Chem. Soc. Jap., 63, 1943 (1990).

22. M.Shibagaki, K.Takahashi, H.Kuno and H.Matsushita, Bull. Chem. Soc. Jap., 61, 328 (1988).

CHAPTER IV
RESULTS AND DISCUSSION

RESULTS AND DISCUSSION

Though rare earth oxides are widely used as catalysts in various types of industries, no effort so far has been made to understand the surface electron properties of many of the rare earth oxides. Among rare earth oxides samarium oxide is the most active and selective catalyst in the formation of C_2 – compounds [1] (selectivity 93%). Cerium oxide is a complete oxidation catalyst and is active in the direct formation of secondary alcohols and ketones from CO and H_2 [2]. These characteristics make the two oxides industrially important. So in this work we have attempted to study the surface electron properties and acidity/basicity of samaria and ceria. Mixed oxides and alumina supported metal oxides are quite often used as catalysts for reactions such as polymerization, carbon monoxide hydrogenation etc. [3,4]. Studies were carried out on binary oxides of samaria with alumina and ceria with alumina. The data have been correlated with their catalytic activity towards reactions such as oxidation (Oppenauer oxidation) and reduction (Meerwein-Ponndorf-Verley reduction).

The surface electron properties of metal oxide depend on the activation temperature. Hence the effect of activation temperature on electron donating capacity is also studied. In the case of paramagnetic metal oxides the extent of electron transfer from metal oxide during chemisorption can be measured as the change in the magnetic moment of the metal oxide. Hence the magnetic properties of metal oxide as a function of equilibrium concentration of the electron acceptor is studied. Another property that is directly related to the electron transfer between adsorbent and the electron acceptor is the surface acidity and basicity of the metal oxides. Hence the surface acidic and basic properties of the oxides are studied using a series of Hammett indicators. In order to correlate electron donating and acid-base properties with the catalytic activity the activity of the oxides have studied for the oxidation/reduction reactions.

The electron donor properties obviously depend on the basicity of the solvent. These properties are studied as a function of the basicity of the solvents, using three solvents, acetonitrile, ethyl acetate and 1,4-dioxane, in the order of increasing basicity. On the surface of metal

oxides the electron donor sites are distributed from low electron affinity to a high electron affinity. The surface electron properties of some of the rare earth oxides have been reported [5-8]. To study the distribution of electron donor sites adsorption of electron acceptors of various electron affinity are studied. They are listed in Table 3.

Table 3: Electron acceptors used

Electron acceptors	Electron affinity (eV)
7,7,8,8-tetracyano quino-dimethane (TCNQ)	2.84
2,3,5,6-tetrachloro 1,4-benzoquinone (Chloranil)	2.40
p-dinitrobenzene (PDNB)	1.77
m-dinitrobenzene (MDNB)	1.26

Both Sm_2O_3 and CeO_2 were prepared by hydroxide method from the respective nitrate solution. They were activated by heating in air for 2 hrs at various temperatures, viz., 300, 500 and 800°C.

The adsorption of PDNB and MDNB on these oxides were so negligible that the amount adsorbed could not be

measured. The adsorption isotherms of TCNQ and chloranil from these solvents may be classified as Langmuir type. It is verified by the linear plot of C_{eq}/C_{ads} against C_{eq} where C_{eq} is the equilibrium concentration in mol dm^{-3} and C_{ads} is the amount adsorbed in mol m^{-2} of the electron acceptor (Fig.2). The limiting amount of electron acceptor adsorbed is determined from the Langmuir plots (Figs.3 and 4). Data are given in Tables 4-30. When electron acceptors were adsorbed the surface of the oxide they showed characteristic colouration due to the interaction between the electron acceptor adsorbed and the oxide surface [9]. Chloranil gave light pink colour and TCNQ gave green colour to the oxide surface. To study nature of interaction reflectance spectra (Fig.5) of adsorbed sample are measured. The bands appearing below 400 nm correspond to physically adsorbed state of neutral TCNQ radical which has the adsorption band at 395 nm [10]. The bands near 600 nm is attributed to the dimeric TCNQ radical which absorbs light at 643 nm [11]. The broad band extending upto 700 nm corresponds to chloranil anion radical [12].

The electronic state of adsorbed species was studied by ESR Spectroscopy in addition to Electronic Spectroscopy. Fig.6 shows the ESR of the sample adsorbed

Fig.2 Linear form of Langmuir isotherm obtained for adsorption of TCNQ and chloranil in acetonitrile on Sm_2O_3 activated at 800°C

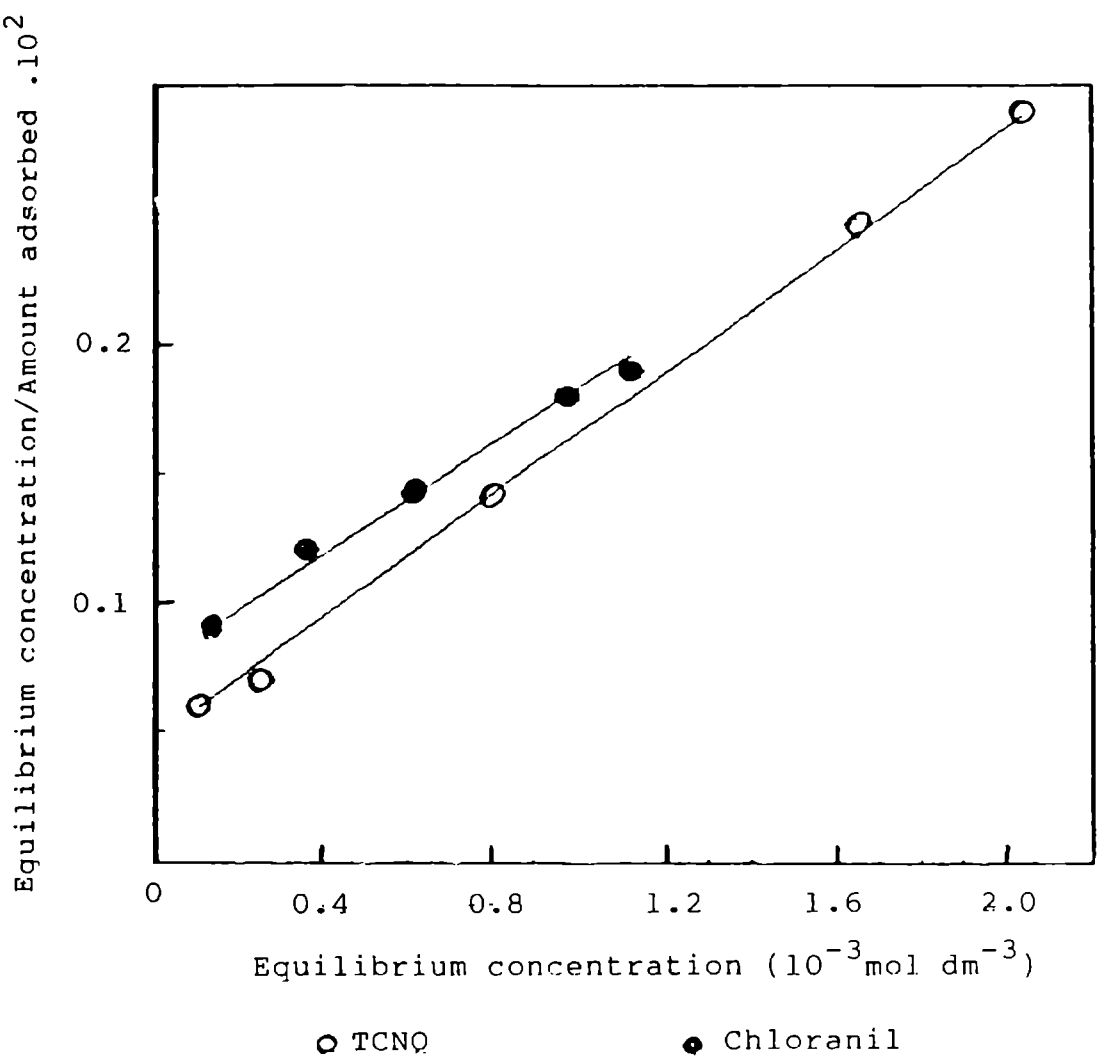

Fig.3 Adsorption isotherms on Sm_2O_3

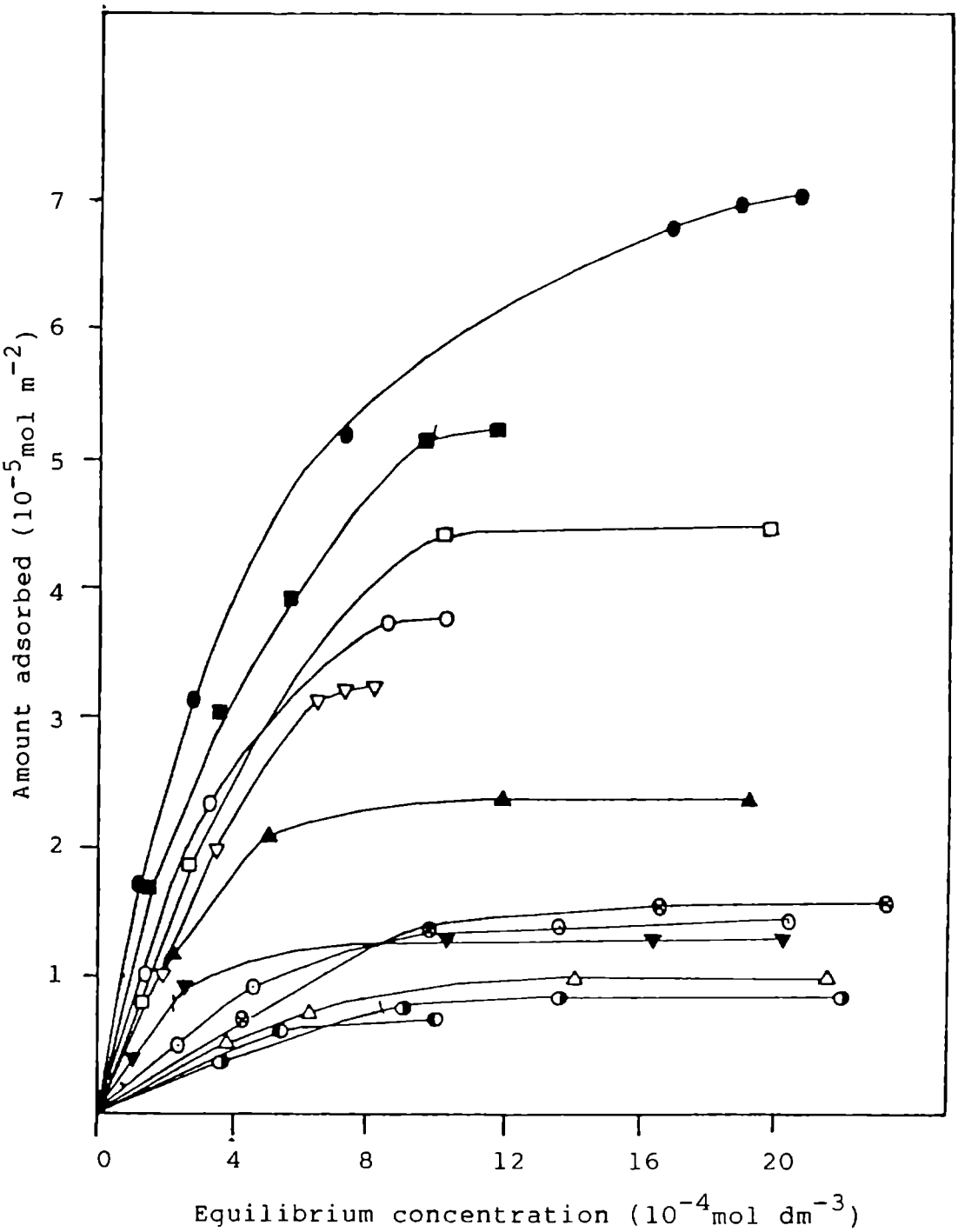

Electron acceptor/Solvent/Activation temperature (°C)
[CA - Chloranil; AN - Acetonitrile; TC - TCNQ: D-Dioxane]

△ CA/AN/300	⊗ CA/AN/500	▪ CA/AN/800
⊙ TC/AN/300	□ TC/AN/500	◍ TC/AN/800
◐ CA/D/300	▼ CA/D/500	▽ CA/D/800
◑ TC/D/300	▲ TC/D/500	○ TC/D/800

Fig.4 Adsorption isotherms on CeO_2

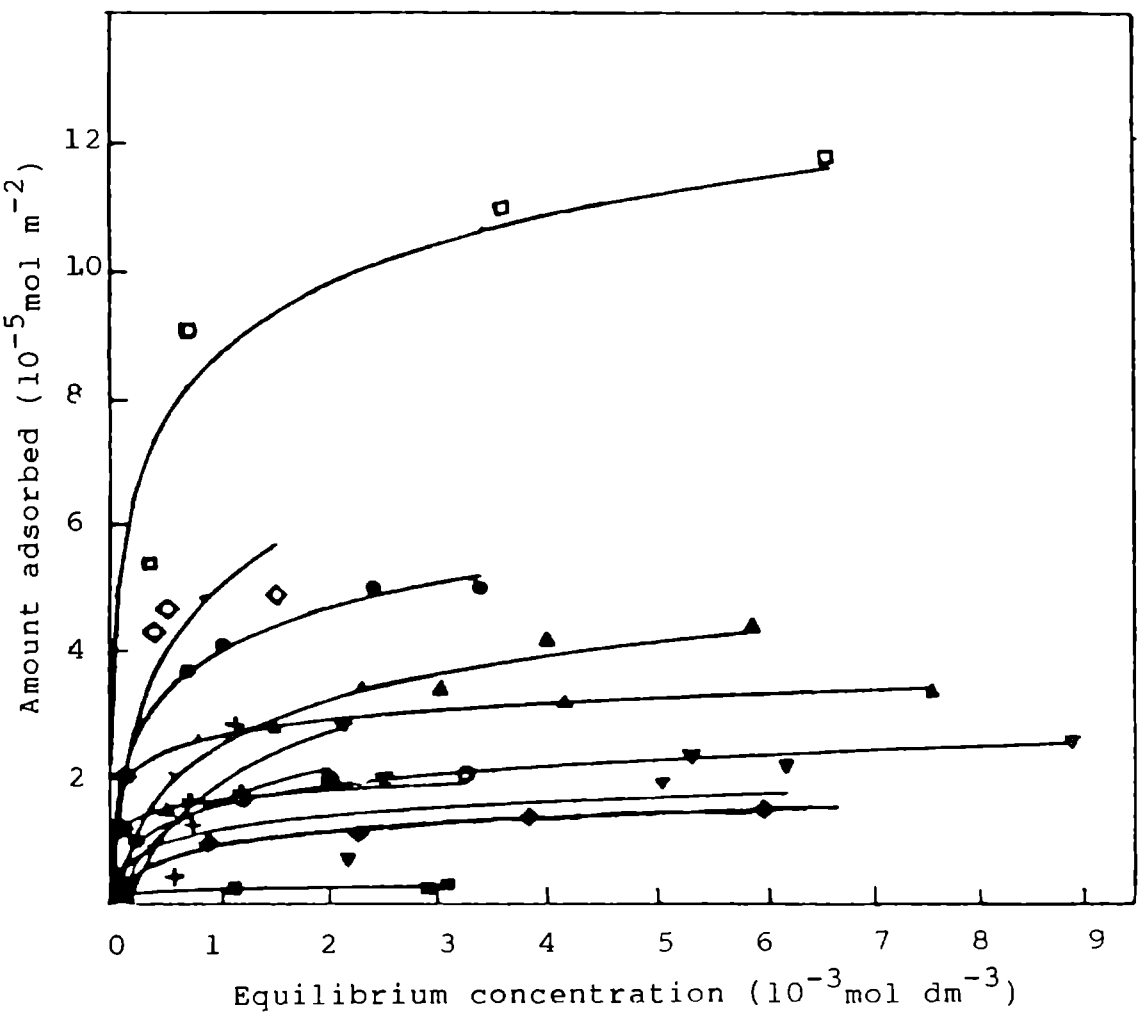

Electron acceptor/Solvent/Activation temperature (°C)

[CA - Chloranil; AN - Acetonitrile; TC - TCNQ; D -1,4-dioxane, EA - Ethyl acetate]

CA/AN/300	CA/AN/500	CA/AN/800
TC/AN/300	TC/AN/500	TC/AN/800
TC/D/300	TC/D/500	TC/D/800
TC/EA/300	TC/EA/500	TC/EA/800

Table 4 : Adsorption of Chloranil on Sm_2O_3

Activation temperature: 300°C Solvent: Acetonitrile

Initial concentration 10^{-3}mol dm^{-3}	Equilibrium concentration 10^{-3}mol dm^{-3}	Amount adsorbed 10^{-5}mol m^{-2}
0.057	0.016	0.111
0.248	0.117	0.392
0.496	0.295	0.581
0.795	0.544	0.613
1.732	1.402	0.981
2.473	2.132	0.990

Table 5 : Adsorption of TCNQ on Sm_2O_3

Activation temperature: 300°C Solvent: Acetonitrile

Initial concentration 10^{-3}mol dm^{-3}	Equilibrium concentration 10^{-3}mol dm^{-3}	Amount adsorbed 10^{-5}mol m^{-2}
0.044	0.023	0.041
0.195	0.114	0.222
0.386	0.235	0.431
0.764	0.463	0.920
2.033	1.353	1.461
2.541	2.051	1.462

Table 6: Adsorption of Chloranil on Sm_2O_3

Activation temperature: 300°C Solvent: 1,4-dioxane

Initial concentration 10^{-3}mol dm^{-3}	Equilibrium concentration 10^{-3}mol dm^{-3}	Amount adsorbed 10^{-5}mol m^{-2}
0.044	0.013	0.111
0.093	0.023	0.202
0.201	0.050	0.461
0.701	0.531	0.540
0.812	0.575	0.721
1.211	0.980	0.722

Table 7: Adsorption of TCNQ on Sm_2O_3

Activation temperature: 300°C Solvent: 1,4-dioxane

Initial concentration 10^{-3}mol dm^{-3}	Equilibrium concentration 10^{-3}mol dm^{-3}	Amount adsorbed 10^{-5}mol m^{-2}
0.250	0.170	0.221
0.491	0.362	0.392
0.732	0.571	0.493
1.721	1.440	0.830
2.450	2.180	0.831

Table 8: Adsorption of TCNQ on Sm_2O_3

Activation temperature: 300°C Solvent: Ethyl acetate

Initial concentration 10^{-3}mol dm^{-3}	Equilibrium concentration 10^{-3}mol dm^{-3}	Amount adsorbed 10^{-5}mol m^{-2}
0.052	0.025	0.083
0.263	0.180	0.254
0.527	0.415	0.337
1.055	0.743	0.946
2.111	1.741	1.114
2.639	2.277	1.123

Table 9: Adsorption of Chloranil on Sm_2O_3

Activation temperature: 500°C Solvent: Acetonitrile

Initial concentration 10^{-3}mol dm^{-3}	Equilibrium concentration 10^{-3}mol dm^{-3}	Amount adsorbed 10^{-5}mol m^{-2}
0.060	0.030	0.124
0.341	0.265	0.577
0.572	0.420	0.635
1.353	1.040	1.312
2.710	2.321	1.623
3.390	2.991	1.632

Table 10: Adsorption of TCNQ on Sm_2O_3

Activation temperature: 500°C Solvent: Acetonitrile

Initial concentration 10^{-3}mol dm^{-3}	Equilibrium concentration 10^{-3}mol dm^{-3}	Amount adsorbed 10^{-5}mol m^{-2}
0.150	0.040	0.472
0.297	0.074	0.929
0.744	0.216	2.199
1.190	0.291	3.749
2.192	1.030	4.431
3.124	1.980	4.440

Table 11: Adsorption of Chloranil on Sm_2O_3

Activation temperature: 500°C Solvent: 1,4-dioxane

Initial concentration 10^{-3}mol dm^{-3}	Equilibrium concentration 10^{-3}mol dm^{-3}	Amount adsorbed 10^{-5}mol m^{-2}
0.080	0.072	0.030
0.397	0.337	0.250
1.191	0.965	0.925
1.986	1.659	1.363
2.384	2.057	1.363

Table 12: Adsorption of TCNQ on Sm_2O_3

Activation temperature: 500°C Solvent: 1,4-dioxane

Initial concentration 10^{-3}mol dm^{-3}	Equilibrium concentration 10^{-3}mol dm^{-3}	Amount adsorbed 10^{-5}mol m^{-2}
0.284	0.015	0.198
0.397	0.203	0.823
0.501	0.219	1.618
1.003	0.474	2.205
1.755	1.177	2.403
2.509	1.933	2.403

Table 13: Adsorption of TCNQ on Sm_2O_3

Activation temperature: 500°C Solvent: Ethyl acetate

Initial concentration 10^{-3}mol dm^{-3}	Equilibrium concentration 10^{-3}mol dm^{-3}	Amount adsorbed 10^{-5}mol m^{-2}
0.067	0.304	0.011
0.303	0.157	0.601
0.607	0.334	1.120
1.214	0.600	2.552
2.428	1.527	3.750
3.036	2.130	3.751

Table 14: Adsorption of Chloranil on Sm_2O_3

Activation temperature: 800°C Solvent: Acetonitrile

Initial concentration 10^{-3}mol dm^{-3}	Equilibrium concentration 10^{-3}mol dm^{-3}	Amount adsorbed 10^{-5}mol m^{-2}
0.403	0.146	1.701
0.806	0.364	2.920
1.216	0.600	3.900
1.752	0.979	5.698
1.949	1.117	5.705

Table 15: Adsorption of TCNQ on Sm_2O_3

Activation temperature: 800°C Solvent: Acetonitrile

Initial concentration 10^{-3}mol dm^{-3}	Equilibrium concentration 10^{-3}mol dm^{-3}	Amount adsorbed 10^{-5}mol m^{-2}
0.382	0.112	1.732
0.850	0.263	3.876
1.549	0.779	5.207
2.734	1.695	6.873
2.980	1.716	7.039
3.122	2.042	7.039

Table 16: Adsorption of Chloranil on Sm_2O_3

Activation temperature: 800°C Solvent: 1,4-dioxane

Initial concentration 10^{-3}mol dm^{-3}	Equilibrium concentration 10^{-3}mol dm^{-3}	Amount adsorbed 10^{-5}mol m^{-2}
0.293	0.143	0.994
0.585	0.300	1.905
0.999	0.527	3.125
1.175	0.673	3.178
1.292	0.808	3.178

Table 17: Adsorption of TCNQ on Sm_2O_3

Activation temperature: 800°C Solvent: 1,4-dioxane

Initial concentration 10^{-3}mol dm^{-3}	Equilibrium concentration 10^{-3}mol dm^{-3}	Amount adsorbed 10^{-5}mol m^{-2}
0.538	0.269	1.771
0.840	0.501	2.252
0.951	0.532	2.781
1.409	0.859	3.683
1.596	1.036	3.686

Table 18: Adsorption of TCNQ on Sm_2O_3

Activation temperature: 800°C Solvent: Ethyl acetate

Initial concentration 10^{-3}mol dm^{-3}	Equilibrium concentration 10^{-3}mol dm^{-3}	Amount adsorbed 10^{-5}mol m^{-2}
0.080	0.060	0.157
0.395	0.323	0.463
0.791	0.585	1.360
1.582	0.111	3.119
3.165	2.120	6.635
3.957	2.955	6.920

Table 19: Adsorption of Chloranil on CeO_2

Activation temperature: 300°C Solvent: Acetonitrile

Initial concentration 10^{-3}mol dm^{-3}	Equilibrium concentration 10^{-3}mol dm^{-3}	Amount adsorbed 10^{-5}mol m^{-2}
0.204	0.164	0.121
0.819	0.223	1.805
2.049	0.677	4.131
2.529	0.990	4.870
4.018	2.462	5.001
5.059	3.398	5.201

Table 20: Adsorption of TCNQ on CeO_2

Activation temperature: 300°C Solvent: Acetonitrile

Initial concentration 10^{-3}mol dm^{-3}	Equilibrium concentration 10^{-3}mol dm^{-3}	Amount adsorbed 10^{-5}mol m^{-2}
0.739	0.014	2.183
1.478	0.139	2.679
2.217	0.499	5.170
5.320	2.449	8.644
7.144	3.220	10.810
10.200	6.589	11.910

Table 21: Adsorption of TCNQ on CeO_2

Activation temperature: 300°C Solvent: 1,4-dioxane

Initial concentration 10^{-3}mol dm^{-3}	Equilibrium concentration 10^{-3}mol dm^{-3}	Amount adsorbed 10^{-5}mol m^{-2}
0.209	0.145	0.094
1.044	0.729	0.170
2.088	1.513	0.728
4.176	3.041	3.426
5.399	4.001	4.194
7.297	5.834	4.405

Table 22: Adsorption of TCNQ on CeO_2

Activation temperature: 300°C Solvent: Ethyl acetate

Initial concentration 10^{-3}mol dm^{-3}	Equilibrium concentration 10^{-3}mol dm^{-3}	Amount adsorbed 10^{-5}mol m^{-2}
0.106	0.040	0.176
0.529	0.105	1.192
1.057	0.132	2.012
2.052	0.384	4.471
2.644	0.502	4.802

Table 23: Adsorption of Chloranil on CeO_2

Activation temperature: 500°C Solvent: Acetonitrile

Initial concentration 10^{-3}mol dm^{-3}	Equilibrium concentration 10^{-3}mol dm^{-3}	Amount adsorbed 10^{-5}mol m^{-2}
0.407	0.003	0.381
0.815	0.029	0.524
1.222	0.223	0.988
2.852	1.196	1.650
4.075	2.024	1.982
5.254	3.272	2.050

Table 24: Adsorption of TCNQ on CeO_2

Activation temperature: 500°C Solvent: Acetonitrile

Initial concentration 10^{-3}mol dm^{-3}	Equilibrium concentration 10^{-3}mol dm^{-3}	Amount adsorbed 10^{-5}mol m^{-2}
0.078	0.001	0.076
2.154	0.134	2.010
4.308	1.490	2.820
7.545	4.118	3.211
10.770	7.553	3.372

Table 25: Adsorption of TCNQ on CeO_2

Activation temperature: 500°C Solvent: 1,4-dioxane

Initial concentration 10^{-3}mol dm^{-3}	Equilibrium concentration 10^{-3}mol dm^{-3}	Amount adsorbed 10^{-5}mol m^{-2}
0.224	0.044	0.181
1.121	0.091	1.028
2.242	1.121	1.619
4.484	2.520	1.954
7.847	5.293	2.525
11.210	8.889	2.549

Table 26: Adsorption of TCNQ on CeO_2

Activation temperature: 500°C Solvent: Ethyl acetate

Initial concentration 10^{-3}mol dm^{-3}	Equilibrium concentration 10^{-3}mol dm^{-3}	Amount adsorbed 10^{-5}mol m^{-2}
0.199	0.144	0.056
0.399	0.216	0.182
0.999	0.575	0.423
1.998	0.738	1.257
3.996	1.121	2.842
4.998	2.143	2.867

Table 27: Adsorption of Chloranil on CeO_2

Activation temperature:800°C Solvent: Acetonitrile

Initial concentration 10^{-3}mol dm^{-3}	Equilibrium concentration 10^{-3}mol dm^{-3}	Amount adsorbed 10^{-5}mol m^{-2}
0.159	0.056	0.098
0.687	0.508	0.171
1.365	1.113	0.240
2.225	2.915	0.295
3.416	3.100	0.301

Table 28: Adsorption of TCNQ on CeO_2

Activation temperature: 800°C Solvent: Acetonitrile

Initial concentration 10^{-3}mol dm^{-3}	Equilibrium concentration 10^{-3}mol dm^{-3}	Amount adsorbed 10^{-5}mol m^{-2}
0.028	0.020	0.077
0.141	0.098	0.403
2.822	2.113	0.670
7.055	5.044	1.916
8.466	6.161	2.191
14.110	11.670	2.323

Table 29: Adsorption of TCNQ on CeO_2

Activation temperature: 800°C Solvent: 1,4-dioxane

Initial concentration 10^{-3}mol dm^{-3}	Equilibrium concentration 10^{-3}mol dm^{-3}	Amount adsorbed 10^{-5}mol m^{-2}
0.151	0.058	0.088
0.757	0.426	0.313
1.514	0.877	0.607
3.028	2.273	0.718
5.299	3.842	1.394
7.571	5.983	1.511

Table 30: Adsorption of TCNQ on CeO_2

Activation temperature: 800°C Solvent: Ethyl acetate

Initial concentration 10^{-3}mol dm^{-3}	Equilibrium concentration 10^{-3}mol dm^{-3}	Amount adsorbed 10^{-5}mol m^{-2}
0.368	0.153	0.204
0.736	0.271	0.484
0.926	0.283	0.606
1.222	0.337	0.842
2.429	0.763	1.642
3.036	1.169	1.776

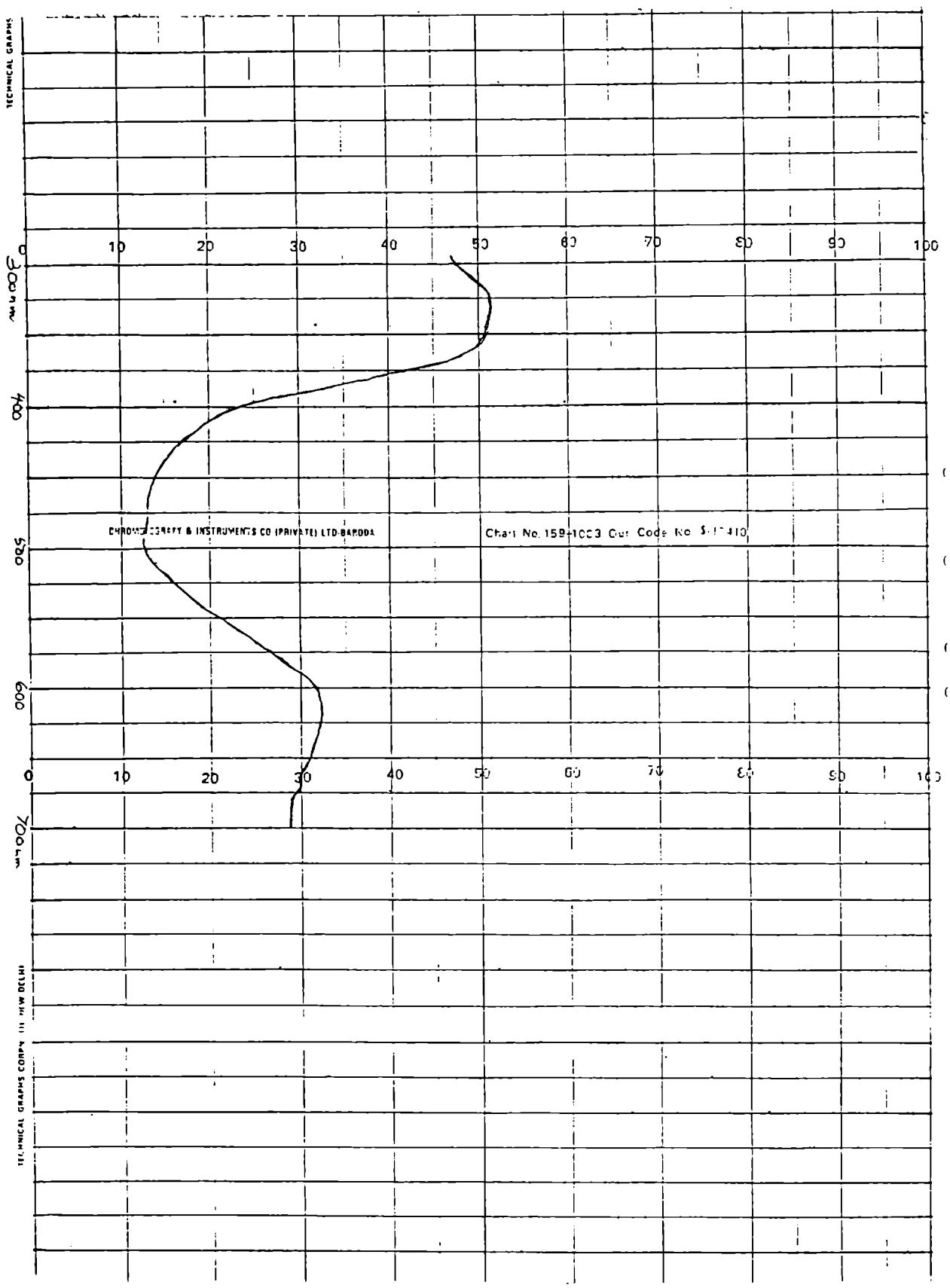
TECHNICAL GRAPHS
0
10
20
30
40
50
60
70
80
90
100
300
400
500
600
700
CHROMO CORRFY & INSTRUMENTS CO (PRIVATE) LTD-BARODA
Chart No. 159-1003 Our Code No.
TECHNICAL GRAPHS COPY (I) NEW DELHI

Fig.5

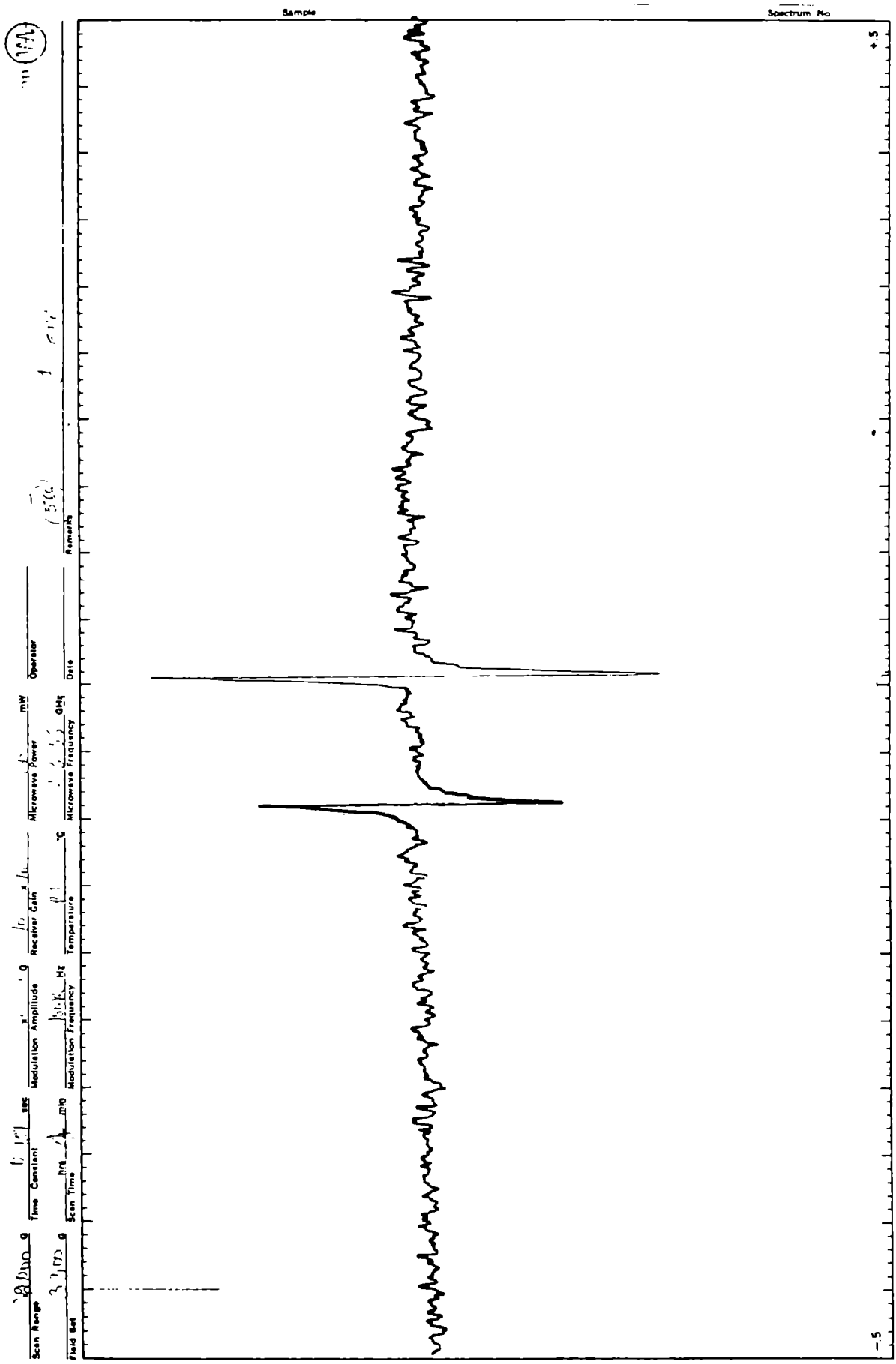
Sample
Spectrum No
+5
-5
Scan Range
Time Constant
Modulation Amplitude
Receiver Gain
Field Set
Scan Time
Modulation Frequency
Temperature
Microwave Power
Microwave Frequency
Operator
Date
Remarks

Fig.6

with TCNQ (C_{ads} = 7.039×10^{-5} mol m^{-2}) on the surface. Samples coloured by TCNQ adsorption gave unresolved ESR Spectra with a g value of 2.003. These spectra have been identified as being those of TCNQ anion radicals [13]. The coloured samples obtained by the adsorption of chloranil gave unresolved ESR spectra having a g value of 2.011 [14]. The radical concentration of TCNQ and chloranil adsorbed are given in Tables 31-34. Figs.7 and 8 show the radical concentration of TCNQ and chloranil against the equilibrium concentration of TCNQ and chloranil in solution. The isotherms obtained are of Langmuir type and is of the same shape as the plot of the amount of electron acceptor adsorbed. Limiting radical concentrations are calculated from the Langmuir plots.

The electron donating capacity of the oxide is found to depend on the electron affinity of the electron acceptor adsorbed. The amount of electron acceptor adsorbed increased with increase in electron affinity of the electron acceptor. Strong electron acceptor like TCNQ is capable of forming anions even from weak donor sites, whereas weak electron acceptor like MDNB is capable of forming anions only at strong donor sites. Hence the limiting radical concentration of the weak electron

Table 31: Adsorption of Chloranil on Sm_2O_3

Activation temperature: 800°C Solvent: Acetonitrile

Initial concentration 10^{-3}mol dm^{-3}	Equilibrium concentration 10^{-3}mol dm^{-3}	Radical concentration 10^{18} spins m^{-2}
0.403	0.146	0.052
0.806	0.364	0.090
1.216	0.600	0.120
1.752	0.979	0.303
1.947	1.117	0.346

Table 32: Adsorption of TCNQ on Sm_2O_3

Activation temperature: 800°C Solvent: Acetonitrile

Initial concentration 10^{-3}mol dm^{-3}	Equilibrium concentration 10^{-3}mol dm^{-3}	Radical concentration 10^{18} spins m^{-2}
0.382	0.112	0.937
0.850	0.263	2.100
1.549	0.779	2.818
2.734	1.695	3.725
2.986	1.916	3.815
3.122	2.042	3.815

Table 33: Adsorption of Chloranil on CeO_2

Activation temperature: 300°C Solvent: Acetonitrile

Initial concentration 10^{-3}mol dm^{-3}	Equilibrium concentration 10^{-3}mol dm^{-3}	Radical concentration 10^{18}spins m^{-2}
0.204	0.164	0.003
0.819	0.223	0.005
2.049	0.667	0.012
2.529	0.990	0.015
4.018	2.402	0.016
5.059	3.398	0.016

Table 34: Adsorption of TCNQ on CeO_2

Activation temperature: 300°C Solvent: Acetonitrile

Initial concentration 10^{-3}mol dm^{-3}	Equilibrium concentration 10^{-3}mol dm^{-3}	Radical concentration 10^{18} spins m^{-2}
0.739	0.014	1.127
1.478	0.139	1.384
2.217	0.499	2.671
5.320	2.449	4.466
7.144	3.220	5.632
10.200	6.589	6.102

Fig.7 Radical concentration of TCNQ and chloranil on Sm_2O_3 Vs. equilibrium concentration of TCNQ and chloranil

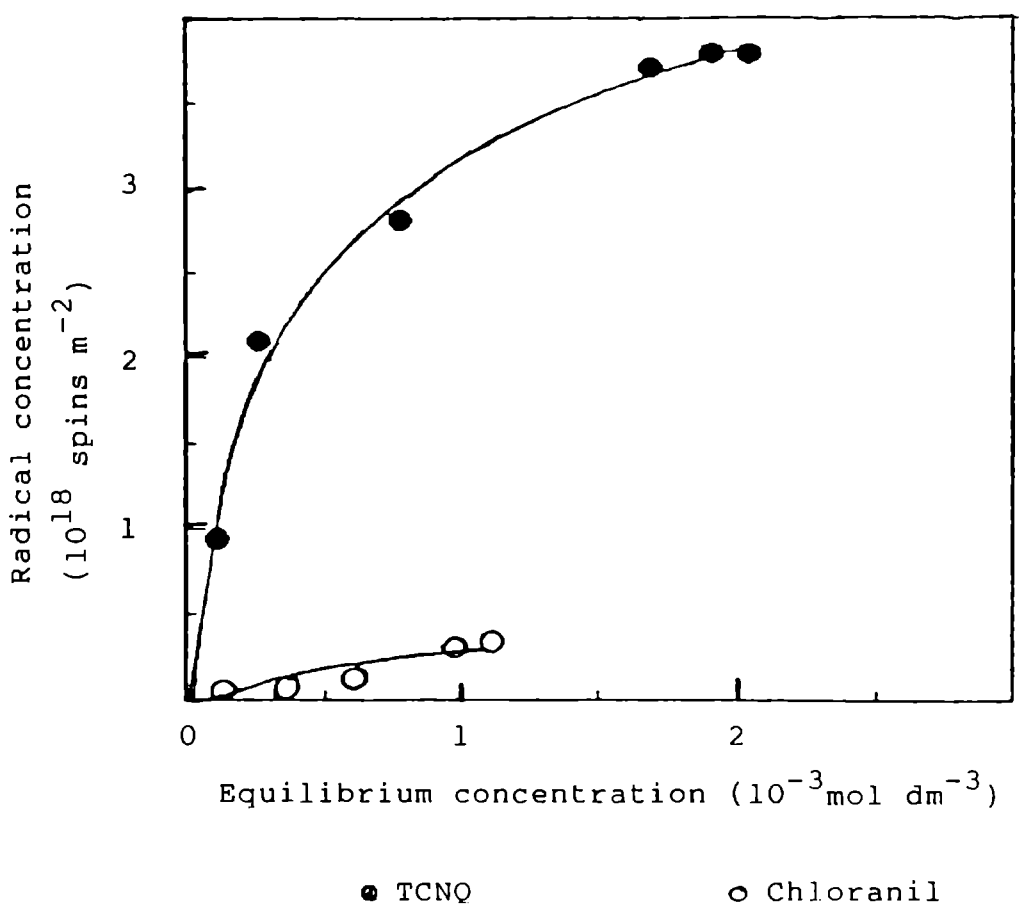

Fig.8 Radical concentration of TCNQ and chloranil on CeO_2 Vs. equilibrium concentration of TCNQ and chloranil.

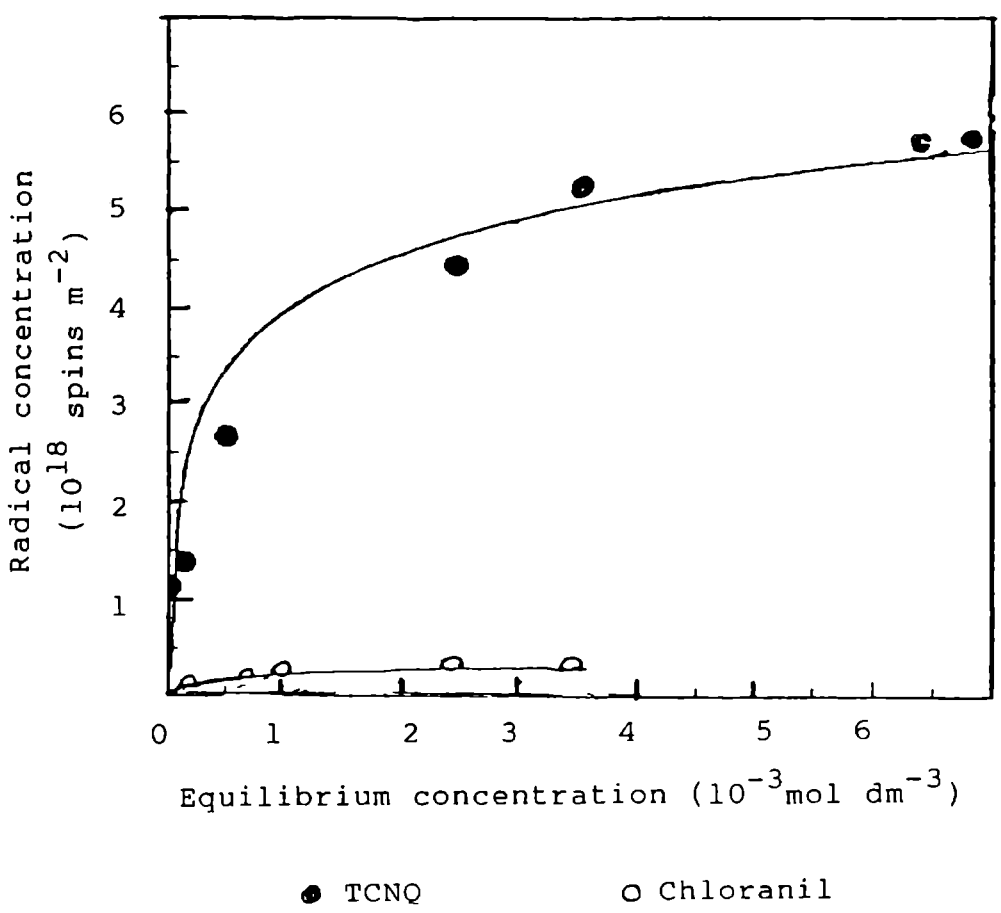

acceptor is a measure of the number of strong donor sites on the surface and that for a strong acceptor is related to the total number of sites (weak and strong donor sites) on the surface. Accordingly the limit of electron transfer from the electron donor site of samaria and ceria is located between 2.40 and 1.77 eV in terms of the electron affinity of the acceptor.

Two possible electron sources exist in oxide surface responsible for electron transfer. One of these has electron trapped in intrinsic defects and the other has hydroxyl ions [15]. At lower activation temperature surface sites may be associated with the presence of unsolvated hydroxyl ions and at higher activation temperature an electron defect centre is produced. It is reported that free electron defect site on metal oxide surface is created at an activation temperature of above 500°C [16]. Fomin et al have shown that electron transfer from OH^- ions can and does occur in certain solvent systems provided a suitable electron acceptor is present [17]. Surface hydroxyls on metal oxides are shown to differ in chemical properties and difference in acidity between hydroxyl groups on several oxide surfaces have been reported [18]. These suggest that hydroxyl ions on metal

oxide surfaces have electron donor sites of varying electron donicity. IR spectral data of samaria and ceria confirm the presence of hydroxyl groups (Fig.9), (Peaks near 3400 cm^{-1}).

The limiting amount of electron acceptor adsorbed on the oxide surface depends on the activation temperature. Figs.10 and 11 show the limiting amount of electron acceptor adsorbed on samaria and ceria as a function of activation temperature. In the case of samaria as the activation temperature increases amount of electron acceptor adsorbed also increases. This trend can be understood as the decrease in concentration of surface hydroxyl ions and the increase in concentration of trapped electron centers with increasing activation temperature. It might be expected that the trapped electron centres are solely responsible for the adsorption of electron acceptor on the surface of rare earth oxide activated at higher temperature and they are stronger reducing agent than hydroxyl ions. From the data it is inferred that the effect of temperature is to increase the concentration of both weak and strong donor sites.

In the case of ceria, the limiting amount adsorbed is higher for activation temperature of 300°C,

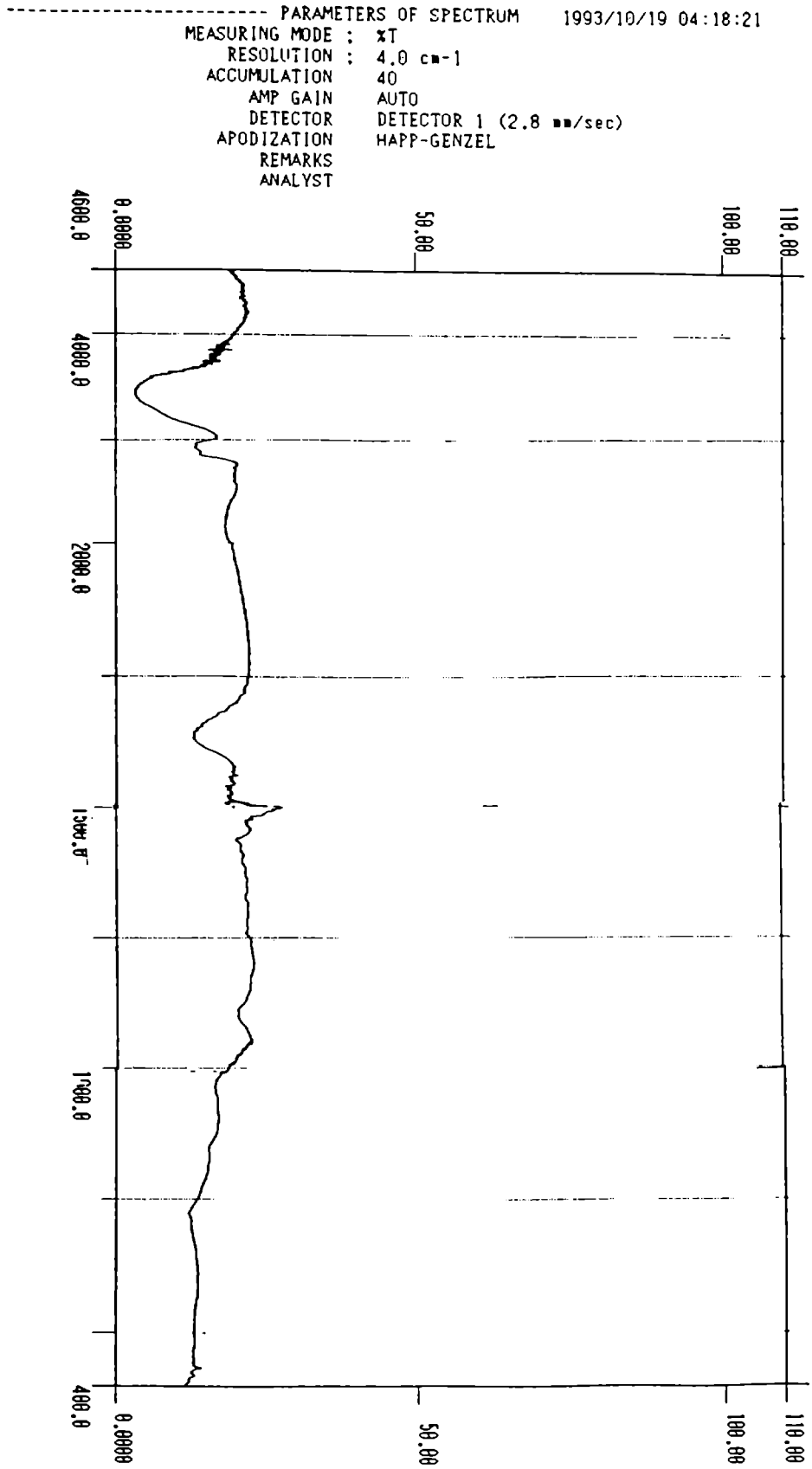

Fig.9

Fig.10 Limiting amount of electron acceptor adsorbed on Sm_2O_3 as a function of activation temperature

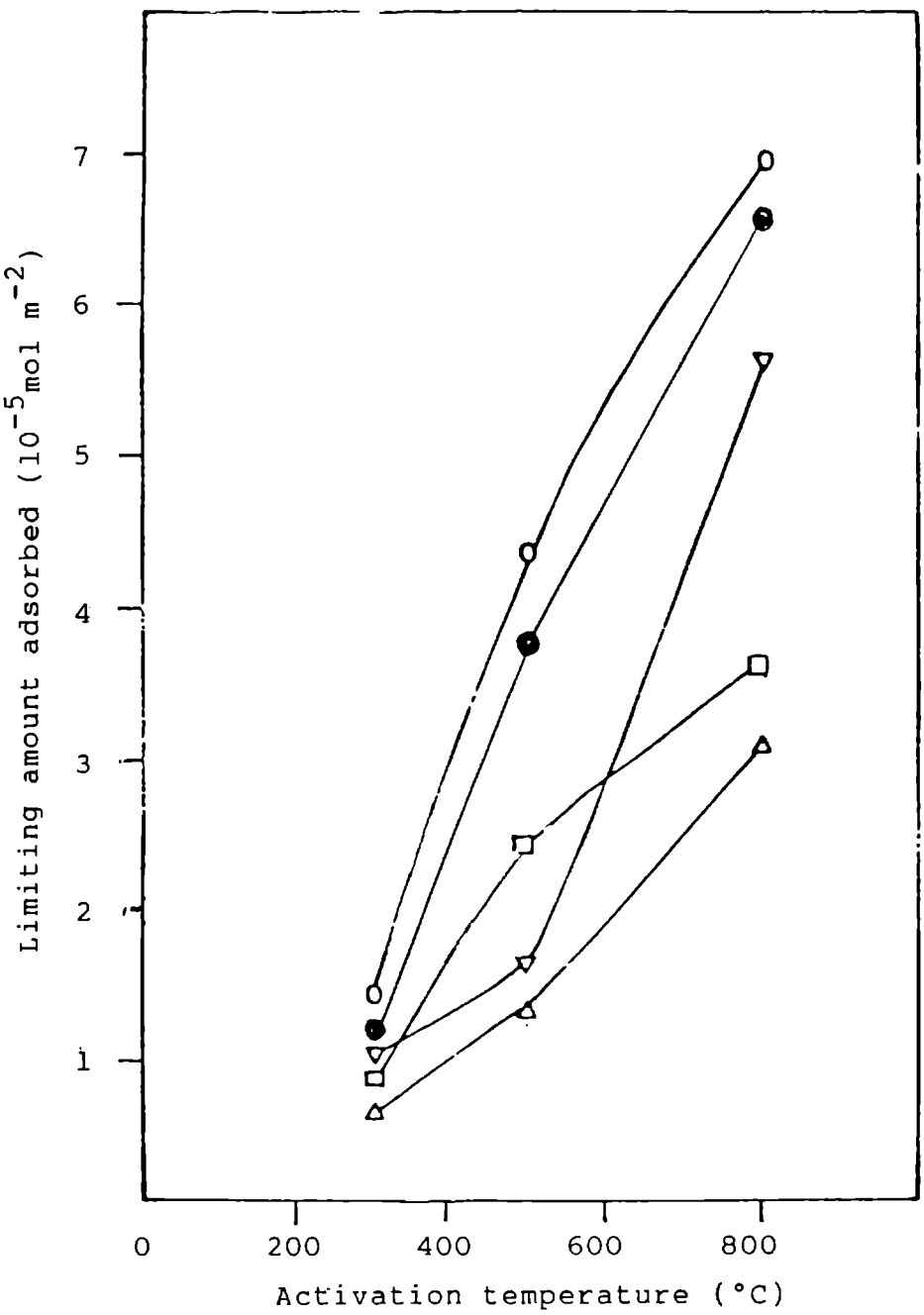

Electron acceptor/solvent

[CA - Chloranil; AN - Acetonitrile; D - Dioxane; TC - TCNQ; EA - Ethyl acetate]

▽ CA/AN
△ CA/D
○ TC/AN
□ TC/D
● TC/EA

Fig.11. Limiting amount of electron acceptor adsorbed on CeO_2 as a function of activation temperature.

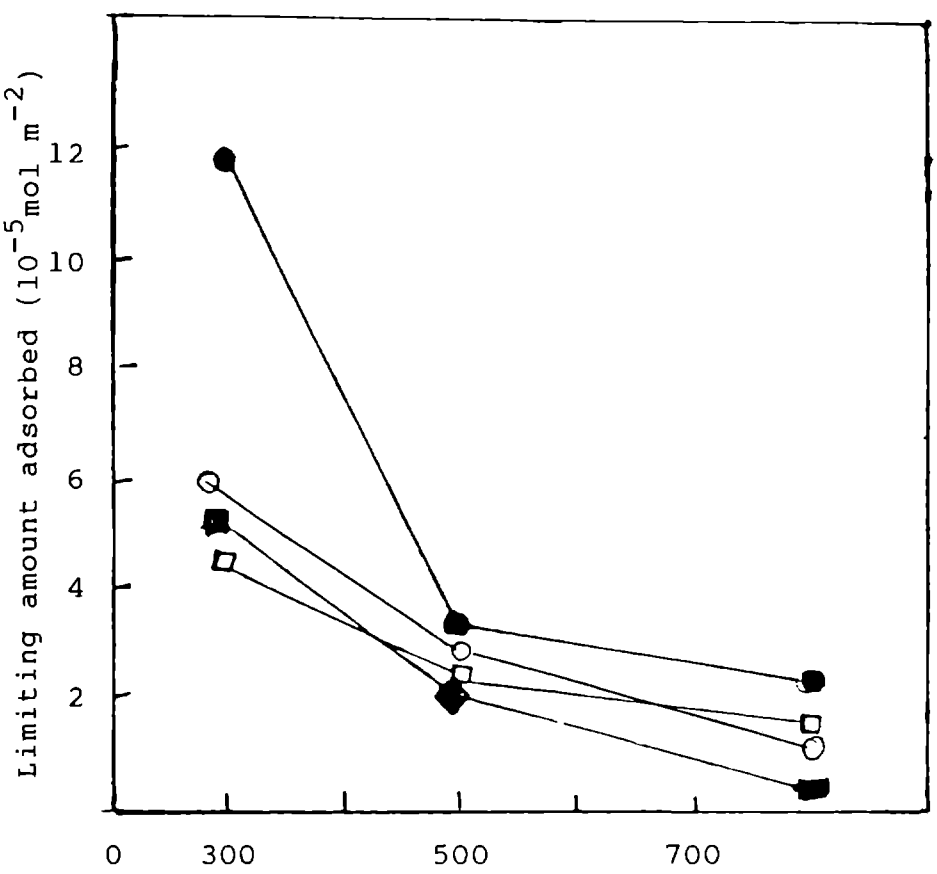

Electron acceptor/solvent

[CA - Chloranil; AN - Acetonitrile; D - Dioxane; TC - TCNQ; EA - Ethyl acetate]

□ CA/AN ■ TC/D

● TC/AN ○ TC/EA

implying that it has higher electron donating capacity compared to those activated at higher temperatures. For ceria as activation temperature increases electronic mobility is decreased [19].

The limiting amount of electron acceptor adsorbed is found to decrease with increase in basicity of the solvent. A very useful approach for relating the interfacial interaction quantitatively has been the Drago equation [20] of enthalpy changes in acid-base complexation. When the Drago equation is applied to this system the basic compound corresponds to the solvents such as acetonitrile, ethyl acetate and 1,4-dioxane and acidic compound to electron acceptor. The values obtained in kcal mol^{-1} are acetonitrile 3.51, ethyl acetate 4.27 and 1,4-dioxane 5.23. The decrease in adsorption of electron acceptor with increasing basicity of solvents shows the competition between basic solvents and basic sites (electron donor sites) of metal oxides for electron acceptors. Thus adsorption on to metal oxides is strongly influenced by interaction between basic solvents and electron acceptors. In the case of ceria as the basicity of the solvent increases the limit of electron transfer shift

from 2.40-1.77 eV to 2.84-2.40 eV in ethyl acetate and 1,4-dioxane. The limiting amount of TCNQ adsorbed on samaria and ceria as a function of acid-base interaction enthalpy are shown in Figs.12 and 13.

During the adsorption of electron acceptor on Sm_2O_3 the magnetic moment of oxide decreases and reaches a limiting value at the same concentration at which limiting amount of electron acceptor is adsorbed. The values are given in Tables 35-38. In Fig.14 magnetic moment of the oxide is plotted as a function of equilibrium concentration of electron acceptors. In the case of CeO_2 due to a diamagnetism appreciable change in magnetic moment could not be measured.

Acid-base strength distribution

Acidity and basicity of Sm_2O_3 and CeO_2 was estimated by titration using Hammett indicators. Acidity at various acid strengths of the oxide was measured by titrating the solid suspended in benzene with a 0.1N solution of n-butylamine in benzene. Basicity was measured by titrating with trichloro acetic acid using the same indicators as those used for acidity measurement. This

Fig.12 Limiting amount of TCNQ adsorbed on Sm_2O_3 as a function of acid-base interaction enthalpy.

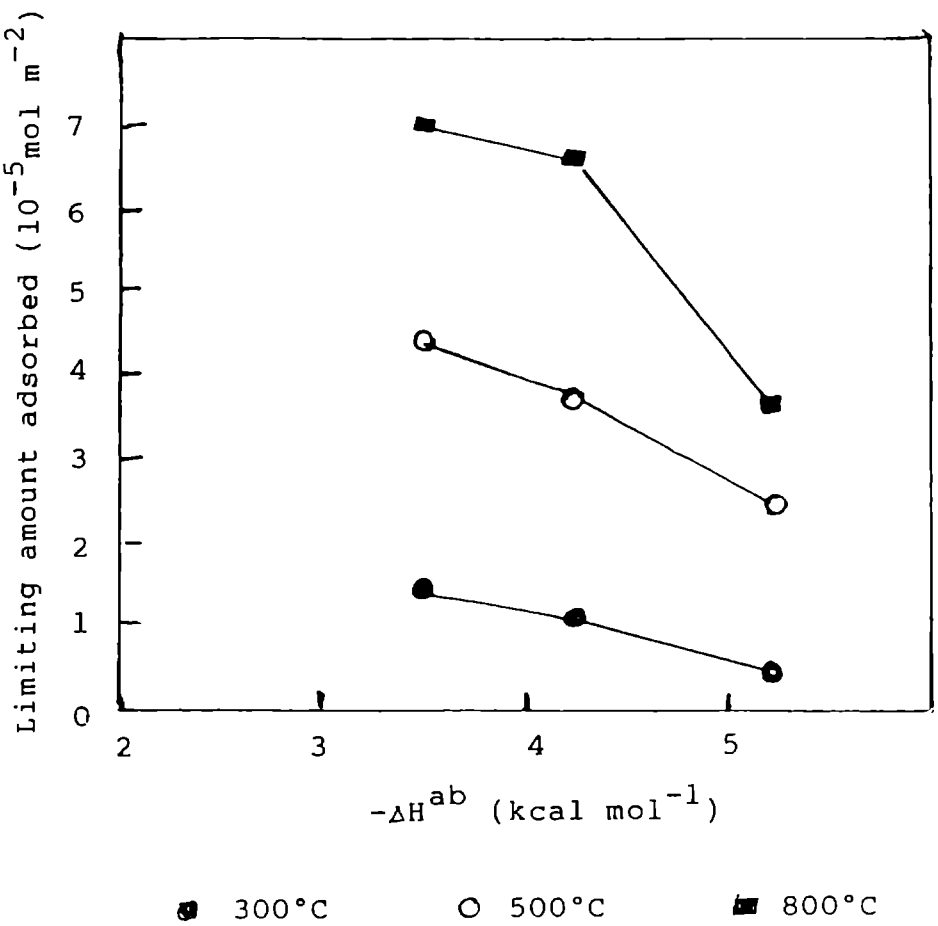

Fig.13 Limiting amount of electron acceptor adsorbed on CeO_2 as a function of acid-base interaction enthalpy.

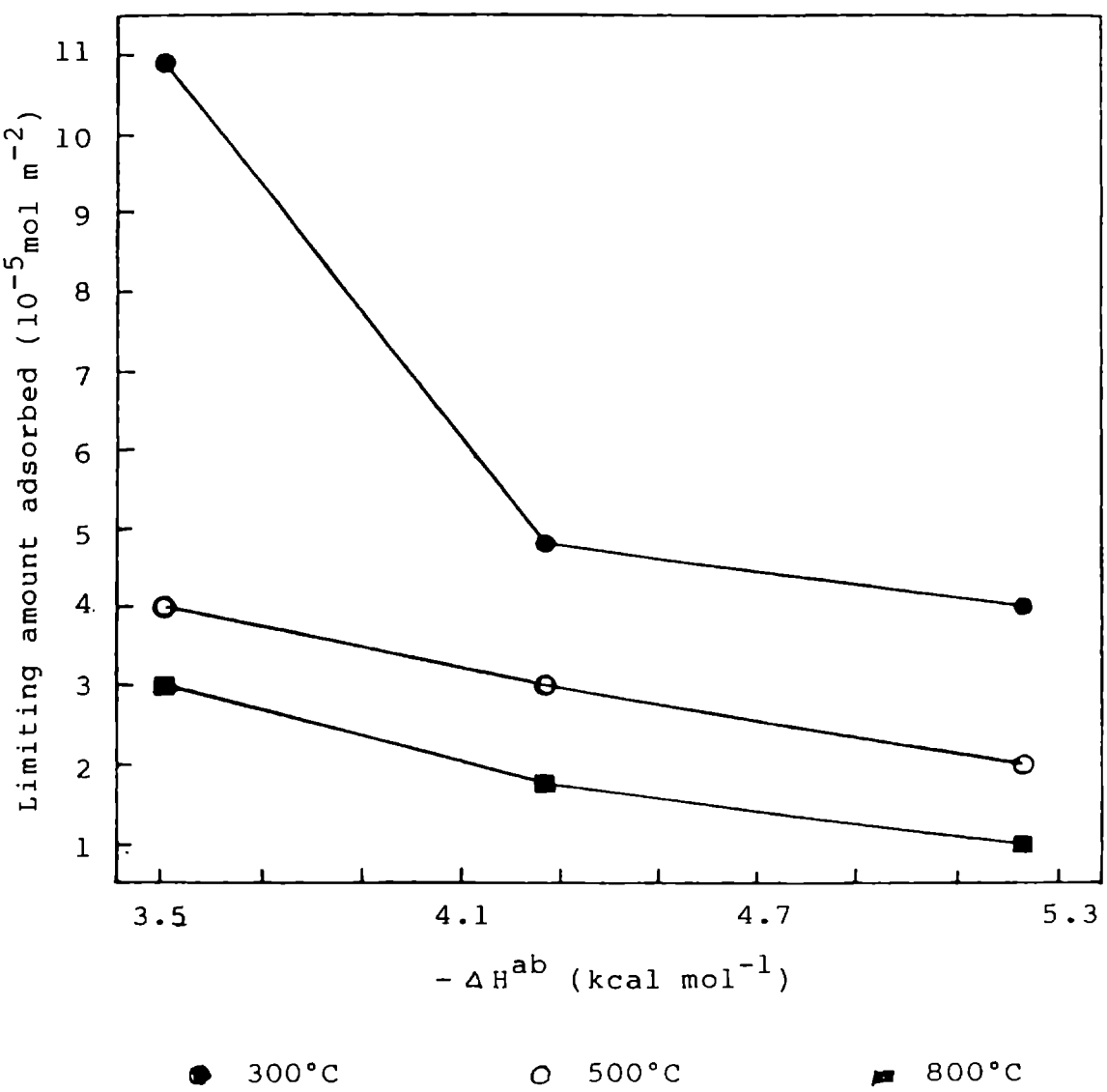

Table 35: Adsorption of Chloranil on Sm_2O_3

Activation temperature: 500°C Solvent: Acetonitrile

Initial concentration 10^{-3}mol dm^{-3}	Equilibrium concentration 10^{-3}mol dm^{-3}	Amount adsorbed 10^{-5}mol m^{-2}	Magnetic moment BM
0	0	0	1.040
0.060	0.030	0.124	1.241
0.345	0.265	0.577	1.202
0.575	0.420	0.035	1.182
0.367	1.040	1.312	1.167
2.714	2.321	1.623	0.970
3.393	2.991	1.632	0.971

Table 36: Adsorption of TCNQ on Sm_2O_3

Activation temperature: 500°C Solvent: Acetonitrile

Initial concentration 10^{-3}mol dm^{-3}	Equilibrium concentration 10^{-3}mol dm^{-3}	Amount adsorbed 10^{-5}mol m^{-2}	Magnetic moment BM
0	0	0	1.840
0.150	0.040	0.472	1.236
0.297	0.074	0.929	1.170
0.744	0.216	2.199	1.071
1.190	0.291	3.749	1.023
2.192	1.030	4.431	0.901
3.124	1.980	4.440	0.882

Table 37: Adsorption of Chloranil on Sm_2O_3

Activation temperature: 500°C Solvent: 1,4-dioxane

Initial concentration 10^{-3}mol dm^{-3}	Equilibrium concentration 10^{-3}mol dm^{-3}	Amount adsorbed 10^{-5}mol m^{-2}	Magnetic moment BM
0	0	0	1.840
0.080	0.012	0.030	1.391
0.397	0.337	0.250	1.291
1.191	0.965	0.925	1.120
1.986	1.659	1.363	1.070
2.384	2.057	1.363	1.062

Table 38: Adsorption of TCNQ on Sm_2O_3

Activation temperature: 500°C Solvent: 1,4-dioxane

Initial concentration 10^{-3}mol dm^{-3}	Equilibrium concentration 10^{-3}mol dm^{-3}	Amount adsorbed 10^{-5}mol m^{-2}	Magnetic moment BM
0	0	0	1.840
0.284	0.015	0.178	1.301
0.397	0.203	0.823	1.222
0.501	0.219	1.618	1.071
1.003	0.474	2.205	1.022
1.755	1.177	2.403	1.002
2.507	1.933	2.403	1.001

Fig.14 Magnetic moment of Sm_2O_3 as a function of equilibrium concentration of electron acceptor.

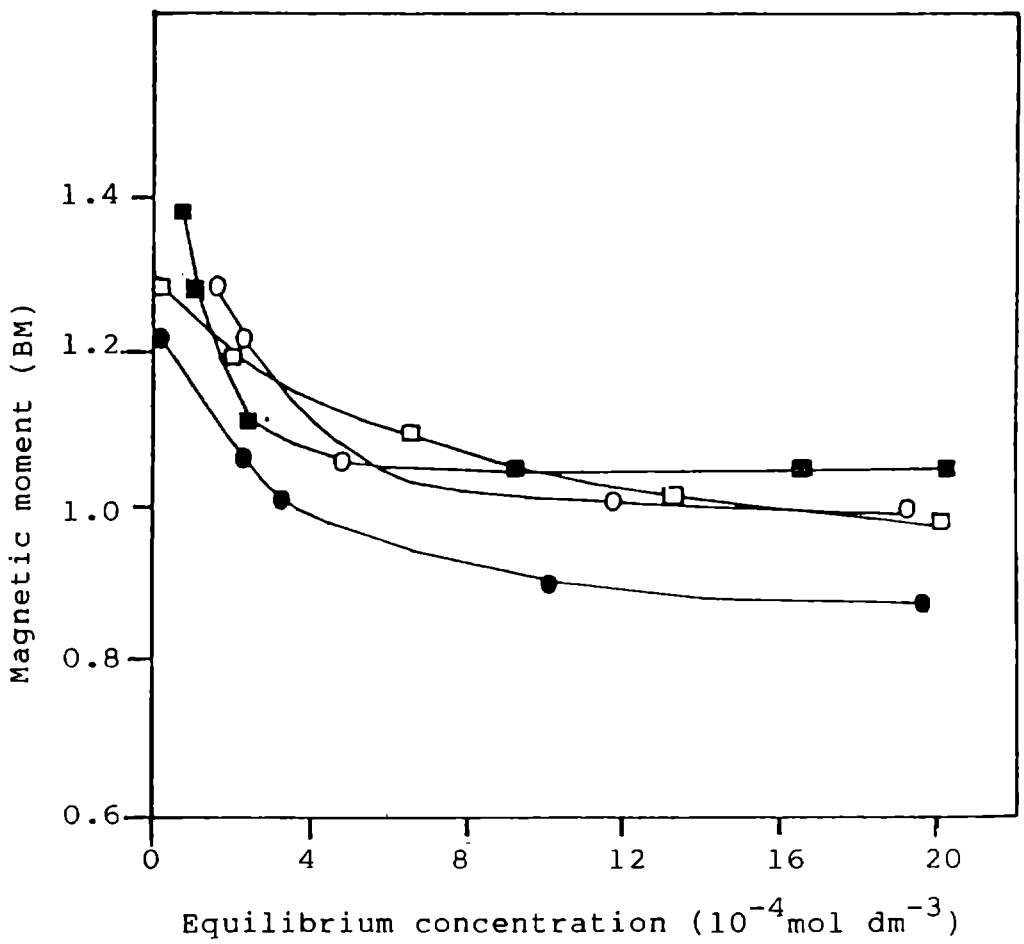

enables us to measure acid-base strength on a common scale. Visible colour change was obtained only for four indicators which are listed in Table 39.

Table 39: Hammett indicators used

Indicators	pKa	C O L O U R	
		Basic	Acidic
p-dimethyl amino azobenzene	+3.3	Yellow	Red
Methyl red	+4.8	Yellow	Red
Neutral red	+6.8	Yellow	Red
Bromothymol blue	+7.2	Blue	Yellow

Figures 15 and 16 show the acidity and basicity of Sm_2O_3 and CeO_2 at various acid-base strengths at different activation temperatures. The data are given in Tables 40 and 41.

The strength of an acidic or basic site can be expressed in terms of the Hammett acidity function H_o [21]. It is measured by using indicators that are adsorbed on the solid surface. If acidic sites of $H_o \leq pK_a$ of the indicator

Fig.15 Acid-base strength of Sm_2O_3 at various activation temperatures.

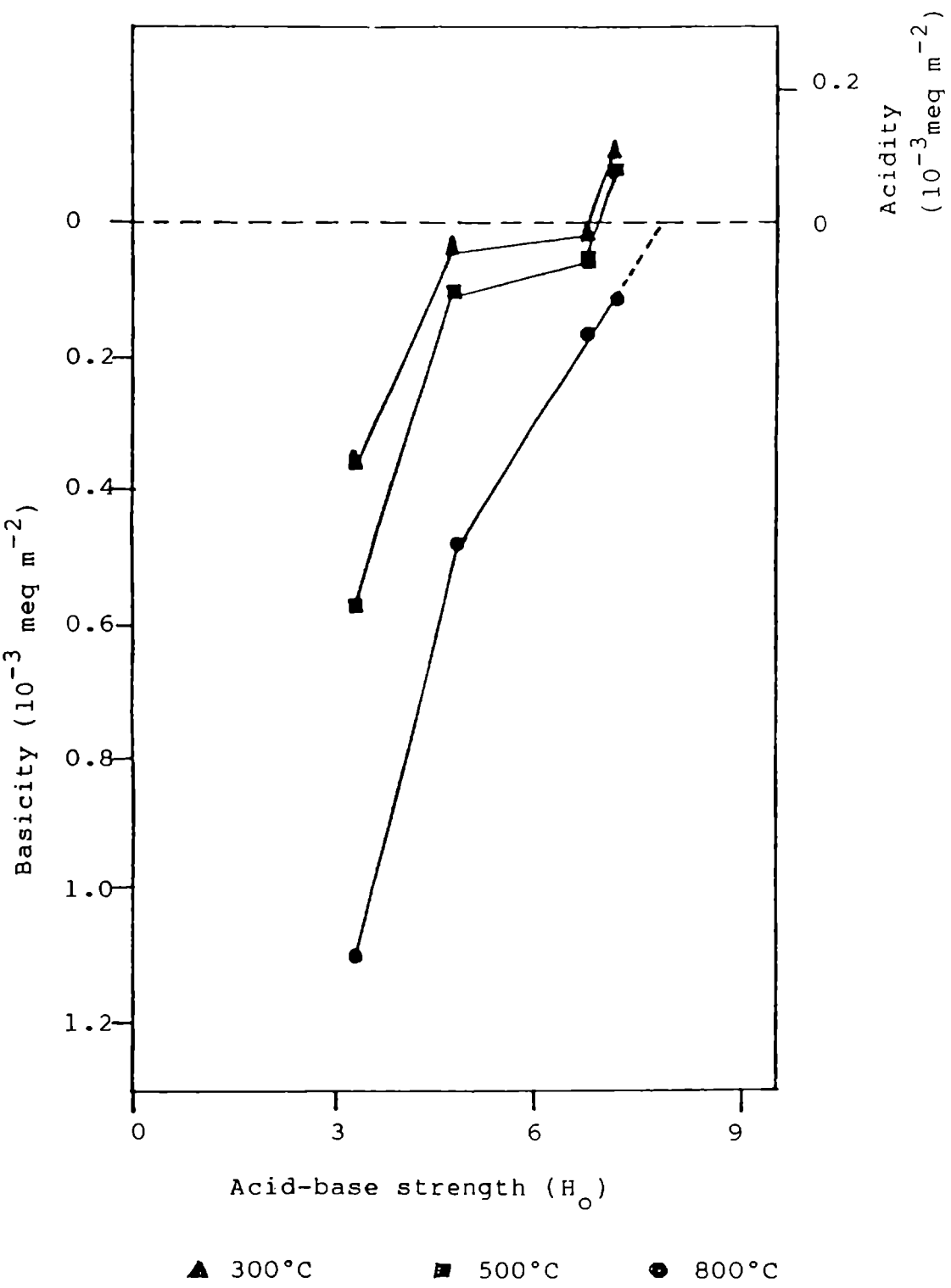

Fig.16 Acid-base strength of CeO_2 at various activation temperatures.

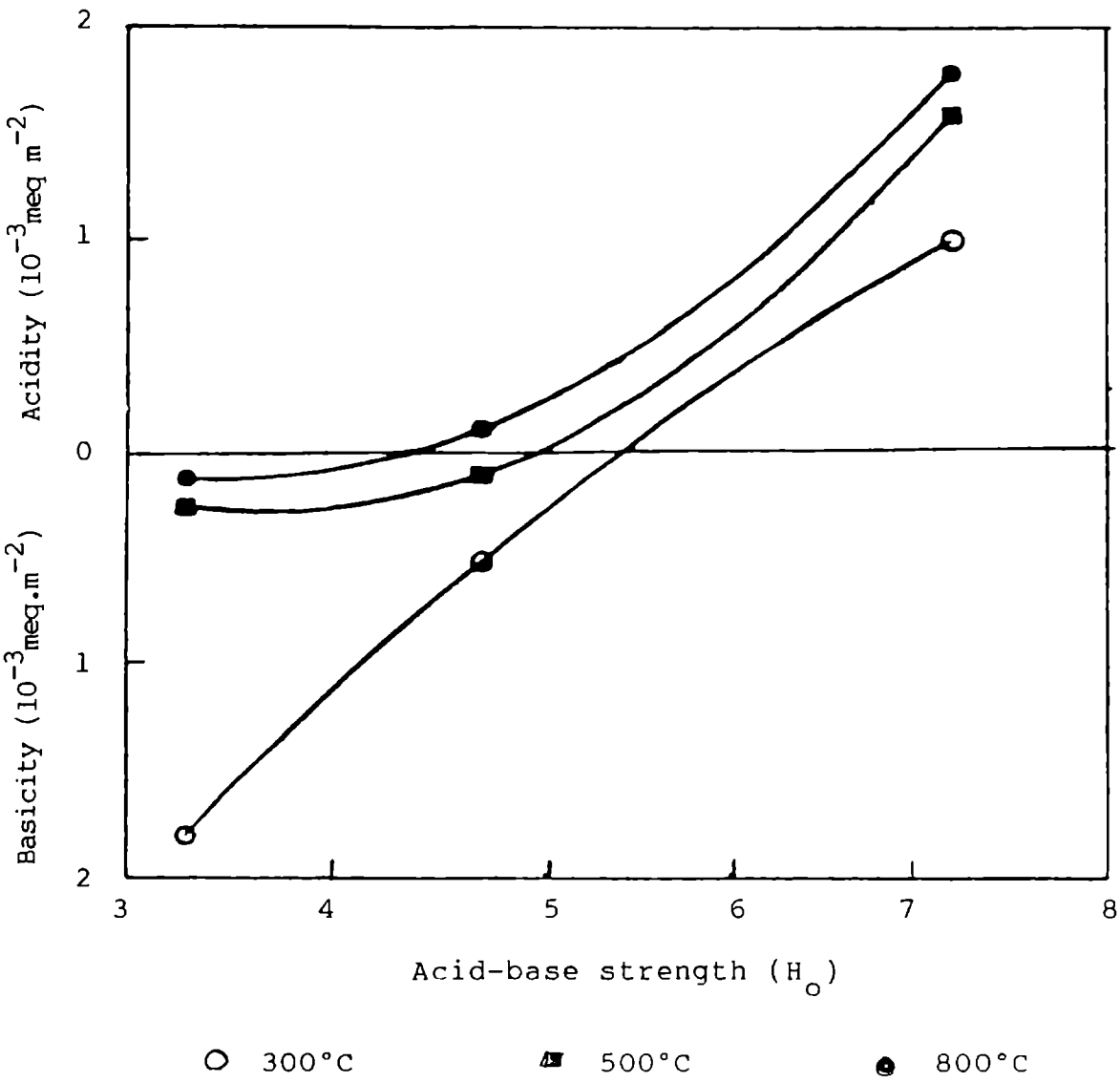

Table 40: Acid-base strength of Sm_2O_3 at various activation temperatures using different Hammett indicators

Temperature (°C)	Basicity (10^{-3}meq m^{-2})				Acidity (10^{-3} meq m^{-2}				
	$H_o \geqslant 3.3$	$H_o \geqslant 4.8$	$H_o \geqslant 6.8$	$H_o \geqslant 7.2$	$H_o \leqslant 3.3$	$H_o \leqslant 4.8$	$H_o \leqslant 6.8$	$H_o \leqslant 7.2$	$H_{o,max}$
300	0.37	0.04	0.04	--	--	--	--	0.11	6.9
500	0.62	0.14	0.06	--	--	--	--	0.10	7.0
800	1.10	4.49	0.16	0.11	--	--	--	--	8.0

Table 41: Acid-base strength of CeO_2 at various activation temperatures using different Hammett indicators

Tamperature (°C)	Basicity (10^{-3} meq m^{-2}				Acidity (10^{-3} meq m^{-2})				
	$H_o \geq 3.3$	$H_o \geq 4.8$	$H_o \geq 6.8$	$H_o \geq 7.2$	$H_o \leq 3.3$	$H_o \leq 4.8$	$H_o \leq 6.8$	$H_o \leq 7.2$	$H_{o,max}$
300	1.08	0.52	--	--	--	--	--	1.02	5.5
500	0.26	0.10	--	--	--	--	--	1.59	5.0
800	0.12	--	--	--	--	0.12	--	1.79	4.3

exist on a solid surface, the colour of the indicator changes to that of its conjugate acid. When a neutral acid indicator is adsorbed on a basic solid, the colour of the indicator changes to that of its conjugate base provided the solid oxide has sufficicient basic strength. Both acidity and basicity were determined on a common H_o scale. The acidity measured with an indicator shows the number of acidic sites whose acid strength $H_o \leq pK_a$ of the indicator, and the basicity shows the number of basic sites whose basic strength $H_\ominus \geq pK_a$ of the indicator. The acid-base strength distribution curves meet at a point on the abscissa, $H_{o,max}$ where acidity = basicity = 0 [22]. $H_{o,max}$ can be regarded as a practical parameter to represent the acid-base properties of solids, which is sensitive to the surface structure.

It is known that a solid with a large negative $H_{o,max}$ value has weak basic sites and that a solid with a large positive $H_{o,max}$ value has strong basic sites [22]. For Sm_2O_3 as activation temperature increases $H_{o,max}$ value increases which shows the increases in basic sites on the oxide surface. This trend is reversed in the case of cerium oxide ie., with increase in activation temperature

$H_{o,max}$ value decreases which in turn shows decrease in basic sites on the oxide.

Electron donating properties of mixed oxide systems

It is well known that two component metal oxide systems exhibit characteristic surface properties which are not qualitatively predictable from consideration of the independent properties of parent oxides. The mixed oxides of ceria with alumina and samaria with alumina were prepared for different weight % of the respective oxides, by co-precipitation method.

The electron donating properties of these mixed oxides were determined by using same set of electron acceptors ie., TCNQ and chloranil in acetonitrile and 1,4-dioxane. The adsorption isotherms obtained are of Langmuir type (Figs.17 and 18). Data are given in Tables 42-89. The limiting amount of electron acceptor adsorbed increases with increase in percentage of rare earth oxide as a consequence of the increase in concentration of Al-O-R bonds, where R stands for rare earth element. Further addition of rare earth oxide decreases the limiting amount without changing the limit of electron transfer. This may be due to the increase in concentration of rare earth oxide

Fig.17 Adsorption isotherms on Sm_2O_3/Al_2O_3

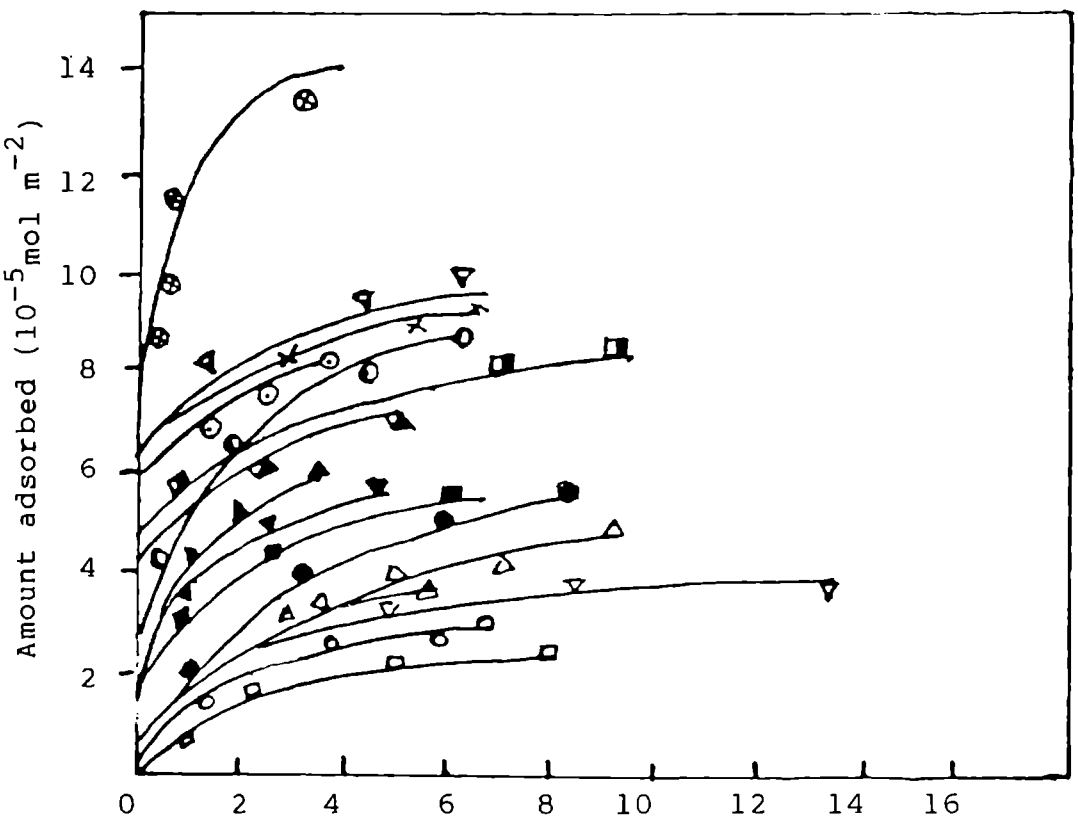

Electron acceptor/solvent/weight % of Sm_2O_3

[CA - Chloranil; AN - Acetonitrile;
TC - TCNQ; D - Dioxane]

CA/AN/10	CA/AN/20	CA/AN/40	CA/AN/75
TC/AN/10	TC/AN/20	TC/AN/40	TC/AN/75
CA/D/10	CA/D/20	CA/D/40	CA/D/75
TC/D/10	TC/D/20	TC/D/40	TC/D/75

Fig.18 Adsorption isotherms on CeO_2/Al_2O_3

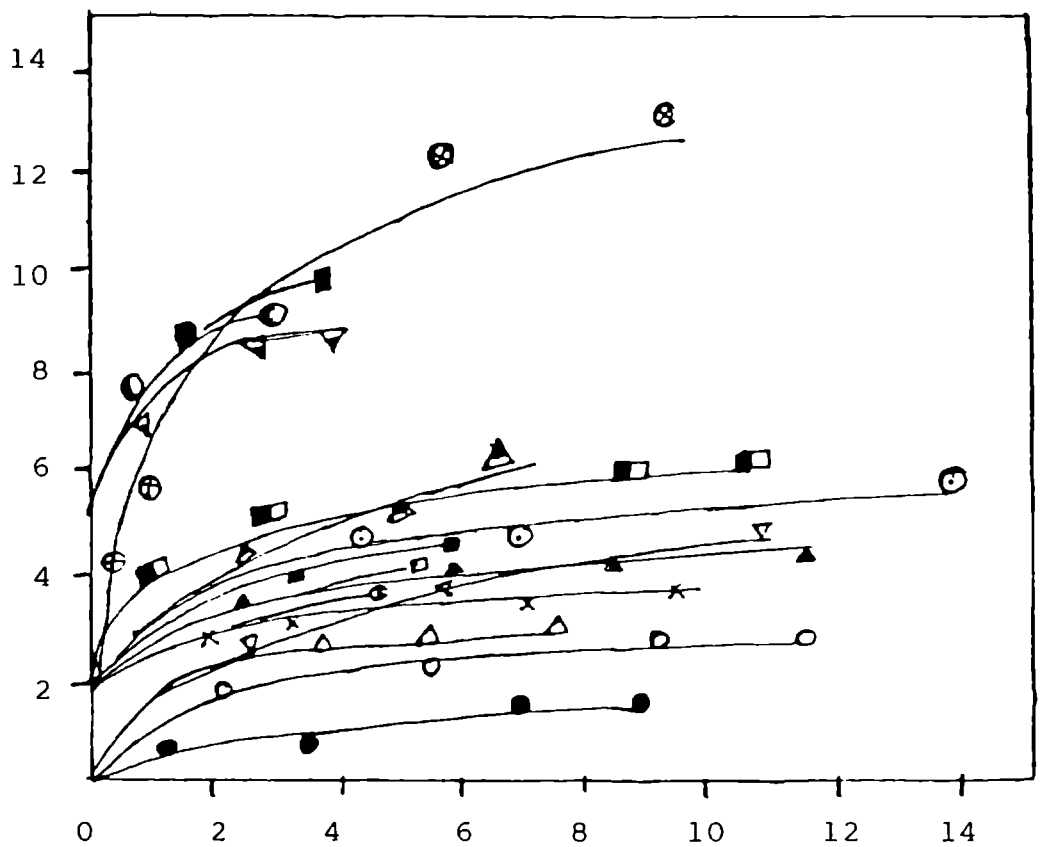

Electron acceptor/solvent/weight % of CeO_2

[CA - Chloranil; AN - Acetonitrile;
TC - TCNQ; D - Dioxane]

CA/AN/10	CA/AN/20	CA/AN/40	CA/AN/80
TC/AN/10	TC/AN/20	TC/AN/40	TC/AN/80
CA/D/10	CA/D/20	CA/D/40	CA/D/80
TC/D/10	TC/D/20	TC/D/40	TC/D/80

Table 42: Adsorption of Chloranil on Al_2O_3

Activation temperature: 500°C Solvent: Acetonitrile

Initial concentration 10^{-3}mol dm^{-3}	Equilibrium concentration 10^{-3}mol dm^{-3}	Amount adsorbed 10^{-5}mol m^{-2}
0.320	0.002	0.334
1.305	0.302	1.032
2.611	1.383	1.264
3.508	4.929	1.646
7,657	5.533	2.183
8.509	6.356	2.218

Table 43: Adsorption of TCNQ on Al_2O_3

Activation temperature: 500°C Solvent: Acetonitrile

Initial concentration 10^{-3}mol dm^{-3}	Equilibrium concentration 10^{-3}mol dm^{-3}	Amount adsorbed 10^{-5}mol m^{-2}
1.460	0.001	1.505
2.920	0.002	3.012
4.381	0.071	4.443
7.302	0.995	6.505
8.481	2.019	6.659
9.424	2.779	6.660

Table 44: Adsorption of Chloranil on Al_2O_3

Activation temperature: 500°C Solvent: 1,4-dioxane

Initial concentration 10^{-3}mol dm^{-3}	Equilibrium concentration 10^{-3}mol dm^{-3}	Amount adsorbed 10^{-5}mol m^{-2}
0.145	0.001	0.149
0.725	0.168	0.574
1.451	0.691	0.783
2.902	1.903	1.011
4.353	3.203	1.186

Table 45: Adsorption of TCNQ on Al_2O_3

Activation temperature: 500°C Solvent: 1,4-dioxane

Initial concentration 10^{-3}mol dm^{-3}	Equilibrium concentration 10^{-3}mol dm^{-3}	Amount adsorbed 10^{-5}mol m^{-2}
1.616	0.008	1.583
3.232	0.874	2.431
6.465	3.602	2.951
8.081	4.664	3.521
12.015	7.671	4.469
13.348	8.950	4.529

Table 46: Adsorption of Chloranil on 5% Sm_2O_3/Al_2O_3

Activation temperature: 500°C Solvent: Acetonitrile

Initial concentration 10^{-3}mol dm^{-3}	Equilibrium concentration 10^{-3}mol dm^{-3}	Amount adsorbed 10^{-5}mol m^{-2}
1.524	0.172	1.378
5.082	3.044	2.075
8.893	6.464	2.298
12.205	10.165	2.589
16.002	13.426	2.619
17.145	14.385	2.628
18.529	15.935	2.649

Table 47: Adsorption of TCNQ on 5% Sm_2O_3/Al_2O_3

Activation temperature: 500°C Solvent: Acetonitrile

Initial concentration 10^{-3}mol dm^{-3}	Equilibrium concentration 10^{-3}mol dm^{-3}	Amount adsorbed 10^{-5}mol m^{-2}
1.022	0.001	1.042
3.408	0.018	3.445
5.964	0.524	5.544
8.784	1.652	7.170
9.760	2.566	7.182
11.900	4.788	7.212

Table 48: Adsorption of Chloranil on 5% Sm_2O_3/Al_2O_3

Activation temperature: 500°C Solvent: 1,4-dioxane

Initial concentration 10^{-3}mol dm^{-3}	Equilibrium concentration 10^{-3}mol dm^{-3}	Amount adsorbed 10^{-5}mol m^{-2}
0.020	0.007	0.013
1.922	1.062	0.981
4.046	2.610	1.462
6.727	5.260	1.555
8.081	6.463	1.630
9.610	7.995	1.641

Table 49: Adsorption of TCNQ on 5% Sm_2O_3/Al_2O_3

Activation temperature: 500°C Solvent: 1,4-dioxane

Initial concentration 10^{-3}mol dm^{-3}	Equilibrium concentration 10^{-3}mol dm^{-3}	Amount adsorbed 10^{-5}mol m^{-2}
0.212	0.018	0.198
1.061	0.028	1.054
2.122	0.059	2.127
4.244	0.521	3.807
7.427	2.461	5.074
8.026	3.041	5.126

Table 50: Adsorption of Chloranil on 10% Sm_2O_3/Al_2O_3

Activation temperature: 500°C Solvent: Acetonitrile

Initial concentration 10^{-3}mol dm^{-3}	Equilibrium concentration 10^{-3}mol dm^{-3}	Amount adsorbed 10^{-5}mol m^{-2}
0.608	0.005	0.543
1.216	0.009	1.088
4.489	1.881	2.373
6.631	3.763	2.610
8.296	5.934	2.661
9.653	6.779	2.664

Table 51: Adsorption of TCNQ on 10% Sm_2O_3/Al_2O_3

Activation temperature: 500°C Solvent: Acetonitrile

Initial concentration 10^{-3}mol dm^{-3}	Equilibrium concentration 10^{-3}mol dm^{-3}	Amount adsorbed 10^{-5}mol m^{-2}
0.265	0.002	0.400
2.658	0.011	2.368
6.087	0.525	5.009
9.789	2.695	6.388
11.175	4.460	7.199
13.108	5.200	7.230

Table 52: Adsorption of Chloranil on 10% Sm_2O_3/Al_2O_3

Activation temperature: 500°C Solvent: 1,4-dioxane

Initial concentration 10^{-3}mol dm^{-3}	Equilibrium concentration 10^{-3}mol dm^{-3}	Amount adsorbed 10^{-5}mol m^{-2}
0.210	0.199	0.090
1.050	0.606	0.405
2.100	0.928	1.079
4.200	2.285	1.749
7.350	4.966	2.269
10.500	7.927	2.330

Table 53: Adsorption of TCNQ on 10% Sm_2O_3/Al_2O_3

Activation temperature: 500°C Solvent: 1,4-dioxane

Initial concentration 10^{-3}mol dm^{-3}	Equilibrium concentration 10^{-3}mol dm^{-3}	Amount adsorbed 10^{-5}mol m^{-2}
1.331	0.050	1.184
2.662	0.104	2.329
5.324	0.970	3.955
7.343	2.577	4.338
8.975	3.170	5.289
10.490	4.641	5.330

Table 54: Adsorption of Chloranil on 15% Sm_2O_3/Al_2O_3

Activation temperature: 500°C Solvent: Acetonitrile

Initial concentration 10^{-3}mol dm^{-3}	Equilibrium concentration 10^{-3}mol dm^{-3}	Amount adsorbed 10^{-5}mol m^{-2}
0.354	0.003	0.361
1.536	1.477	1.143
4.609	3.026	1.631
10.361	7.424	3.032
16.176	12.572	3.639
20.220	16.702	3.648

Table 55: Adsorption of TCNQ on 15% Sm_2O_3/Al_2O_3

Activation temperature: 500°C Solvent: Acetonitrile

Initial concentration 10^{-3}mol dm^{-3}	Equilibrium concentration 10^{-3}mol dm^{-3}	Amount adsorbed 10^{-5}mol m^{-2}
1.599	0.004	1.646
2.986	0.015	3.061
8.578	2.041	6.795
11.946	4.464	7.719
12.382	4.607	8.018
14.933	6.404	8.816
16.220	7.561	8.840

Table 56: Adsorption of Chloranil on 15% Sm_2O_3/Al_2O_3

Activation temperature: 500°C Solvent: 1,4-dioxane

Initial concentration 10^{-3}mol dm^{-3}	Equilibrium concentration 10^{-3}mol dm^{-3}	Amount adsorbed 10^{-5}mol m^{-2}
0.239	0.044	0.260
1.198	0.400	0.823
2.396	0.929	1.512
4.792	2.632	2.232
11.980	9.090	2.921
12.540	9.710	2.989

Table 57: Adsorption of TCNQ on 15% Sm_2O_3/Al_2O_3

Activation temperature: 500°C Solvent: 1,4-dioxane

Initial concentration 10^{-3}mol dm^{-3}	Equilibrium concentration 10^{-3}mol dm^{-3}	Amount adsorbed 10^{-5}mol m^{-2}
0.658	0.001	0.679
1.646	0.027	1.670
3.292	0.983	2.438
4.988	0.989	4.030
11.520	5.807	5.920
16.460	10.620	5.998

Table 58: Adsorption of Chloranil on 20% Sm_2O_3/Al_2O_3

Activation temperature: 500°C Solvent: Acetonitrile

Initial concentration 10^{-3}mol dm^{-3}	Equilibrium concentration 10^{-3}mol dm^{-3}	Amount adsorbed 10^{-5}mol m^{-2}
1.822	0.105	1.907
4.993	2.013	3.200
8.613	5.120	3.459
10.493	7.177	3.749
14.576	10.996	4.108
18.220	14.360	4.141

Table 59: Adsorption of TCNQ on 20% Sm_2O_3/Al_2O_3

Activation temperature: 500°C Solvent: Acetonitrile

Initial concentration 10^{-3}mol dm^{-3}	Equilibrium concentration 10^{-3}mol dm^{-3}	Amount adsorbed 10^{-5}mol m^{-2}
1.622	0.005	1.734
3.053	0.008	3.271
8.226	1.595	7.119
12.115	3.944	8.773
13.387	4.569	9.468
15.885	7.047	9.509

Table 60: Adsorption of Chloranil on 20% Sm_2O_3/Al_2O_3

Activation temperature: 500°C Solvent: 1,4-dioxane

Initial concentration 10^{-3}mol dm^{-3}	Equilibrium concentration 10^{-3}mol dm^{-3}	Amount adsorbed 10^{-5}mol m^{-2}
0.341	0.272	0.734
1.394	0.360	1.109
2.789	1.063	1.850
4.170	3.220	2.088
11.940	8.432	3.760
17.060	13.540	3.780

Table 61: Adsorption of TCNQ on 20% Sm_2O_3/Al_2O_3

Activation temperature: 500°C Solvent: 1,4-dioxane

Initial concentration 10^{-3}mol dm^{-3}	Equilibrium concentration 10^{-3}mol dm^{-3}	Amount adsorbed 10^{-5}mol m^{-2}
0.324	0.001	0.334
1.486	0.021	1.511
2.972	0.165	2.953
8.110	2.118	6.172
12.976	5.670	7.510
16.220	8.938	7.532

Table 62: Adsorption of Chloranil on 40% Sm_2O_3/Al_2O_3

Activation temperature: 500°C Solvent: Acetonitrile

Initial concentration 10^{-3}mol dm^{-3}	Equilibrium concentration 10^{-3}mol dm^{-3}	Amount adsorbed 10^{-5}mol m^{-2}
0.181	0.001	0.279
0.905	0.084	1.264
1.811	0.094	2.780
2.717	0.102	4.023
6.340	2.126	6.496
9.057	4.630	6.798

Table 63: Adsorption of TCNQ on 40% Sm_2O_3/Al_2O_3

Activation temperature: 500°C Solvent: Acetonitrile

Initial concentration 10^{-3}mol dm^{-3}	Equilibrium concentration 10^{-3}mol dm^{-3}	Amount adsorbed 10^{-5}mol m^{-2}
0.472	0.001	0.725
1.180	0.016	1.794
2.360	0.047	3.557
4.220	0.060	7.167
8.024	0.675	11.300
11.800	3.110	13.360

Table 64: Adsorption of Chloranil on 40% Sm_2O_3/Al_2O_3

Activation temperature: 500°C Solvent: 1,4-dioxane

Initial concentration 10^{-3}mol dm^{-3}	Equilibrium concentration 10^{-3}mol dm^{-3}	Amount adsorbed 10^{-5}mol m^{-2}
0.233	0.126	0.165
1.168	0.793	0.576
2.336	0.838	1.589
5.840	3.288	3.927
9.344	5.980	5.177
11.680	8.314	5.177

Table 65: Adsorption of TCNQ on 40% Sm_2O_3/Al_2O_3

Activation temperature: 500°C Solvent: 1,4-dioxane

Initial concentration 10^{-3}mol dm^{-3}	Equilibrium concentration 10^{-3}mol dm^{-3}	Amount adsorbed 10^{-5}mol m^{-2}
0.387	0.026	0.184
0.967	0.046	1.464
2.422	0.224	3.886
4.844	1.618	4.973
9.689	3.957	8.849
12.110	6.237	9.030

Table 66: Adsorption of Chloranil on 75% Sm_2O_3/Al_2O_3

Activation temperature: 500°C Solvent: Acetonitrile

Initial concentration 10^{-3}mol dm^{-3}	Equilibrium concentration 10^{-3}mol dm^{-3}	Amount adsorbed 10^{-5}mol m^{-2}
0.814	0.656	0.404
1.623	1.191	1.108
2.435	1.741	1.832
4.885	3.523	3.306
6.493	4.987	3.890
8.117	6.506	4.144

Table 67: Adsorption of TCNQ on 75% Sm_2O_3/Al_2O_3

Activation temperature: 500°C Solvent: Acetonitrile

Initial concentration 10^{-3}mol dm^{-3}	Equilibrium concentration 10^{-3}mol dm^{-3}	Amount adsorbed 10^{-5}mol m^{-2}
0.254	0.001	0.653
0.636	0.003	1.633
1.273	0.022	3.218
1.909	0.099	4.642
4.456	1.446	7.703
6.366	3.363	7.739

Table 68: Adsorption of Chloranil on 75% Sm_2O_3/Al_2O_3

Activation temperature: 500°C Solvent: 1,4-dioxane

Initial concentration 10^{-3}mol dm^{-3}	Equilibrium concentration 10^{-3}mol dm^{-3}	Amount adsorbed 10^{-5}mol m^{-2}
0.124	0.004	0.030
0.621	0.183	0.125
1.243	0.470	1.983
1.865	0.980	2.387
4.974	3.853	2.876
6.218	5.027	3.043

Table 69: Adsorption of TCNQ on 75% Sm_2O_3/Al_2O_3

Activation temperature: 500°C Solvent: 1,4-dioxane

Initial concentration 10^{-3}mol dm^{-3}	Equilibrium concentration 10^{-3}mol dm^{-3}	Amount adsorbed 10^{-5}mol m^{-2}
0.107	0.002	0.067
0.533	0.012	1.338
1.067	0.043	2.727
2.135	1.007	2.886
4.270	2.206	5.321
5.338	3.161	5.506

Table 70: Adsorption of Chloranil on 10% CeO_2/Al_2O_3

Activation temperature: 500°C Solvent: Acetonitrile

Initial concentration 10^{-3}mol dm^{-3}	Equilibrium concentration 10^{-3}mol dm^{-3}	Amount adsorbed 10^{-5}mol m^{-2}
1.032	0.027	0.971
2.064	0.166	1.742
4.128	0.968	2.910
7.224	3.348	3.561
10.320	5.944	3.582

Table 71: Adsorption of TCNQ on 10% CeO_2/Al_2O_3

Activation temperature: 500°C Solvent: Acetonitrile

Initial concentration 10^{-3}mol dm^{-3}	Equilibrium concentration 10^{-3}mol dm^{-3}	Amount adsorbed 10^{-5}mol m^{-2}
1.380	0.001	1.262
2.760	0.043	4.998
5.521	0.051	5.993
11.041	1.618	8.662
13.800	3.858	8.693

Table 72: Adsorption of Chloranil on 10% CeO_2/Al_2O_3

Activation temperature: 500°C Solvent: 1,4-dioxane

Initial concentration 10^{-3}mol dm^{-3}	Equilibrium concentration 10^{-3}mol dm^{-3}	Amount adsorbed 10^{-5}mol m^{-2}
0.209	0.137	0.067
1.062	0.531	0.487
2.124	1.247	0.579
4.248	3.574	0.623
8.496	7.008	1.371
10.601	8.910	1.380

Table 73: Adsorption of TCNQ on 10% CeO_2/Al_2O_3

Activation temperature: 500°C Solvent: 1,4-dioxane

Initial concentration 10^{-3}mol dm^{-3}	Equilibrium concentration 10^{-3}mol dm^{-3}	Amount adsorbed 10^{-5}mol m^{-2}
1.128	0.107	0.938
2.250	0.238	1.853
4.500	2.208	2.120
9.003	5.220	3.482
11.250	5.587	4.801
12.241	6.557	4.920

Table 74: Adsorption of Chloranil on 20% CeO_2/Al_2O_3

Activation temperature: 500°C Solvent: Acetonitrile

Initial concentration 10^{-3}mol dm^{-3}	Equilibrium concentration 10^{-3}mol dm^{-3}	Amount adsorbed 10^{-5}mol m^{-2}
0.293	0.024	0.238
1.464	0.122	1.237
2.928	0.482	2.255
5.856	2.538	3.059
11.710	7.609	3.782
14.640	10.440	3.873

Table 75: Adsorption of TCNQ on 20% CeO_2/Al_2O_3

Activation temperature: 500°C Solvent: Acetonitrile

Initial concentration 10^{-3}mol dm^{-3}	Equilibrium concentration 10^{-3}mol dm^{-3}	Amount adsorbed 10^{-5}mol m^{-2}
0.353	0.003	0.332
1.764	0.010	1.617
3.528	0.016	3.529
7.040	0.631	5.911
14.080	3.769	9.518
17.640	5.882	10.836

Table 76: Adsorption of Chloranil on 20% CeO_2/Al_2O_3

Activation temperature: 500°C Solvent: 1,4-dioxane

Initial concentration 10^{-3}mol dm^{-3}	Equilibrium concentration 10^{-3}mol dm^{-3}	Amount adsorbed 10^{-5}mol m^{-2}
1.240	0.751	0.451
2.480	1.094	1.282
4.960	2.145	1.678
6.832	4.770	1.899
9.920	7.440	2.805
12.400	9.244	2.930

Table 77: Adsorption of TCNQ on 20% CeO_2/Al_2O_3

Activation temperature: 500°C Solvent: 1,4-dioxane

Initial concentration 10^{-3}mol dm^{-3}	Equilibrium concentration 10^{-3}mol dm^{-3}	Amount adsorbed 10^{-5}mol m^{-2}
0.244	0.041	0.186
1.220	0.222	0.921
2.440	0.313	1.962
4.880	1.634	3.547
8.540	2.757	5.202
12.200	6.546	5.333

Table 78: Adsorption of Chloranil on 40% CeO_2/Al_2O_3

Activation temperature: 500°C Solvent: Acetonitrile

Initial concentration 10^{-3}mol dm^{-3}	Equilibrium concentration 10^{-3}mol dm^{-3}	Amount adsorbed 10^{-5}mol m^{-2}
0.352	0.017	0.225
1.760	0.103	0.912
3.520	1.014	3.129
7.040	4.440	3.560
13.020	8.760	5.208
17.600	13.900	5.320

Table 79: Adsorption of TCNQ on 40% CeO_2/Al_2O_3

Activation temperature: 500°C Solvent: Acetonitrile

Initial concentration 10^{-3}mol dm^{-3}	Equilibrium concentration 10^{-3}mol dm^{-3}	Amount adsorbed 10^{-5}mol m^{-2}
0.389	0.001	0.485
1.947	0.089	2.322
3.894	0.480	4.263
5.841	1.387	5.600
15.570	5.630	12.713
19.470	9.293	13.430

Table 80: Adsorption of Chloranil on 40% CeO_2/Al_2O_3

Activation temperature: 500°C Solvent: 1,4-dioxane

Initial concentration 10^{-3}mol dm^{-3}	Equilibrium concentration 10^{-3}mol dm^{-3}	Amount adsorbed 10^{-5}mol m^{-2}
0.295	0.032	0.329
1.478	0.758	0.899
2.956	1.533	1.773
5.912	3.841	2.585
10.930	7.359	4.396
14.780	11.213	4.490

Table 81: Adsorption of TCNQ on 40% CeO_2/Al_2O_3

Activation temperature: 500°C Solvent: 1,4-dioxane

Initial concentration 10^{-3}mol dm^{-3}	Equilibrium concentration 10^{-3}mol dm^{-3}	Amount adsorbed 10^{-5}mol m^{-2}
0.301	0.009	0.364
1.507	0.192	1.635
3.016	0.241	3.459
6.028	2.001	5.020
12.050	7.620	5.432
15.070	10.526	5.531

Table 82: Adsorption of Chloranil on 60% CeO_2/Al_2O_3

Activation temperature: 500°C Solvent: Acetonitrile

Initial concentration 10^{-3}mol dm^{-3}	Equilibrium concentration 10^{-3}mol dm^{-3}	Amount adsorbed 10^{-5}mol m^{-2}
0.132	0.002	0.152
0.659	0.006	0.909
1.318	0.032	1.781
2.636	0.326	3.215
5.218	2.056	4.398
6.523	3.302	4.482

Table 83: Adsorption of TCNQ on 60% CeO_2/Al_2O_3

Activation temperature: 500°C Solvent: Acetonitrile

Initial concentration 10^{-3}mol dm^{-3}	Equilibrium concentration 10^{-3}mol dm^{-3}	Amount adsorbed 10^{-5}mol m^{-2}
0.318	0.001	0.441
1.589	0.004	2.205
3.178	0.012	4.448
4.767	0.231	6.634
11.700	3.827	10.957
15.890	7.817	11.235

Table 84: Adsorption of Chloranil on 60% CeO_2/Al_2O_3

Activation temperature: 500°C Solvent: 1,4-dioxane

Initial concentration 10^{-3}mol dm^{-3}	Equilibrium concentration 10^{-3}mol dm^{-3}	Amount adsorbed 10^{-5}mol m^{-2}
0.131	0.042	0.124
0.655	0.048	0.844
2.260	0.591	2.324
4.520	2.260	3.145
8.205	5.820	3.520
10.250	7.572	3.727

Table 85: Adsorption of TCNQ on 60% CeO_2/Al_2O_3

Activation temperature: 500°C Solvent: 1,4-dioxane

Initial concentration 10^{-3}mol dm^{-3}	Equilibrium concentration 10^{-3}mol dm^{-3}	Amount adsorbed 10^{-5}mol m^{-2}
0.154	0.019	0.188
0.772	0.043	0.482
1.544	0.496	1.458
3.089	1.284	2.526
6.178	2.918	4.532
7.723	4.441	4.565

Table 86: Adsorption of Chloranil on 80% CeO_2/Al_2O_3

Activation temperature: 500°C Solvent: Acetonitrile

Initial concentration 10^{-3}mol dm^{-3}	Equilibrium concentration 10^{-3}mol dm^{-3}	Amount adsorbed 10^{-5}mol m^{-2}
0.288	0.007	0.449
1.410	0.162	2.039
2.880	0.963	3.061
5.760	3.202	4.084
10.900	8.267	4.082
14.401	11.902	4.084

Table 87: Adsorption of TCNQ on 80% CeO_2/Al_2O_3

Activation temperature: 500°C Solvent: Acetonitrile

Initial concentration 10^{-3}mol dm^{-3}	Equilibrium concentration 10^{-3}mol dm^{-3}	Amount adsorbed 10^{-5}mol m^{-2}
0.832	0.001	1.327
1.663	0.148	2.633
3.326	0.274	4.874
6.648	1.299	8.541
8.315	2.702	8.968

Table 88: Adsorption of Chloranil on 80% CeO_2/Al_2O_3

Activation temperature: 500°C Solvent: 1,4-dioxane

Initial concentration 10^{-3}mol dm^{-3}	Equilibrium concentration 10^{-3}mol dm^{-3}	Amount adsorbed 10^{-5}mol m^{-2}
1.318	0.336	1.568
2.636	1.329	2.087
5.272	3.570	2.590
9.755	8.131	2.601
13.180	11.500	2.680

Table 89: Adsorption of TCNQ on 80% CeO_2/Al_2O_3

Activation temperature: 500°C Solvent: 1,4-dioxane

Initial concentration 10^{-3}mol dm^{-3}	Equilibrium concentration 10^{-3}mol dm^{-3}	Amount adsorbed 10^{-5}mol m^{-2}
0.191	0.019	0.273
0.954	0.206	1.194
1.908	0.475	2.286
3.817	1.540	3.511
7.253	5.054	3.636
9.544	7.245	3.671

Fig.19 Limiting amount of electron acceptor adsorbed as a function of composition of Sm_2O_3/Al_2O_3.

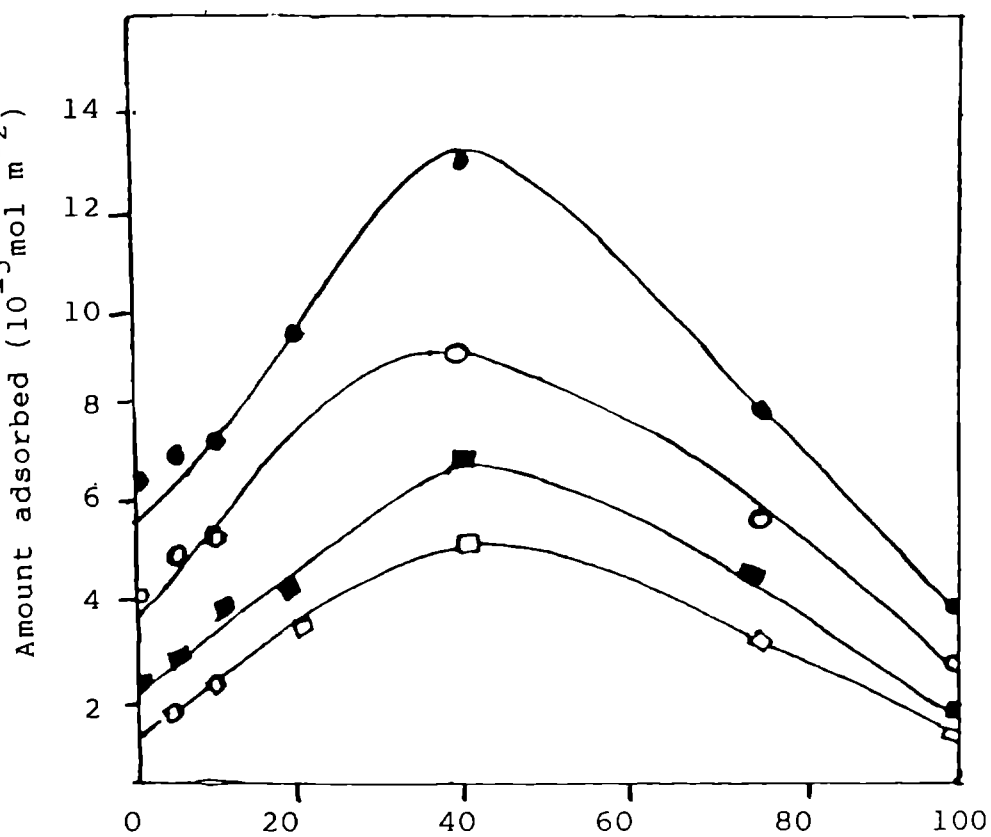

Electron acceptor/solvent

[CA - Chloranil; AN - Acetonitrile;
TC - TCNQ; D - Dioxane]

CA/AN CA/D

TC/AN TC/D

Fig.20 Limiting amount of electron acceptor adsorbed as a function of composition of CeO_2/Al_2O_3.

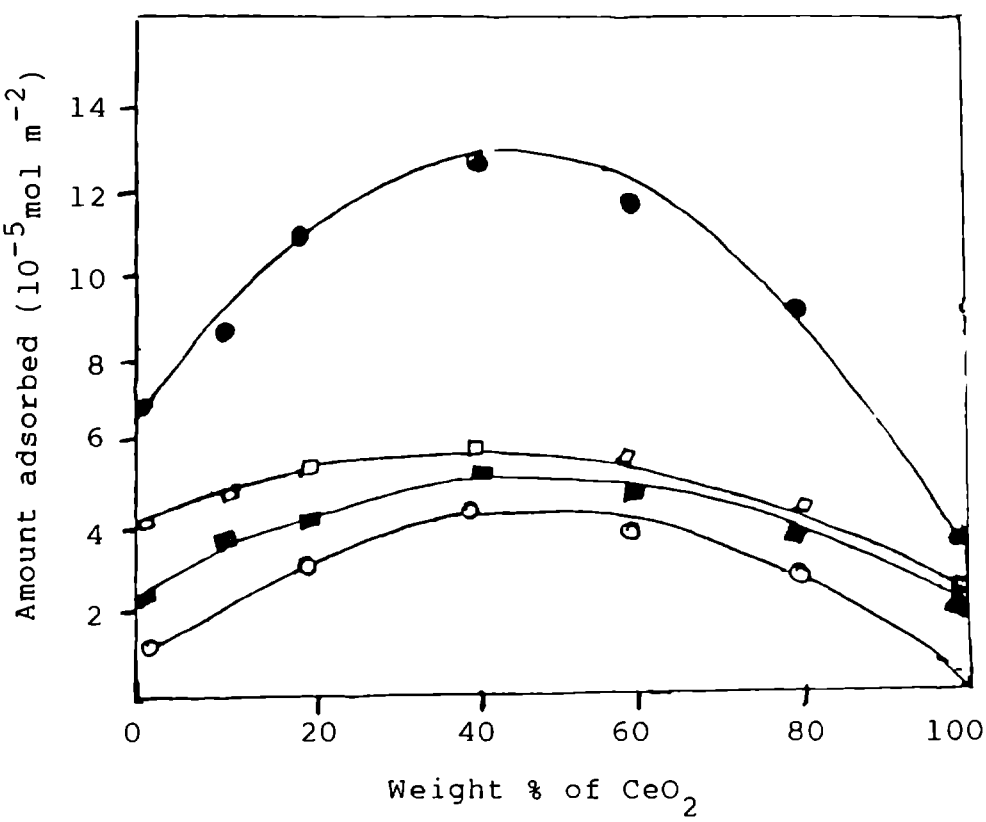

Fig.21 Acid-base strength distribution of Sm_2O_3/Al_2O_3

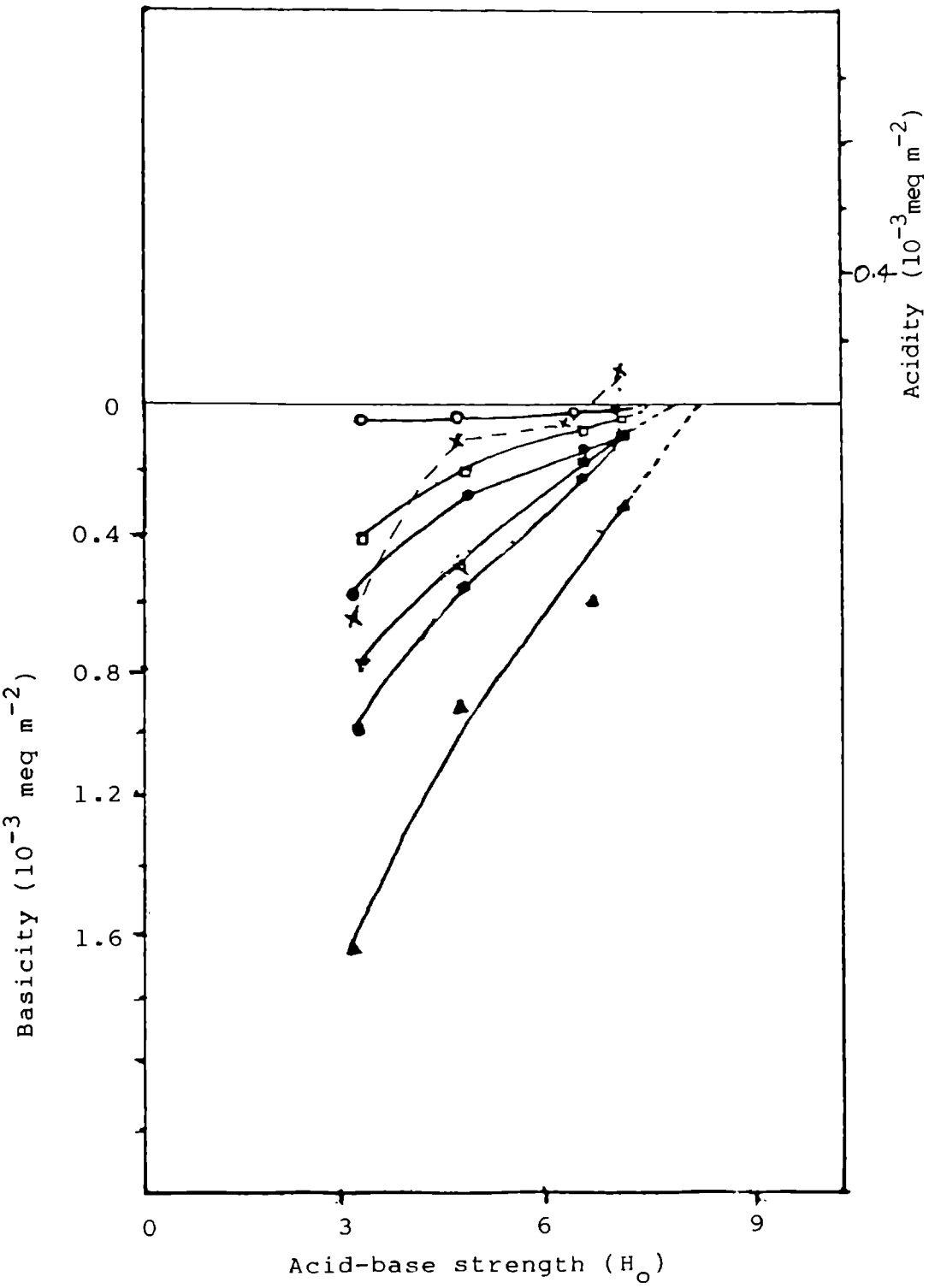

Fig.22 Acid-base strength distribution of CeO_2/Al_2O_3

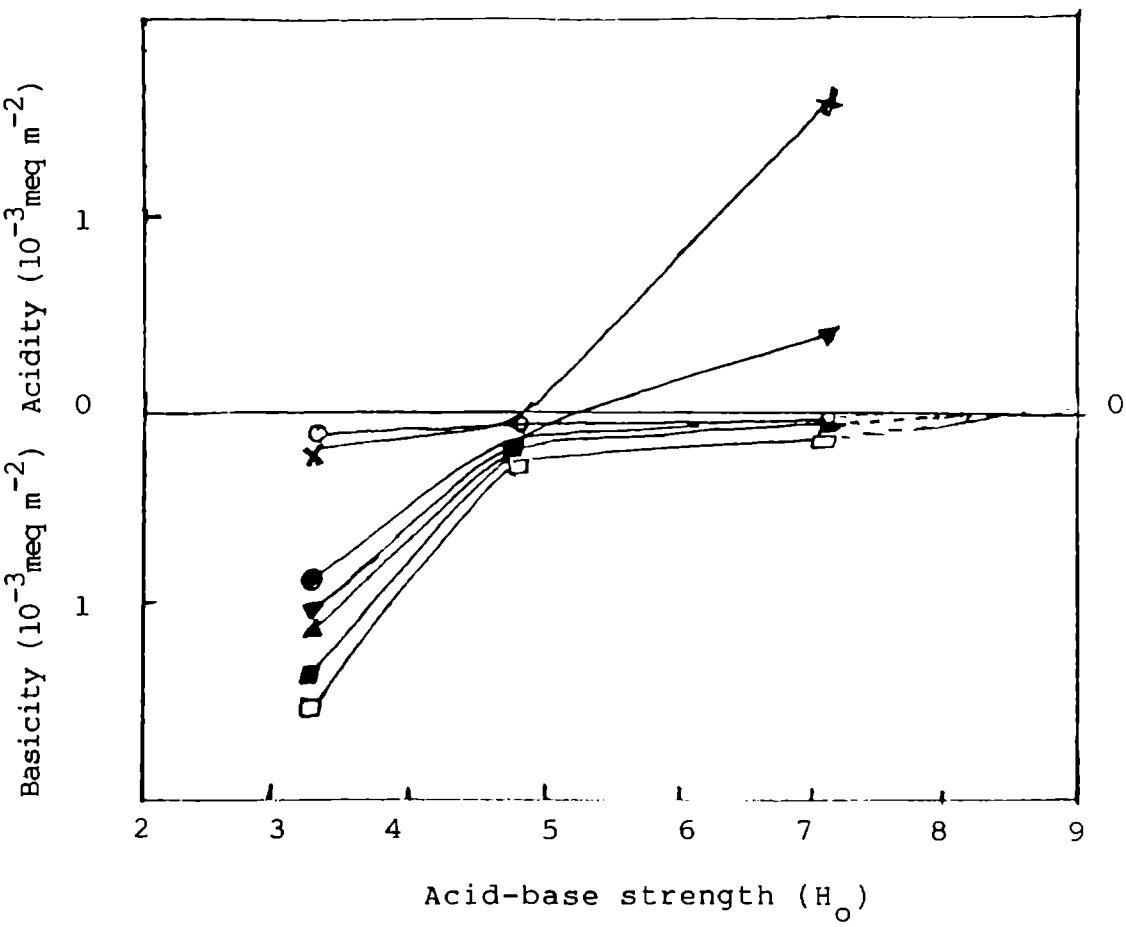

- Al_2O_3
- 10% CeO_2/Al_2O_3
- 20% CeO_2/Al_2O_3
- 40% CeO_2/Al_2O_3
- 60% CeO_2/Al_2O_3
- 80% CeO_2/Al_2O_3
- CeO_2

Table 90: Acidity and basicity of Sm_2O_3/Al_2O_3

Oxides	Basicity (10^{-3}meq m^{-2})				Acidity (10^{-3}meq m^{-2})				
	$H_o \geq 3.3$	$H_o \geq 4.8$	$H_o \geq 6.8$	$H_o \geq 7.2$	$H_o \leq 3.3$	$H_o \leq 4.8$	$H_o \leq 6.8$	$H_o \leq 7.2$	$H_{o,max}$
100% Sm_2O_3 [500°C]	0.62	0.14	0.06	-	-	-	-	0.10	7.0
100% Al_2O_3 [500°C]	0.04	0.03	0.01	0.01	-	-	-	-	7.5
5% Sm_2O_3/Al_2O_3	0.42	0.20	0.10	0.05	-	-	-	-	7.5
10% Sm_2O_3/Al_2O_3	0.61	0.27	0.18	0.09	-	-	-	-	8.0
15% Sm_2O_3/Al_2O_3	0.82	0.51	0.20	0.10	-	-	-	-	8.0
20% Sm_2O_3/Al_2O_3	0.96	0.69	0.31	0.16	-	-	-	-	8.0
40% Sm_2O_3/Al_2O_3	1.68	0.72	0.61	0.30	-	-	-	-	8.5
75% Sm_2O_3/Al_2O_3	1.15	0.64	0.25	0.12	-	-	-	-	7.5

Table 91: Acidity and basicity of CeO_2/Al_2O_3

Oxides	Basicity (10^{-3}meq m^{-2})				Acidity (10^{-3}meq m^{-2})				
	$H_o \geq 3.3$	$H_o \geq 4.8$	$H_o \geq 6.8$	$H_o \geq 7.2$	$H_o \leq 3.3$	$H_o \leq 4.8$	$H_o \leq 6.8$	$H_o \leq 7.2$	$H_{o,max}$
100% CeO_2 [500°C]	0.73	0.10	-	-	-	-	-	1.59	5.0
100% Al_2O_3 [500°C]	0.04	0.03	0.01	0.01	-	-	-	-	7.5
10% CeO_2/Al_2O_3	0.91	0.11	-	0.06	-	-	-	-	8.4
20% CeO_2/Al_2O_3	1.41	0.21	-	0.09	-	-	-	-	8.4
40% CeO_2/Al_2O_3	1.57	0.28	-	0.12	-	-	-	-	8.5
60% CeO_2/Al_2O_3	1.16	0.21	-	0.09	-	-	-	-	8.4
80% CeO_2/Al_2O_3	1.10	0.15	-	-	-	-	-	0.35	5.4

in the mixed oxide lattice because rare earth oxide has lower electron donicity than Al_2O_3. Figs.19 and 20 show the variation in the limiting amounts of electron acceptor adsorbed as a function of composition of mixed oxides.

The surface electron properties of alumina are promoted by the rare earth oxide without changing the limit of electron transfer. The concentration and strength of acidic and basic sites on the surface of these mixed oxides are measured by titration method using Hammett indicators (Figs.21 and 22). Data are given in Tables 90-91. $H_{o,max}$ value parallel the electron donating properties of the mixed oxides.

Catalytic activity

In order to correlate electron donating and acid-base properties of the oxides with their catalytic activity the following reactions were studied:

I. Reduction of

(i) Cyclohexanone

(ii) Acetophenone and

(iii) Benzophenone in presence of isopropanol,

II. Oxidation of cyclohexanol in presence of benzophenone using these oxides as catalysts

When a ketone in the presence of a base is used as the oxidising agent the reaction is known as Oppenauer oxidation. This reaction is the reverse of Meerwein-Ponndorf-Verley type reduction of ketones. Oppenauer oxidation of secondary alcohols proceeds efficiently using benzophenone as the hydrogen acceptor [23]. It has high ability for oxidising the alcohol and to resist aldol condensation [24]. The catalytic activity of these oxides can be rationalized in terms of the mechanism (Scheme I) proposed by Shibagaki et al [25] for oxidation and reduction using ZrO_2 as the catalyst. It has already been established from primary, kinetic isotope effect studies that k_3 is the rate determining step [25]. The mechanism involves hydride transfer from alcohol to the carbonyl carbon of the ketone. Lewis basicity of the catalyst surface favours the hydride transfer.

Sm_2O_3 and CeO_2 activated at 300, 500 and 800°C and mixed oxides of these rare earth oxides with alumina are found to be effective catalysts for the oxidation-reduction reactions. Data are given in Tables 92-95.

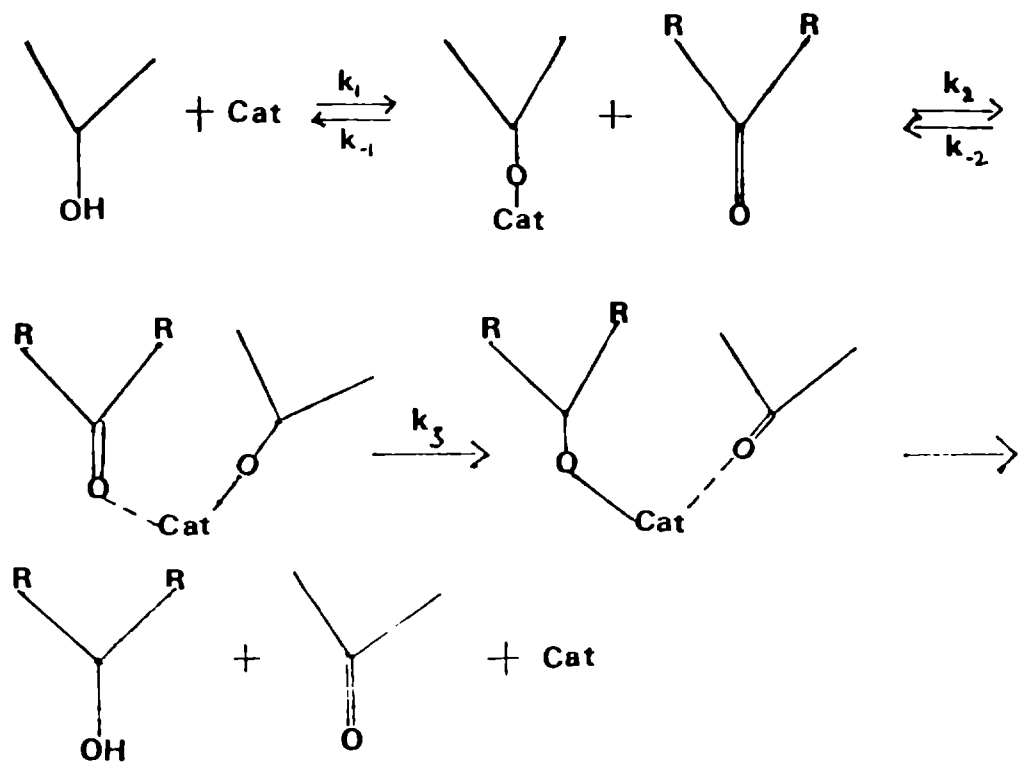

Scheme 1

Table 92: Oxidation of cyclohexanol to cyclohexanone with benzophenone

Catalyst	Conversion %	Rate constant $s^{-1}\ m^{-2}$
Sm_2O_3 [300°C]	52.99	3.183×10^{-6}
Sm_2O_3 [500°C]	66.48	7.170×10^{-6}
Sm_2O_3 [800°C]	92.85	4.950×10^{-5}
Al_2O_3 [500°C]	55.55	2.306×10^{-6}
5% Sm_2O_3/Al_2O_3	80.08	2.425×10^{-6}
10% Sm_2O_3/Al_2O_3	82.71	4.438×10^{-6}
20% Sm_2O_3/Al_2O_3	91.08	7.213×10^{-6}
40% Sm_2O_3/Al_2O_3	92.89	1.120×10^{-5}
75% Sm_2O_3/Al_2O_3	74.32	9.448×10^{-6}
CeO_2 [300°C]	68.75	5.113×10^{-6}
CeO_2 [500°C]	60.20	1.593×10^{-6}
CeO_2 [800°C]	58.22	1.453×10^{-6}
10% CeO_2/Al_2O_3	81.38	2.505×10^{-6}
20% CeO_2/Al_2O_3	84.15	2.631×10^{-6}
40% CeO_2/Al_2O_3	93.47	9.470×10^{-6}
60% CeO_2/Al_2O_3	81.76	5.463×10^{-6}
80% CeO_2/Al_2O_3	72.84	1.773×10^{-6}

Reaction temperature 110°C

Table 93: Reduction of cyclohexanone to cyclohexanol with 2-propanol

Catalyst	Conversion %	Rate constant $s^{-1}\ m^{-2}$
Sm_2O_3 [300°C]	-	--
Sm_2O_3 [500°C]	29.31	1.468×10^{-7}
Sm_2O_3 [800°C]	82.00	8.763×10^{-7}
Al_2O_3 [500°C]	32.18	2.085×10^{-8}
5% Sm_2O_3/Al_2O_3	39.82	2.664×10^{-8}
10% Sm_2O_3/Al_2O_3	57.83	5.608×10^{-8}
20% Sm_2O_3/Al_2O_3	62.25	7.451×10^{-8}
40% Sm_2O_3/Al_2O_3	71.63	2.133×10^{-7}
75% Sm_2O_3/Al_2O_3	52.27	1.633×10^{-7}
CeO_2 [300°C]	47.93	1.511×10^{-7}
CeO_2 [500°C]	2.00	1.073×10^{-8}
CeO_2 [800°C]	-	--
10% CeO_2/Al_2O_3	33.93	2.879×10^{-8}
20% CeO_2/Al_2O_3	40.57	3.703×10^{-8}
40% CeO_2/Al_2O_3	53.68	7.758×10^{-8}
60% CeO_2/Al_2O_3	51.35	7.738×10^{-8}
80% CeO_2/Al_2O_3	35.42	5.338×10^{-8}

Reaction temperature: 80°C.

Table 94: Reduction of acetophenone to 2-phenylethanol with 2-propanol

Catalyst	Conversion %	Rate constant $s^{-1}\ m^{-2}$
Sm_2O_3 [300°C]	-	--
Sm_2O_3 [500°C]	71.97	3.421×10^{-7}
Sm_2O_3 [800°C]	85.47	9.789×10^{-7}
Al_2O_3 [500°C]	-	--
5% Sm_2O_3/Al_2O_3	29.29	2.733×10^{-9}
10% Sm_2O_3/Al_2O_3	38.35	3.396×10^{-8}
20% Sm_2O_3/Al_2O_3	57.82	7.150×10^{-8}
40% Sm_2O_3/Al_2O_3	94.40	4.981×10^{-7}
75% Sm_2O_3/Al_2O_3	91.93	4.065×10^{-7}

Reaction temperature 80°C

Table 95: Reduction of benzophenone to diphenylcarbonol with 2-propanol

Catalyst	Conversion %	Rate constant $s^{-1}\ m^{-2}$
Sm_2O_3 [300°C]	-	--
Sm_2O_3 [500°C]	8.70	2.821×10^{-8}
Sm_2O_3 [800°C]	82.00	8.220×10^{-7}
Al_2O_3 [500°C]	-	--
5% Sm_2O_3/Al_2O_3	-	--
10% Sm_2O_3/Al_2O_3	2.70	1.921×10^{-8}
20% Sm_2O_3/Al_2O_3	31.82	2.175×10^{-8}
40% Sm_2O_3/Al_2O_3	37.84	9.643×10^{-8}
75% Sm_2O_3/Al_2O_3	37.09	7.061×10^{-8}

Reaction temperature: 80°C

Among the three ketones, reduction of benzophenone is the slowest because of the lower electron density at the carbonyl carbon of benzophenone [23].

The reaction was followed by CHEMITO 8510 gas Chromatograph. No by products were detected. The kinetics of these reactions have also been studied. The activity is reported as the first order rate coefficient per unit area of the catalyst surface. The rate coefficients are determined from the graphical method (Figs.23-26).

The rate of oxidation and reduction increases with increase in basicity of the oxide. For Sm_2O_3 as activation temperature increases the catalytic activity also increases and highest activity was shown by Sm_2O_3 activated at 800°c. Cerium oxide is effective only in the reduction of cyclohexanone. The activity of CeO_2 for oxidation-reductions is low compared to Sm_2O_3. As the activation temperature increases the catalytic activity of ceria decreases which parallel their basicities. The catalytic activity of samaria and ceria as a function of activation temperature are shown in Figs.27 and 28.

Fig.23 Kinetics of oxidation of cyclohexanol on Sm_2O_3 catalyst activated at different temperatures.

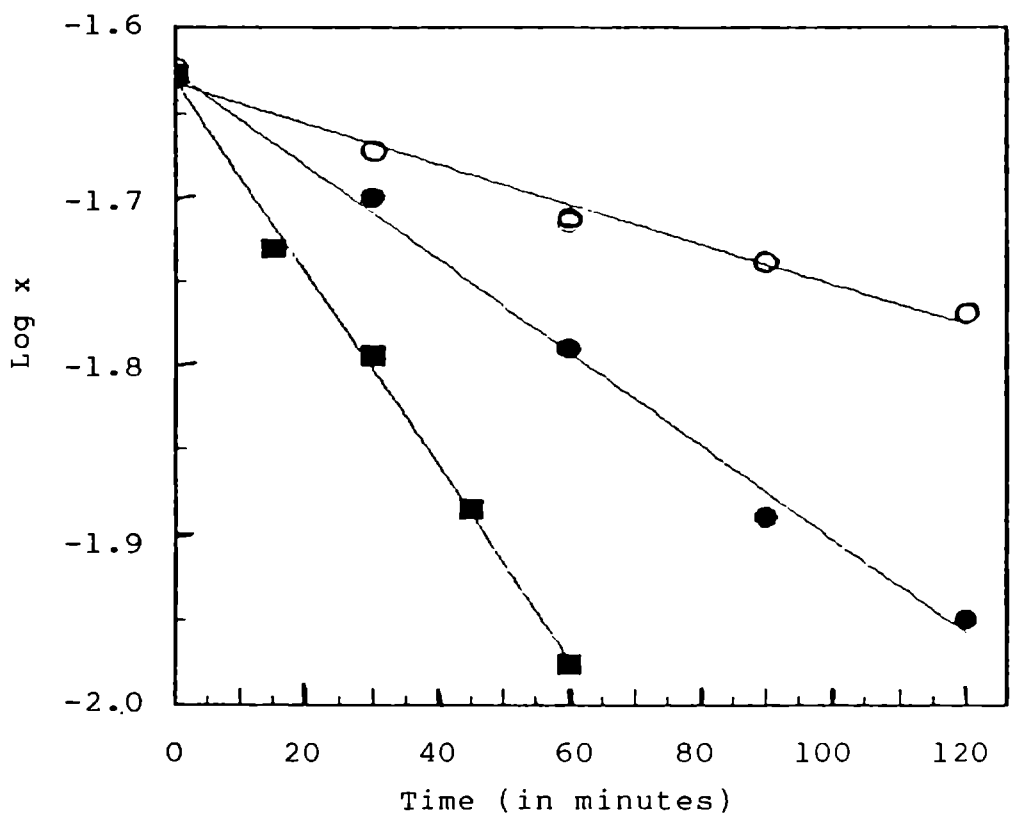

X is the concentration of cyclohexanol.

○ 300°C ● 500°C ■ 800°C

Fig.24 Kinetics of oxidation of cyclohexanol on CeO_2 catalyst activated at different temperatures.

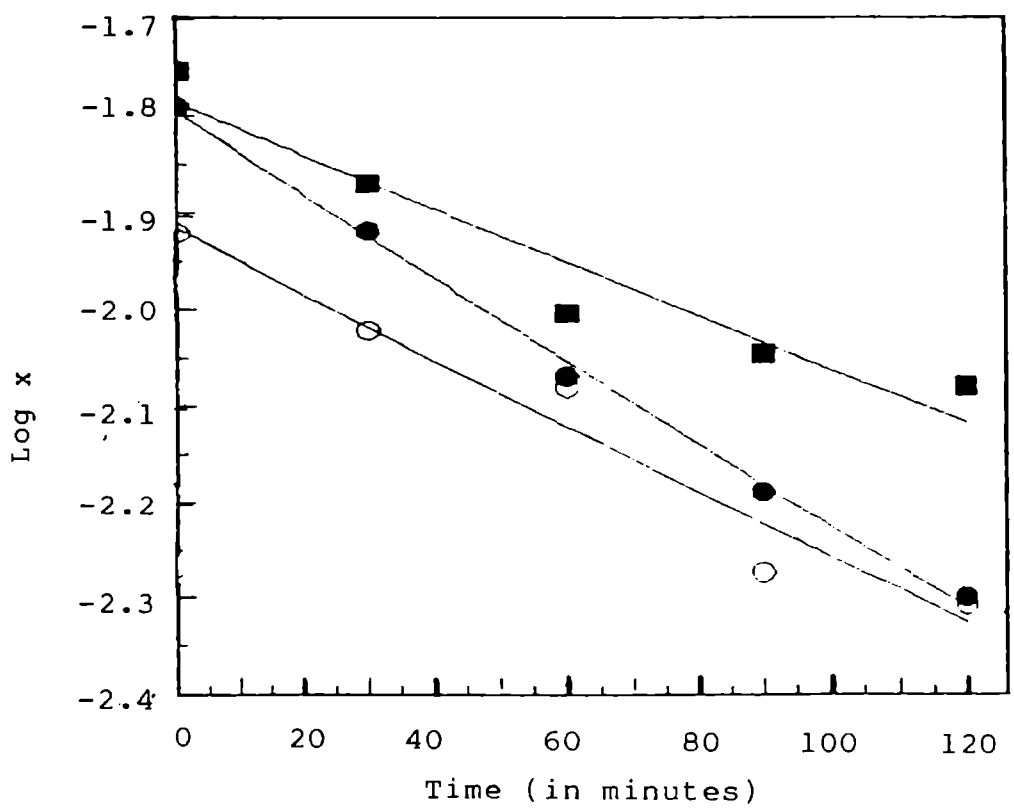

X is the concentration of cyclohexanol

○ 300°C ● 500°C ▣ 800°C

Fig.25 Kinetics of oxidation of cyclohexanol on Sm_2O_3/Al_2O_3 catalyst with different compositions.

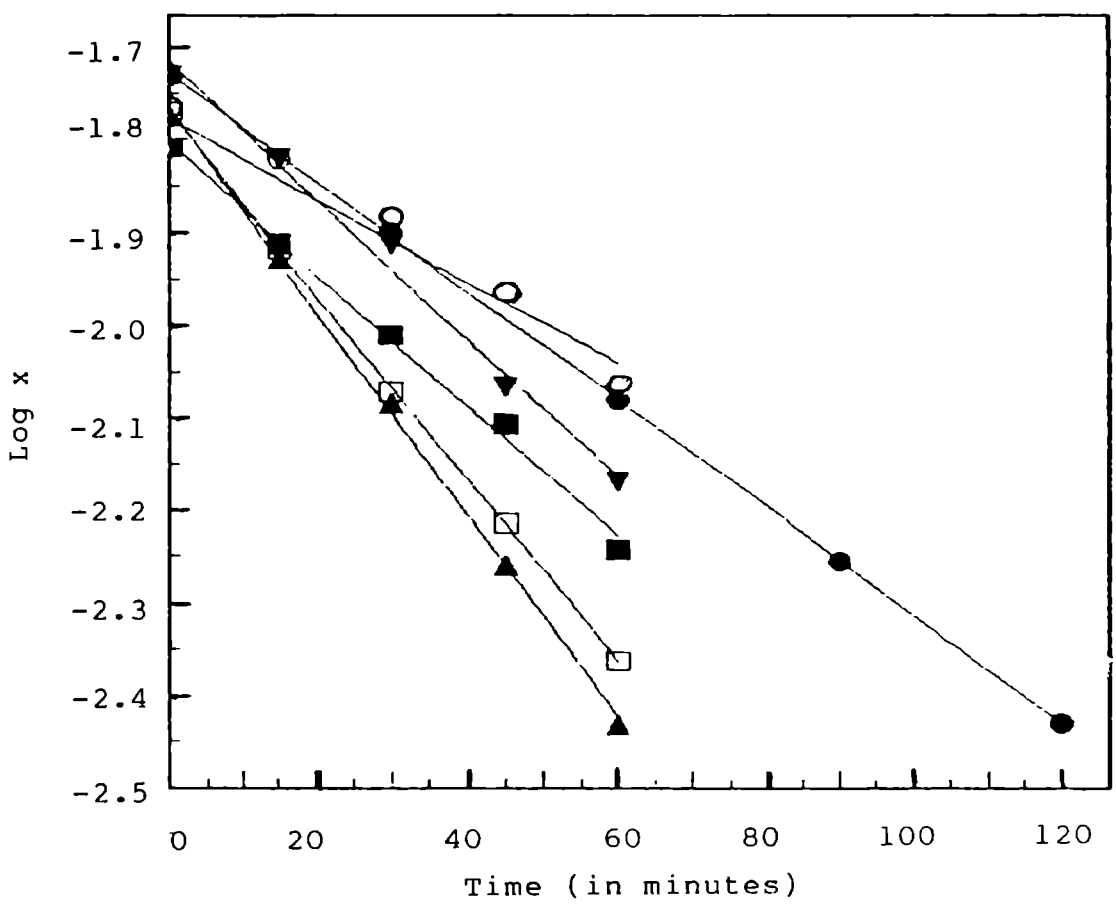

X is the concentration of cyclohexanol.

- 5% Sm_2O_3/Al_2O_3
- 10% Sm_2O_3/Al_2O_3
- 20% Sm_2O_3/Al_2O_3
- 40% Sm_2O_3/Al_2O_3
- 75% Sm_2O_3/Al_2O_3
- Al_2O_3

Fig.26 Kinetics of oxidation of cyclohexanon on CeO_2/Al_2O_3 catalyst with different compositions.

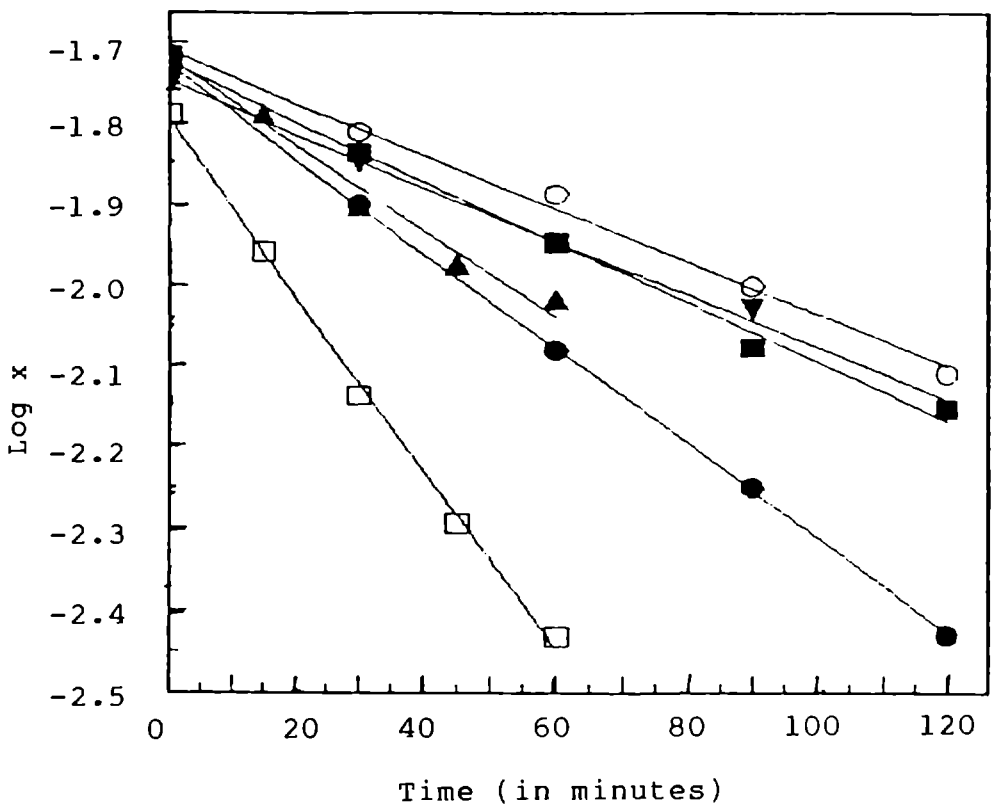

X is the concentration of cyclohexanol.

- O 10% CeO_2/Al_2O_3
- ▼ 20% CeO_2/Al_2O_3
- □ 40% CeO_2/Al_2O_3
- ▲ 60% CeO_2/Al_2O_3
- ■ 80% CeO_2/Al_2O_3
- ● Al_2O_3

Fig.27 Catalytic activity for reduction as a function of activation temperature.

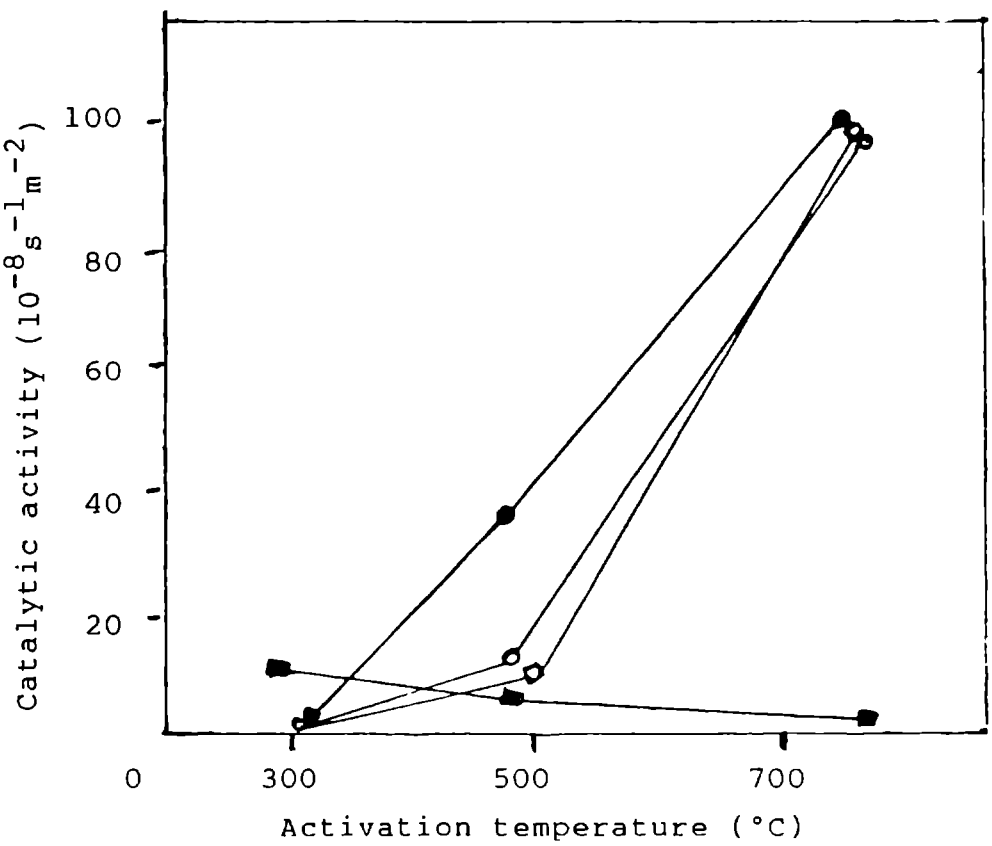

○ Rate constant for the reduction of cyclohexanone

● Rate constant for the reduction of acetophenone

□ Rate constant for the reduction of benzophenone (on Sm_2O_3)

■ Rate constant for the reduction of cyclohexanone on CeO_2

Fig.28 Catalytic activity for oxidation as a function of activation temperature.

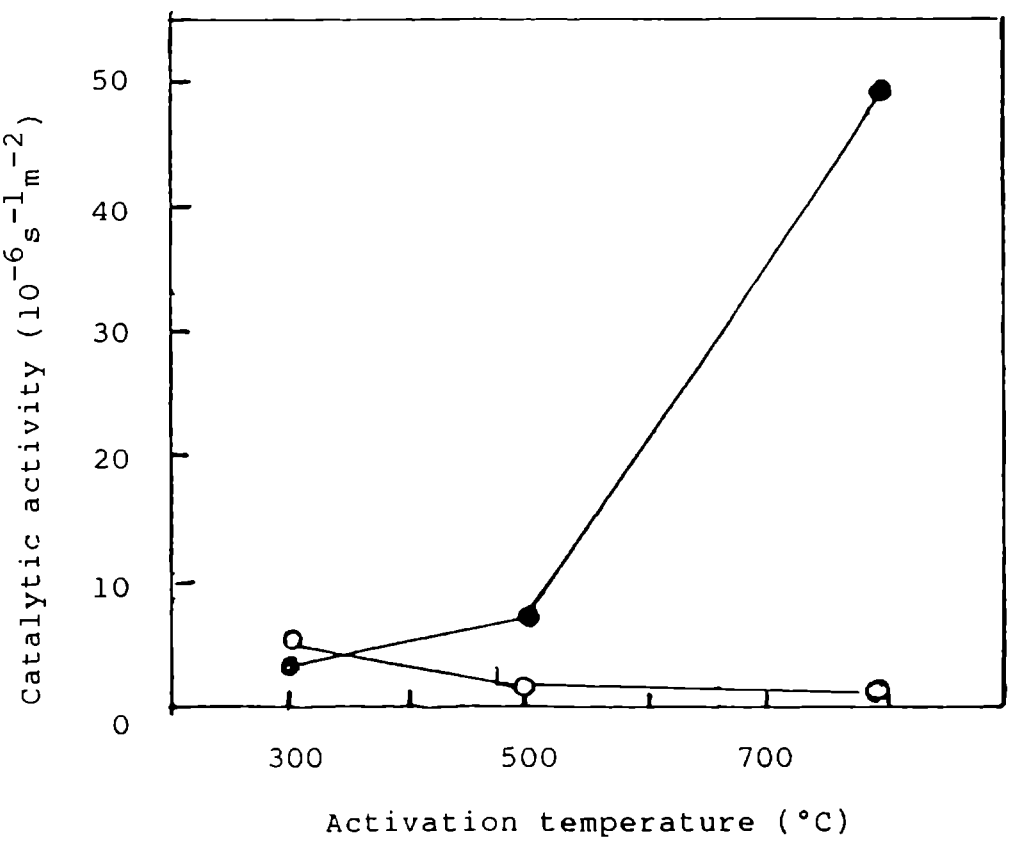

● Rate constant for the oxidation of cyclohexanol on Sm_2O_3

○ Rate constant for the oxidation of cyclohexanol on CeO_2.

Fig.29 Catalytic activity for reduction as a function of composition of Sm_2O_3/Al_2O_3 and CeO_2/Al_2O_3

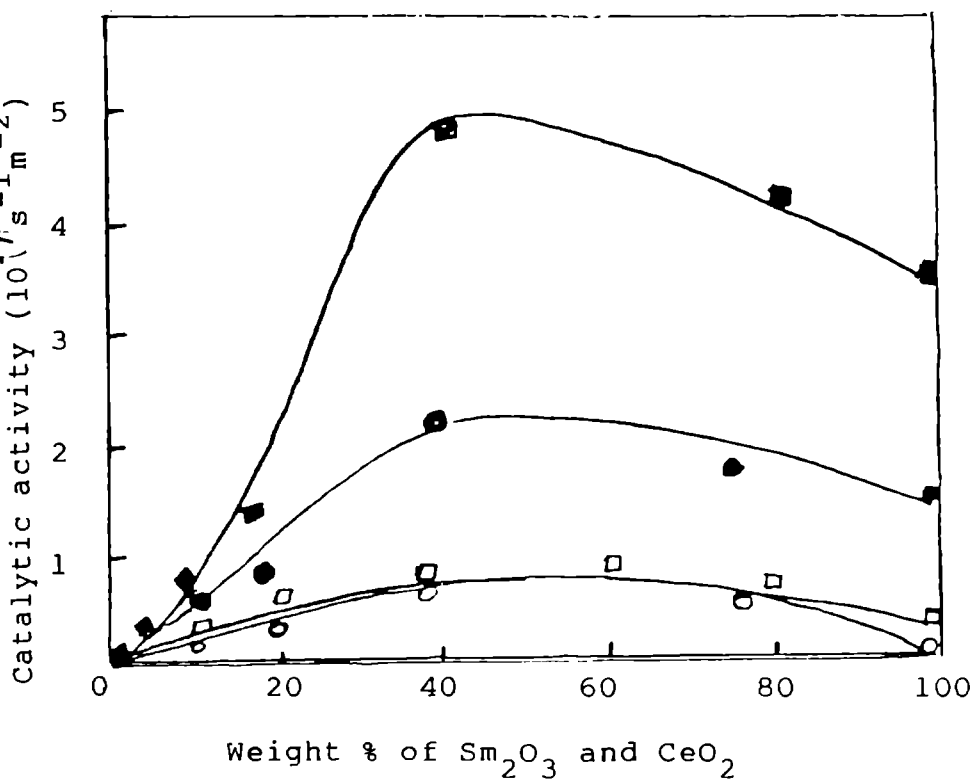

● Rate constant for the reduction of cyclohexanone

▬ Rate constant for the reduction of acetophenone

○ Rate constant for the reduction of benzophenone (on Sm_2O_3/Al_2O_3)

□ Rate constant for the reduction of cyclohexanone on CeO_2/Al_2O_3

Fig.30 Catalytic activity for oxidation as a function of composition of Sm_2O_3/Al_2O_3 and CeO_2/Al_2O_3.

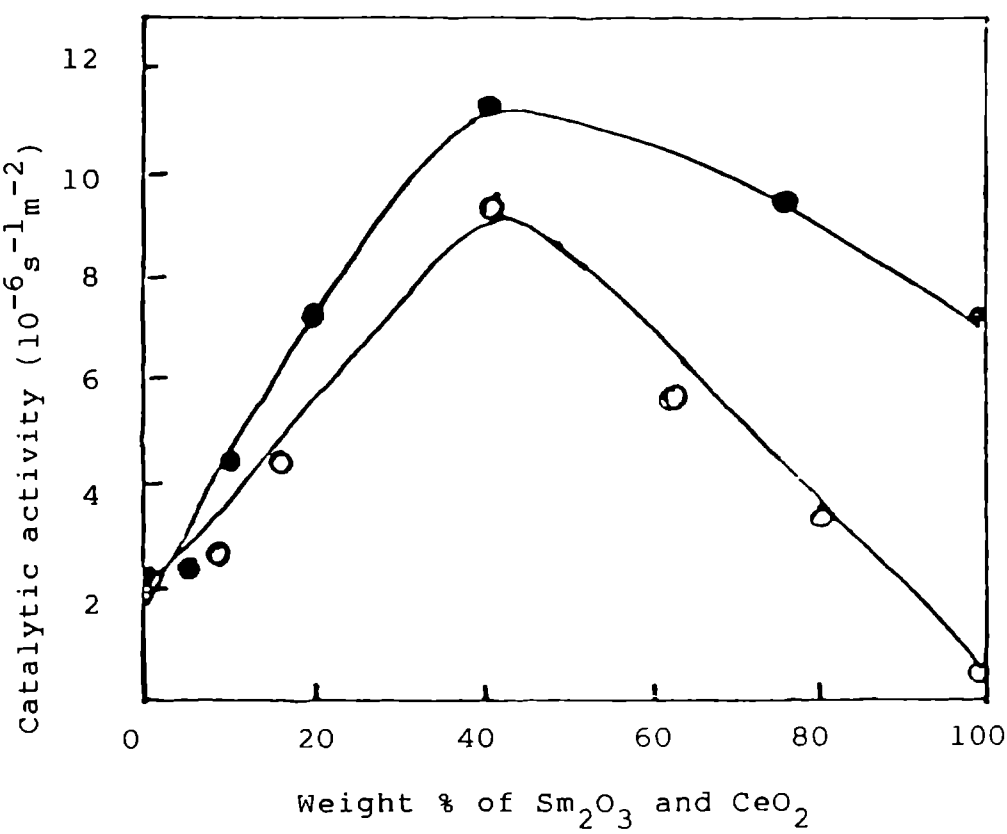

● Rate constant for the oxidation of cyclohexanol on Sm_2O_3/Al_2O_3.

○ Rate constant for the oxidation of cyclohexanol on CeO_2/Al_2O_3.

Fig.31 Limiting amount of electron acceptor adsorbed and catalytic activity as a function of activation temperature of Sm_2O_3.

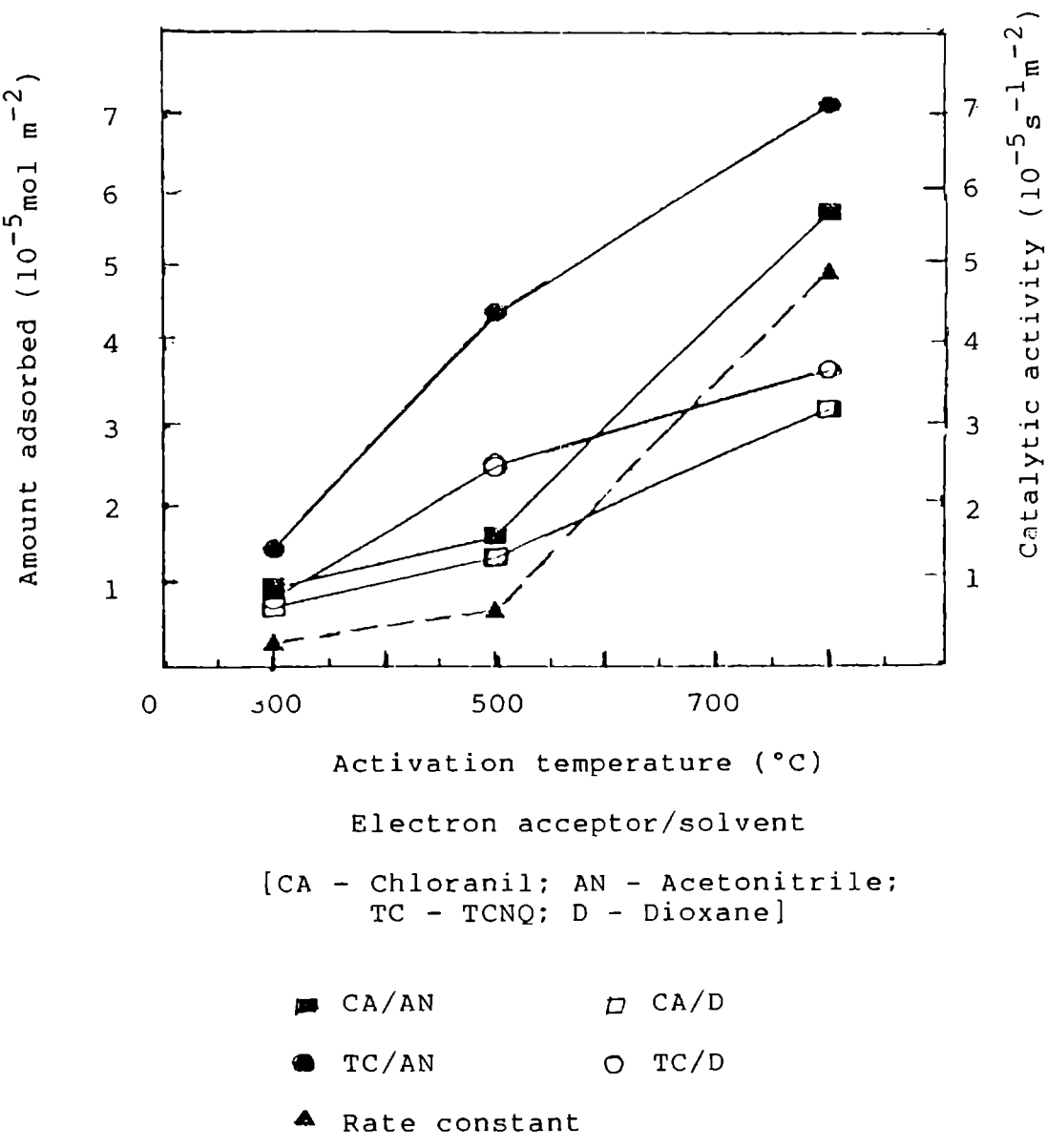

Fig.32 Limiting amount of electron acceptor adsorbed and catalytic activity as a function of activation temperature of CeO_2.

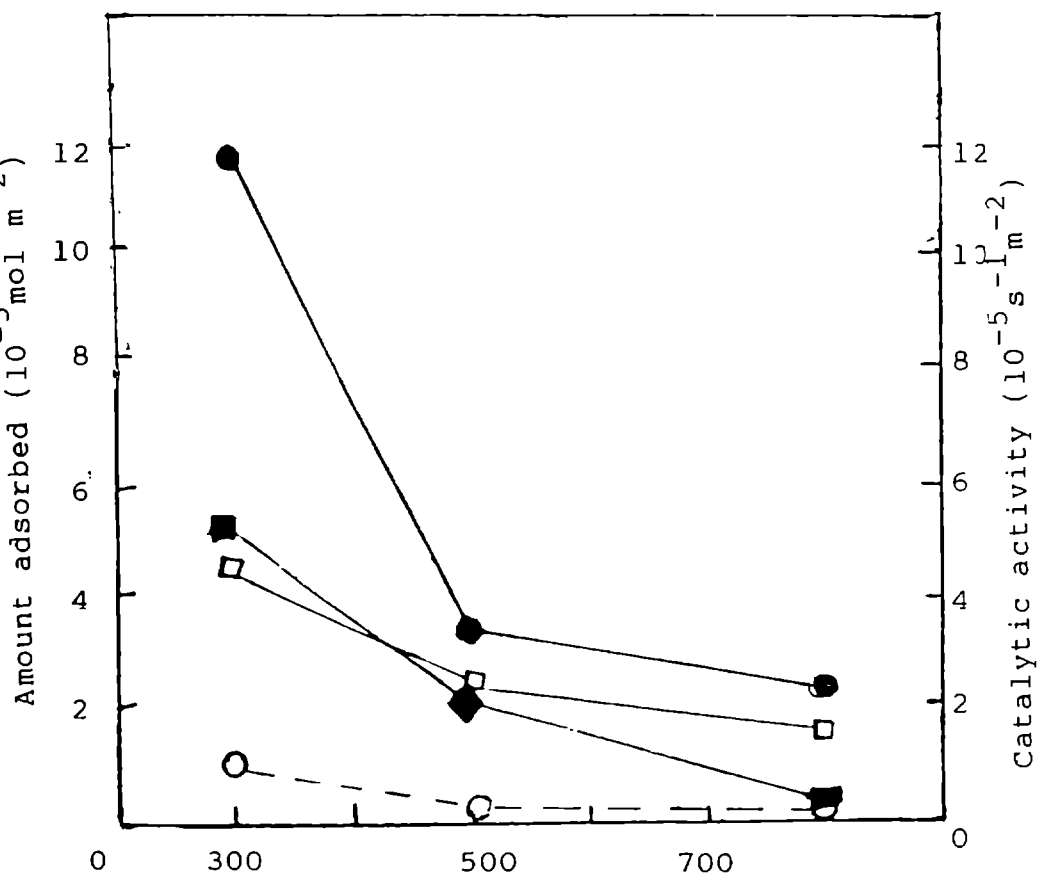

Electron acceptor/solvent

[CA - Chloranil; AN - Acetonitrile;
TC - TCNQ; D - Dioxane]

□ CA/AN

● TC/AN ■ TC/D

○ Rate constant.

Fig.33 Limiting amount of electron acceptor adsorbed and catalytic activity Vs. composition of Sm_2O_3/Al_2O_3.

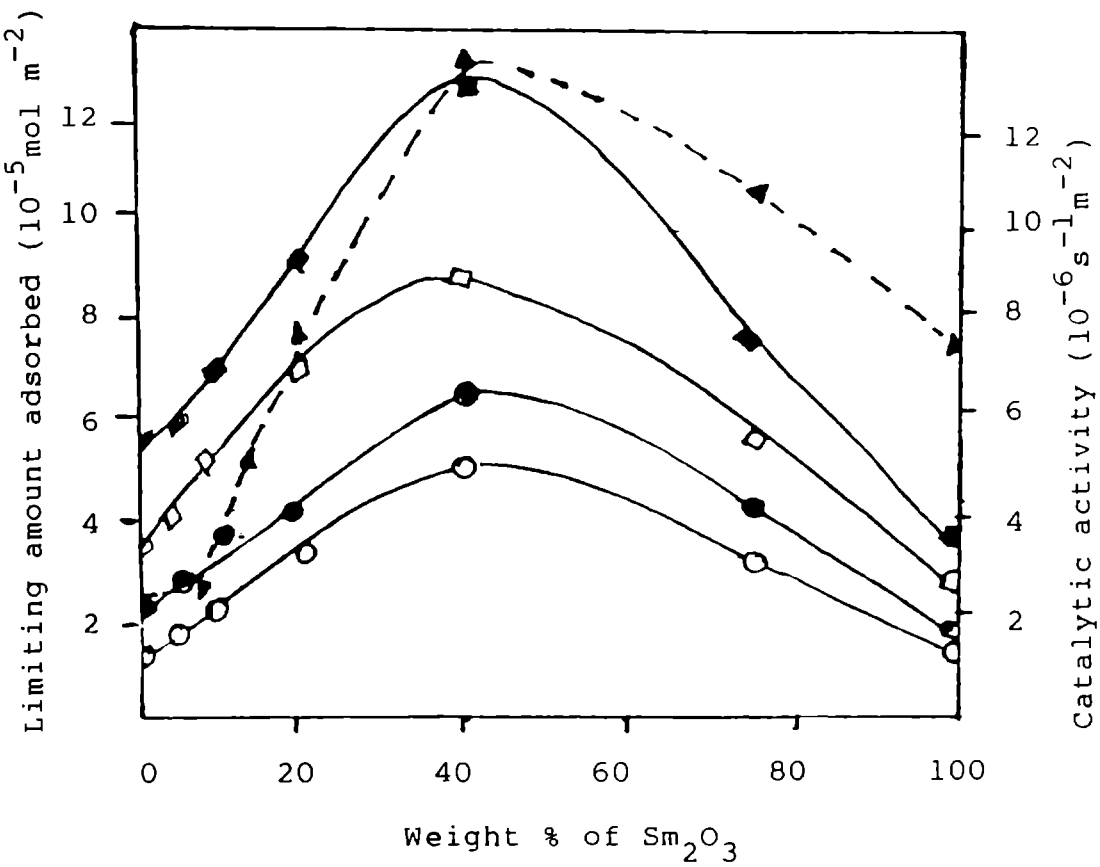

Electron acceptor/solvent

[CA - Chloranil; AN - Acetonitrile;
TC - TCNQ; D - Dioxane]

● CA/AN ○ CA/D

■ TC/AN □ TC/D

▲ Rate constant.

Fig.34 Limiting amount of electron acceptor adsorbed and catalytic activity Vs. composition of CeO_2/Al_2O_3.

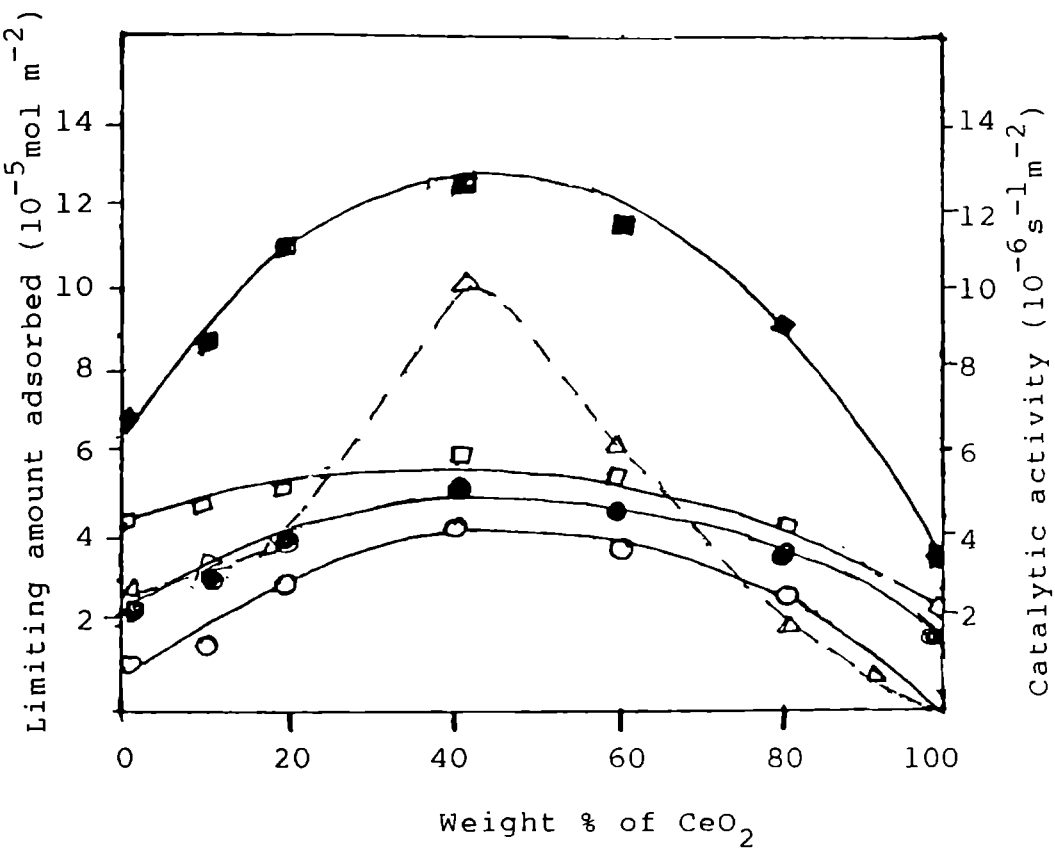

Electron acceptor/solvent

[CA - Chloranil; AN - Acetonitrile; TC - TCNQ; D - Dioxane]

● CA/AN ○ CA/D

■ TC/AN □ TC/D

△ Rate constant.

In the case of mixed oxides the catalytic activity (both the oxidation and reduction) increases up to a certain composition and then decreases (Figs.29-30). Here also activity parallel the basicity of the catalysts. The change in catalytic activity as a function of activation temperature and composition is comparable with the plots of limiting amount of electron acceptor adsorbed as a function of composition and temperature (Figs.31-34). Electron donicity and catalytic activity increases with increase in basicity of the catalyst.

REFERENCES

1. K.Otsuka, K.Jinno and A.Morikawa, Chem. Lett., 499 (1985).

2. K.Kushihashi, K.Maruya, K.Domen and T.Onishi, J. Chem. Soc. Chem. Commun. No.3, 259 (1992).

3. O.Johnson, J. Phys. Chem. 59, 827 (1955).

4. T.Arai, K.Maruya, K.Domen and T.Onishi, Bull. Chem. Soc. Jap., 62, 349 (1989).

5. S.Sugunan and G.Devika Rani, J. Mat. Sci. Lett. 43, 375 (1991).

6. S.Sugunan and Devika Rani, J. Mat. Sci. Lett. 10, 887 (1991).

7. S.Sugunan and K.B.Sherly, Indian J. Chem. 32A, 489 (1993).

8. S.Sugunan and G.Devika Rani, J. Mat. Sci. 28, 4811 (1993).

9. M.Che, C,Naccache and B.Imelik, J. Catal., 24, 328 (1972).

10. D.S.Acker and W.R.Hertler, J. Am. Chem. Soc. 84, 328 (1962).

11. R.H.Boyd and W.D.Philips, J. Chem. Phys., 43, 2927 (1965).

12. R.Foster and T.J.Thomson, Trans. Faraday Soc., 58, 860 (1962).

13. H.Hosaka, T.Fujiwara and K.Meguro, Bull. Chem. Soc. Jap., 44, 2616 (1971).

14. K.Esumi and K.Meguro, J. Japan Color. Material, 48, 539 (1975).

15. K.Meguro and K.Esumi, J. Colloid. Interface Sci., 59, 93 (1973).

16. B.D.Flockhart, J.A.N.Scott and R.C.Pink, Trans. Faraday Soc., 62, 730 (1966).

17. G.V.Fomin, L.A.Blyumenfield and V.I.Sukhorukov, Proc. Acad. Sci., USSR, 157, 819 (1964).

18. M.L.Hair and W.Hertle, J. Phys. Chem. 74, 91 (1970).

19. R.Bluementhal, P.W.Lee and R.J.Panlener, J. Electrochem. Soc., 118, 123 (1971).

20. R.S.Drago, L.B.Parr and C.S.Chamberlain, J. Am. Chem. Sco., 99, 3203 (1977).

21. L.P.Hammett and A.J.Deyrup, J. Am. Chem. Soc., 54, 2721 (1932).

22. T.Yamanaka and K.Tanabe, J. Phys. Chem. 80, 1725 (1976).

23. H.Kuno, T.Takahashi, M.Shibagaki and H.Matsushita, Bull. Chem. Soc. Jap., 63, 1943 (1990).

24. H.Kuno, K.Takahashi, M.Shibagaki and H.Matsushita, Bull. Chem. Soc. Jap., 64, 312 (1991).

25. M.Shibagaki, K.Takahashi and H.Matsushita, Bull. Chem. Soc. Jap., 61, 328 (1988).

CONCLUSION

CONCLUSION

Systematic study of the correlation between catalytic activity, acid-base and electron-donor properties on the rare earth oxide surfaces have revealed the following results.

The amount of electron acceptor adsorbed on the rare earth oxide surface depend on the activation temperature of the oxide, basicity of the solvent and the electron affinity of the electron acceptor. The limiting amount of electron acceptor adsorbed on the oxide surface increases with increase in activation temperature of the oxide, increase in electron affinity of the electron acceptor and decrease in basicity of the solvent.

The limit of electron transfer from the oxide surface to the electron acceptor is between 2.40 and 1.77 eV for Sm_2O_3 in all the systems, but in the case of ceria the limit of electron transfer shift from 2.40-1.77 eV to 2.84-2.40 eV in 1,4-dioxane and ethyl acetate. In the case of mixed oxides surface electron properties of alumina are modified by the rare earth oxide without changing the limit of electron transfer.

The change in magnetic moment during adsorption of electron acceptors on paramagnetic oxides is a measure of the extent of electron transfer during adsorption.

The electron donor power of oxide surface increase with basic strength of surface measured as its $H_{o,max}$ value. The order of basic strength parallels the order of electron donor sites present on oxides.

Sm_2O_3 and mixed oxides of samarium, aluminium and cerium with aluminium are found to be effective in the liquid phase oxidation-reduction reactions. In the case of pure CeO_2, it is effective only for lower activation temperatures (300°C). These reactions showed a first order dependence on the concentration of the reactant. The data on catalytic activity parallel the electron donating and acid-base properties of the oxides.

LIST OF PAPERS PUBLISHED/COMMUNICATED

1. S.Sugunan and J.M.Jalaja, "Electron donating, acid-base and magnetic properties of samaria catalyst", J.Adhesion Sci. Technol. (in Press).

2. S.Sugunan and J.M.Jalaja, "Electron donating and acid-base properties of cerium oxide and its mixed oxides with alumina", Collect. Czech. Chem. Commun. (in Press).

3. S.Sugunan and J.M.Jalaja, "Electron donating properties and catalytic activity of cerium oxide and its mixed oxides with alumina", Indian J. Chem. (in Press).

4. S.Sugunan and J.M.Jalaja, "Electron donating properties and catalytic activity of samarium oxide and its mixed oxides with alumina", Communicated to React. Kinet. Catal. Lett.